University of Ghana http://ugspace.ug.edu.gh

UNIVERSITY OF GHANA

STRUCTURAL AND PETROLOGICAL EVOLUTION OF THE SHAI HILLS TECTONIC SUTURE ZONE, SOUTHEASTERN GHANA.

BY

FOSU THOMAS

(10279668)

THIS THESIS IS SUBMITTED TO THE UNIVERSITY OF GHANA, LEGON IN PARTIAL FULFILMENT OF THE REQUIREMENT FOR THE AWARD OF MPHIL GEOLOGY DEGREE.

JULY, 2015.

University of Ghana http://ugspace.ug.edu.gh

DECLARATION

This is to certify that this thesis is the result of research undertaken by Fosu Thomas towards the award of Master of Philosophy degree in Geology in the Department of Earth Science, University of Ghana, under the supervision of Prof. P.M. Nude and Dr. J.M. Kutu.

…… Date: …….

Fosu Thomas

(Student)

…… Date: ……..

Prof. P.M. Nude

(Supervisor)

…… Date: ……..

Dr. J.M. Kutu

(Co-Supervisor)

University of Ghana http://ugspace.ug.edu.gh

ABSTRACT

High Pressure (HP) mafic granulites (mafic garnet gneisses) in the Shai Hills suture zone occur as NE/SW trending isolated inselbergs in the Accra plains. They characterize the suture zone rocks of the Pan-African orogeny in Ghana. Various aspects of the Shai Hills suture rocks have been studied yet relatively little is known about its structural and deformational evolution. This work presents a new research into the structural, petrological and deformational evolution highlighting on metamorphism, petrogenesis and tectonic setting of the unique suture zone in Ghana by integrating field work, petrographic studies and whole rock major, minor and trace element (including REE) geochemical data.

The high pressure granulites have undergone prograde metamorphism during subduction and followed by later retrograde metamorphism as a result of later exhumation. They record at least four distinct metamorphic episodes of which early prograde mineral assemblages are represented by mineral inclusions of hornblende + ilmenite within some porphyroblastic garnets and clinopyroxenes. The peak assemblage is characterized by granulite metamorphic assemblages of porphyroblastic garnet + clinopyroxene + quartz + plagioclase. The peak granulite stage was followed by three successive retrogressive facies stages during exhumation. The hornblende-granulite stage followed peak granulite stage and is characterized by the introduction of dark red hornblende and corona texture of clinopyroxene around garnet. This stage was then followed by amphibolite stage with the introduction of green hornblende rims of some clinopyroxene and garnet. The introduction of chlorite and epidote defines the greenschist metamorphic assemblage stage in the rock.

University of Ghana http://ugspace.ug.edu.gh

The terrane has undergone three main deformational stages: D_1, D_2 and D_3. The D_1 and D_2 are characterized by ductile deformation while the D_3 is characterized by brittle deformation. Shear sense indicators in the terrane indicate an early dextral shearing and later sinistral shearing.

Geochemical data suggest that, the high pressure granulitic rocks may have preserved the geochemical imprints of their magmatic basaltic protoliths where the rocks are mainly characterized by Island Arc Tholeiite (IAT) imprints with few with ocean crust (N-MORB) imprints. The HP granulite displays trace elements patterns similar to that of the mafic granulite lower crust (LC) composition. They show depletions in HREEs and have enrichment of LREEs. They are depleted in Cs, Rb and Th with enrichment in Ba and Sr. They also display averagely positive Eu anomaly which is similar to the lower crust (LC).

The combination of petrography, mineral compositions, micro and macro structures and geochemical data suggest that the rocks may have undergone initial crustal thickening during subduction and collision related tectonic processes accompanied by prograde metamophism followed by exhumation, cooling and retrogression.

University of Ghana http://ugspace.ug.edu.gh

DEDICATION

I dedicate this work to the Holy Trinity, my late father Mr. Philip Kojo Fosu and to my ever supporting and loving family.

University of Ghana http://ugspace.ug.edu.gh

ACKNOWLEDGEMENTS

I thank the Almighty God for making it possible for me to undertake this project successfully. Throughout this project, the Lord has shown his mercies upon me and has provided me with good health that enabled me to complete the project successfully, thank you Lord.

Secondly I would like to say a very big thank you to my supervisor, Prof. P.M Nude and my co-supervisor, Dr. J.M Kutu, and to the Dean of the School of Physical and Mathematical Science, University of Ghana, Prof. Daniel Asiedu and Emmanuel K. Abitty for providing me with the necessary assistance and taking time to shape and fine-tune this project, God bless you all.

To the entire staff of Earth Science Department, University of Ghana (UG), I say thank you so much and may God bless you for the time and patience you had for me during this project. To my colleague Emmanuel Nyavor, I say thank you so much for helping me during the field work and to the Assembly man and the people of Dedenya for providing me accommodation and other support throughout my stay during the field work, God bless you all. To my friends, Edmund Yeboah, Manesseh Kodji Zodji, Asem Enoch and co., I say God bless you all for the various ways you contributed to the realization of the project, it has been a wonderful time having you around.

Last but not the least, I would like to say thank you so much to my brother Theophilus Atta Fosu and to all my relatives for the many supports that you have offered me.

University of Ghana http://ugspace.ug.edu.gh

TABLE OF CONTENTS

DECLARATION ii

ABSTRACT iii

DEDICATION v

ACKNOWLEDGEMENTS vi

LIST OF TABLES xi

LIST OF FIGURES xii

LIST OF ABBREVIATIONS xvii

1.0 INTRODUCTION 1

1.1 Background 1

1.2 Objectives 2

1.3 Project Area 3

1.3.1 Accessibility 6

1.3.2 Physical Features 6

1.3.3 Climate 6

1.3.4 Vegetation 7

1.3.5 Relief 7

1.3.6 Settlement, Population and Occupation 8

University of Ghana http://ugspace.ug.edu.gh

1.4 Structure of the Thesis 8

2.0 REGIONAL GEOLOGY AND GEOLOGICAL SETTING 10

2.1 Buem Structural Units 11

2.2 Togo Structural Unit 12

2.3 Dahomeyan Structural Unit 13

2.4 Previous Work 17

3.0 METHODOLOGY 20

3.1 Desk Study and Literature Survey 20

3.2 Tools and Equipment 21

3.3 Field Methods and Sampling 21

3.3.1 Reconnaissance Survey 22

3.3.2 Mapping Procedures 22

3.4 Post Field Procedures 24

3.4.1 Thin section Preparation 25

3.4.2 Geochemical Analysis 26

3.4.3 Map Digitization, Stereographic projections and Cross Section Drawing. 27

4.0 RESULTS 28

4.1 Field Relation and Petrography 28

University of Ghana http://ugspace.ug.edu.gh

4.1.1 Mafic Garnet Gneisses 30

4.1.2 Pyroxene Bearing Amphibolite 47

4.1.3 Pyroxenite 51

4.1.4 Fault Breccia 54

4.2 Deformations, Structures and Kinematics 56

4.2.1 Gneissic Bands and Foliations. 56

4.2.2 Mineral lineation. 60

4.2.3 Ptygmatic Folds 64

4.2.4 Faults 66

4.2.5 Joints 70

4.2.6 Boudins 70

4.3 Major and Trace Element Geochemistry 72

4.3.1 Major Element Geochemistry 72

4.3.2 Trace Element Geochemistry 78

5.0 DISCUSSIONS 91

5.1 Field Relation and Petrography 94

5.2 Metamorphism 100

5.3 Deformations, Structures and Kinematics 101

University of Ghana http://ugspace.ug.edu.gh

5.3.1 D_1 Deformation 102

5.3.2 D_2 Deformation 103

5.3.3 D_3 Deformation 104

5.4 Geochemistry 106

5.4.1 Classification 106

5.4.2 Tectonic Setting 109

5.4.3 Petrogenesis 116

6.0 CONCLUSIONS AND RECOMMENDATIONS 125

REFERENCES 130

APPENDIX 144

University of Ghana http://ugspace.ug.edu.gh

LIST OF TABLES

Table 1: Average modal composition (vol %) of minerals in the garnet hornblende gneiss.45

Table 2: Average modal composition (vol%) of minerals in the pyroxene garnet gneiss..... 47

Table 3: Average modal composition (vol %) of minerals in pyroxene bearing Amphibolite. 51

Table 4: Average modal composition (vol%) of minerals in pyroxenite. 54

Table 5: Average modal composition (vol%) of minerals in fault breccia..... 55

Table 6: Structural attitude (degree) of foliation planes. 58

Table 7: Structural attitude (degree) of mineral lineation. 61

Table 8: Structural attitude (degree) of Ptygmatic fold axis..... 64

Table 9: Structural attitude (degree) of faults planes in the area. 67

Table 10: Major and trace elements composition of the pyroxene garnet gneiss..... 75

Table 11: Major and trace elements composition of garnet hornblende gneiss. 76

Table 12: Major and trace elements composition. 77

University of Ghana http://ugspace.ug.edu.gh

LIST OF FIGURES

Figure 1.1: Geological map of Ghana with the study area shown by the black rectangle. (Compiled from Bates (1995), Hasting (1982), Davis, et. al (1994))..... 4

Figure 1.2: Topographical Map of the study area..... 5

Figure 2.1: Tectonic map of the Dahomeyides of southeastern Ghana (after Attoh, 1998) showing the location of the study area. 16

Figure 4.1: Outcrop map of the study Area. 29

Figure 4.2: Field photographs showing (a) subhorizontal layers of mafic and felsic bands in mafic garnet gneiss; at Eastern Quarries, Mampong Hill (b) Compositional felsic bands in the mafic garnet gneiss at Mampong Hill (c) Porphyroblastic garnet of different sizes at PW Quarries, Naglayo Hills (d) Alternating bands of mafic, felsic and garnet bands in the mafic garnet gneiss at the West Coast Quarries, Naglayo Hills..... 31

Figure 4.3: Field Photographs showing (a) compositional bands with stretched hornblendes (b) Compositional bands folded into ptygmatic fold (c) Ptygmatic folds (d) Pressure Shadow formed at the edges of porphyroblastic garnet minerals..... 34

Figure 4.4: Field photographs showing (a) stretched pyroxenite within the mafic garnet gneisses at the Shai Hill Game Reserve (b) brittle fault at the PW Quarries; Naglayo Hill (c) brittle fault zone observed at PW Quarries at Naglayo Hill (d) Joints found at the Shai Hill game reserve. 35

Figure 4.5: (a) Photomicrograph showing garnet minerals. Plane polarized light (Ppl) (b) Photomicrograph showing garnet and clinopyroxene porphyroblast (Ppl) (c) Garnet porhyroblast with hornblende inclusion (Ppl) (d) Poikiloblastic texture of garnet with inclusions of quartz and opaque minerals (Ppl). Garnet (Grt), Plagioclase (Pl),

University of Ghana http://ugspace.ug.edu.gh

Microcline (Mc), Pyroxene (Px), Clinopyroxene (Cpx), Orthopyroxene (Opx), Hornblende (Hbl), Quartz (Qtz), Chlorite (Chl), Opaque mineral (Op)..... 40

Figure 4.6: (a) Photomicrograph showing Clinopyroxene porphyroblast with rims of chlorite with the S_1 foliation around it. (Ppl). (b) Photomicrograph showing Clinopyroxene porphyroblast with rims of chlorite. (Xpl). (c) Hornblende rims around broken Clinopyroxene (Ppl) (d) Hornblende rims around broken Clinopyroxene (Xpl). Same Abbreviations are used. 41

Figure 4.7: (a) and (b) Photomicrographs are showing porphyroblastic Clinopyroxene with rims of hornblende intracrystalline fractures. (Ppl) (c) and (e) Broken and cracked Clinopyroxene porphyroblast (Ppl) (d) and (f) Broken Clinopyroxene porphyroblast. (Xpl). Same Abbreviations are used. 42

Figure 4.8: (a) Photomicragh showing deformed pre kinematic garnet porphyroblast with rims of hornblende and S_1 foliation wrapping around it. (Ppl). (b) Syn kinematic garnet with inclusion of Clinopyroxenes. (Xpl). (c) Garnet with rutile exsolution (Xpl). (d) Syn kinematic garnets (Ppl). (e) Garnet porphroblast with inclusions of quartz and plagioclase (Xpl). (f) Corona texture of Clinopyroxenes and quartz around garnet porphyroblast (Ppl). Same Abbreviations are used. 43

Figure 4.9: (a) Photomicrograph showing L_1 mineral lineation in the S_1 foliation. (b) Photomicrograph showing deformed polysynthetic twining in plagioclase and deformed quartz. (Ppl). Same Abbreviations are used. 44

Figure 4.10: Photomicrograph showing garnet hornblende gneiss. (Xpl) Same Abbreviations are used. 45

Figure 4.11: Photomicrographs of pyroxene garnet gneiss. (Xpl). Same Abbreviations are used. 46

Figure 4.12: Field photograph of pyroxene bearing amphibolite. 48

University of Ghana http://ugspace.ug.edu.gh

Figure 4.13: Field photograph of amphibolite tectonically welded into host mafic garnet gneiss at Eastern quarries, Mampong Hill. (b) Gradational contact between the amphibolite and the mafic garnet garnet gneiss. 48

Figure 4.14: Photomicrographs of pyroxene bearing amphibolite. (Ppl). Same Abbreviations are used. 50

Figure 4.15: Field photograph showing pyroxenite thrusted into the mafic garnet gneiss at Eastern Quarries. Mampong Hill. 52

Figure 4.16: Field photograph showing pyroxenites boudins in the mafic garnet gneiss at PW Quarries. Naglayo hill. 52

Figure 4.17: (a) and (c) Photomicrographs showing Clinopyroxene (Cpx) and Orthopyroxene (Opx) in the pyroxenite. (Ppl). (b) and (d) Photomicrographs showing Clinopyroxene (Cpx) and Orthopyroxene (Opx) in the pyroxenite. (Xpl). Same Abbreviations are used. 53

Figure 4.18: Photomicrograph of the Fault Breccia. (Ppl). Same Abbreviations are used.... 55

Figure 4.19: Field photographs showing gneissic banding and foliations in the mafic garnet gneisses. Shai hills. 57

Figure 4.20: (a) Poles plot of foliations in mafic garnet gneisses (b) Poles plot with plane to poles plot in the mafic garnet gneiss. 59

Figure 4.21: Contoured poles-density plot of foliations in mafic garnet gneisses. 59

Figure 4.22: Stretched hornblende within compositional banding in the mafic garnet gneiss. 60

Figure 4.23: Shows Poles plot of lineations in mafic garnet gneisses. 62

University of Ghana http://ugspace.ug.edu.gh

Figure 4.24: Photograph showing dextral sense of shearing by sheared pyroxenite boudin in the mafic garnet gneiss during D_1 deformation at Shai Forest reserve..... 63

Figure 4.25: Photograph showing dextral sense by clockwise rotation of garnet in the mafic garnet gneiss during D_1 deformation at PW Quarries, Naglayo Hill..... 63

Figure 4.26: Poles plot of fold axis of ptymatic folds. 65

Figure 4.27: Field photograph showing normal faults in the mafic garnet gneiss at PW Quarries, Mampong Hill. 66

Figure 4.28: Poles plot of faults in the mafic garnet gneisses. 68

Figure 4.29: Photograph showing overall sinistral sense of shear during the D_3 deformations. 69

Figure 4.30: Structural map of the study area..... 71

Figure 4.31: Chondrite-normalised plots of the REE composition of the rocks in the study area (a) Pyroxene garnet gneisses. (b) Garnet hornblende gneiss. With lower crust (LC) and Normal MORB (N-MORB). 81

Figure 4.32: Chondrite-normalised plots of the REE composition of the rocks in the study area (c) Pyroxene bearing amphibolite (d) fault breccia and pyroxenite. With lower crust (LC) and Normal MORB (N-MORB). 82

Figure 4.33: Chondrite normalized plots of the incompatible trace element composition of the rock in the study area. (A) Pyroxene garnet gneisses (B) Garnet hornblende gneisses 84

Figure 4.34: Chondrite normalized plots of the incompatible trace element composition of the rock in the study area. (C) Pyroxene bearing amphibolite (D) Fault breccia (E) Pyroxenite. 85

University of Ghana http://ugspace.ug.edu.gh

Figure 4.35: N MORB normalized plots of the incompatible trace element composition of the mafic garnet gneisses. (A) Pyroxene Garnet Gneiss (B) Garnet Hornblende Gneiss. 87

Figure 4.36: Chondrite normalized plots of transition element composition of the rocks in the study area. (A) Pyroxene garnet gneiss (B) Garnet hornblende gneiss. 89

Figure 4.37: Chondrite normalized plots of transition element composition of the rocks in the study area. (C) Pyroxene bearing amphibolite (D) Fault breccia (E) Pyroxenite.90

Figure 5.1: Geological map of the area. 92

Figure 5.2: Cross section of the Study area. 93

Figure 5.3: Geochemical classifications of rocks in the study area using TAS diagram (a) Le Bas et al., (1986) (b) Cox et al., (1979). 107

Figure 5.4: Classification plot of SiO_2 Versus K_2O (after Peccerillo and Taylor, 1974). ... 108

Figure 5.5: Tectonic discrimination diagram Cr vs Y plot (Fields for MORB and IAT after Pearce et al., 1984)..... 110

Figure 5.6: Tectonic discrimination diagram of Ti vs Zr plot (Pearce and Can, 1973)..... 111

Figure 5.7: Tectonic discrimination diagram of MgO-FeO-Al2O3 (Pearce et al., 1977). .. 112

Figure 5.8: Tectonic discrimination diagram of MnO_2, TiO_2 and P_2O_5 (Mullen, 1983)..... 113

Figure 5.9: AFM diagram showing samples from the study area (After Irvine and Barager, 1971). 118

Figure 5.10: Proposed model for the Pan African suture zone in Ghana based on Wilson cycle reconstructions. (Modified after Attoh and Nude, 2008). 124

University of Ghana http://ugspace.ug.edu.gh

LIST OF ABBREVIATIONS

WAC - West African Craton

SE - South East

NW - North West

NE - North East

ENE - East North East

WSW - West South West

NNW - North North West

SSE - South South East

HIPGE - High Pressure Granulites and Eclogites

UHP - Ultra High Pressure

HP - High Pressure

TSB - Trans Saharan Belt

Ma - Million Years

Ga - Billion Years

GPa - Giga Pascal

REE - Rare Earth Element

HREE - Heavy Rare Earth Element

LREE - Light Rare Earth Element

MREE - Middle Rare Earth Element

HFSE – High Field Strength Element

LILE – Large Ion Lithophile Element

University of Ghana http://ugspace.ug.edu.gh

ICP-AES - Inductively Coupled Plasma Atomic Emission Spectrometry

ICP-MS - Inductively Coupled Plasma Mass Spectrometry

Fig - Figure

PPL - Plane Polarized Light

XPL - Cross Polarized Light

CIPW - Cross Iddings Pirsson-Washington

Wt.% - Weight Percentage

Ppm - Part per million

Norm - Normative

MORB - Mid Ocean Ridge Basalt

E-MORB - Enriched Mid Ocean Ridge Basalt

N-MORB - Depleted Mid Ocean Ridge Basalt

LC - Lower Crust

IAT- Island Arc Tholeiite

TAS - Total Alkalis and Silica

CAB - Continental Alkaline Basalt

OIA - Ocean Island Alkali Basalt

Mg# - Magnesium Number

GPS - Global Positioning System

Grt – Garnet

Pl – Plagioclase

Mc – Microcline

University of Ghana http://ugspace.ug.edu.gh

Px – Pyroxene

Cpx – Clinopyroxene

Opx – Orthopyroxene

Hbl – Hornblende

Qtz – Quartz

Chl – Chlorite

Op – Opaque mineral

University of Ghana http://ugspace.ug.edu.gh

CHAPTER ONE

1.0 INTRODUCTION

1.1 Background

In the Pan-African Dahomeyide orogenic belt, the granulitic, eclogitic or mafic to ultramafic Dérouvarou (Benin), Kabye-Kpaza, Djabatouré-Anié, Agou-Ahito (Togo) and Akuse or Shai (Ghana) Hills constitute series of mountains consisting the suture zone (Affaton and Tairou, 2012). The Pan-African Dahomeyide orogen of western Africa represents a model of collision belt between the passive continental margin of the West African craton (WAC) and a group of eastern plates, the Benino-Nigerian shields (Affaton et al., 1980). This orogen in West Africa is the southern extension of the 2000 km long Trans-Saharan belt which formed on the eastern margin of the West African Craton (Attoh et al., 2007).

The Pan-African belt has been subdivided into three main units (Affaton et al., 1980): the western external units, thus the deformed edge of the West African craton (WAC) with its cover rocks consisting of craton verging nappes and thrust sheets bounded by ductile shear zones; Buem and Atacora structural units, the eastern internal units, exotic rocks that form the granitoid gneiss complexes east of the suture zone and thirdly, the suture zone. Numerous ultrabasic and basic bodies of various sizes are scattered throughout the suture zone and display contrasted lithological and metamorphic features (Me´not, 1980). Along this suture zone, high-pressure granulites and eclogites (HIPGE) of basaltic composition are the dominant rock types (Attoh, 1998a; Agbossoumonde et al., 2001; Attoh and Morgan, 2004). There are some amphibolite rocks in association with the high-pressure granulites

University of Ghana http://ugspace.ug.edu.gh

and eclogites (HIPGE). The distinctive mafic and ultramafic rocks in the suture can be traced more or less continuously for about 1000 km and are referred to as the Shai Hills Gneisses in southeastern Ghana (Attoh et al., 1997), Kabye Complex in northern Togo and rocks of the Agou Complex in southwestern Togo (Sylvain et al., 1986; Agbossoumonde, 1998).

Various petrological and geochronological investigations have been conducted on the highly metamorphosed and deformed rocks of the Shai Hill suture. However, the Dahomeyide suture zone located in Ghana (Shai Hills) have received relatively little attention, especially on its structural and deformational evolution compared to other Pan African suture zones rocks. Most studies in the area do not sufficiently lay emphasis on the structural and time relation between deformations. This research intends to contribute to the structural characterization and provide detailed sequential deformational events characterizing the Shai hills suture zone rocks.

1.2 Objectives

The objectives of this research are to;

1. determine the structural and deformational evolution of the rock units of the suture zone.
2. determine the paragenesis of the main rock facies.
3. establish the time relation between deformations and structures in the area.
4. deduce field relations of the rocks in the study area; produce a structural map and a composite geological map with cross section of the area.

University of Ghana http://ugspace.ug.edu.gh

The key outcome of this research program is the documentation of regular structural geometry at macro to micro scale and the interpretation of the distribution of the structures throughout the study area and timing of deformational events in the area which have not been dealt with sufficiently.

To achieve these objectives, first, the geographical and the geological settings of the Shai Hill suture zone rocks are described relative to the regional context. This is followed by a stepwise presentation of results from this study. The results and their interpretations are treated in detail to finally arrive at conclusions, where a geodynamic model for the Shai Hills suture zone is proposed.

1.3 Project Area

The Shai Hills area is located in the Dangme West District of the Greater Accra Region Ghana. It is bounded by the coordinates (0°01'E, 5° 56' N) (0° 06'E, 5° 56'N), (0° 01'E, 5° 50'N) and (0°, 06'E, 5° 50'N). It is within the field sheet number 0500A1. It has an approximate area of about 60km^2. The Shai Hills area is a hub of several stone quarries which generate huge revenue for Ghana through taxes.

University of Ghana http://ugspace.ug.edu.gh

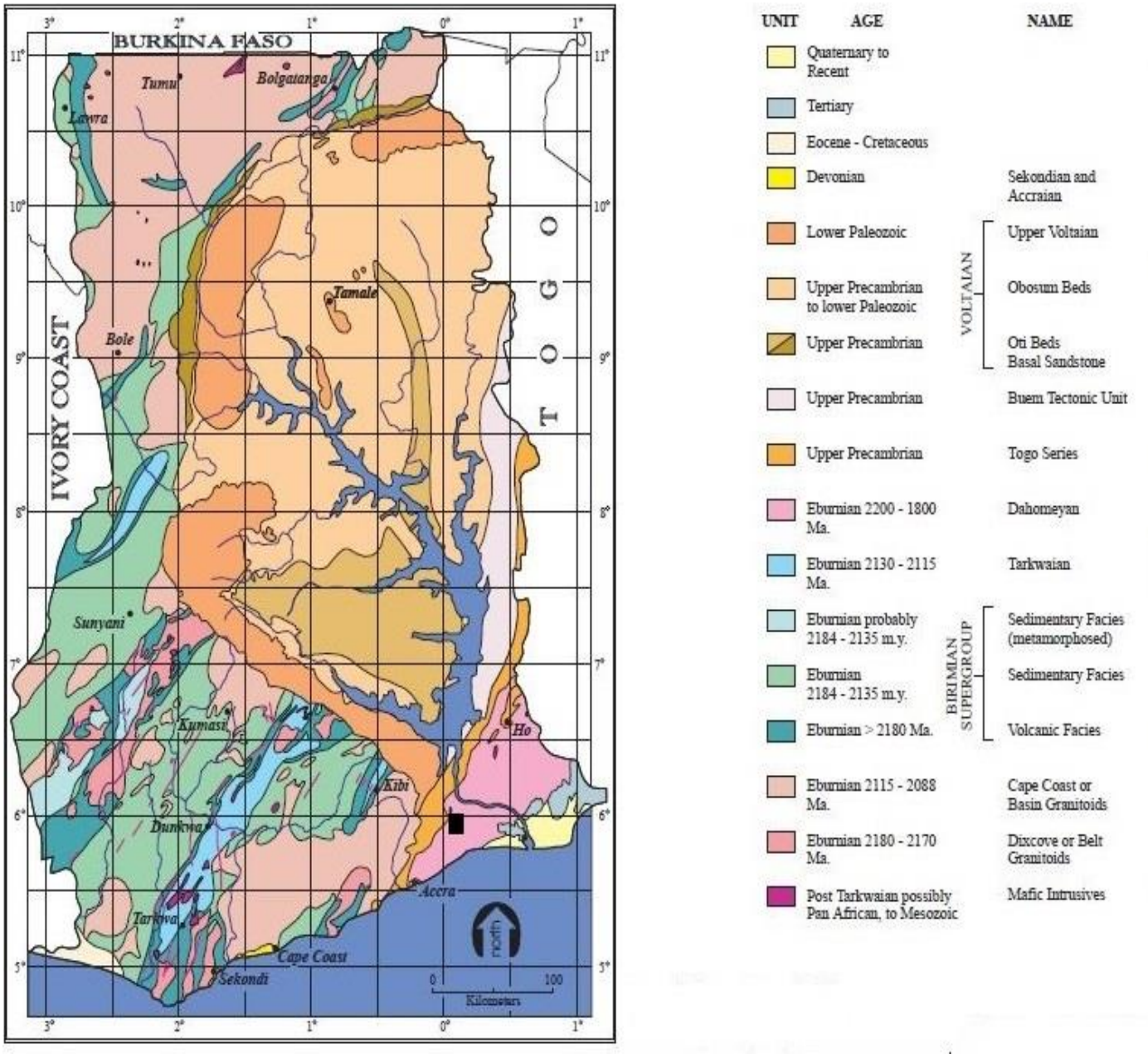

Figure 1.1: Geological map of Ghana with the study area shown by the black rectangle. (Compiled from Bates (1995), Hasting (1982), Davis, et. al (1994))

University of Ghana http://ugspace.ug.edu.gh

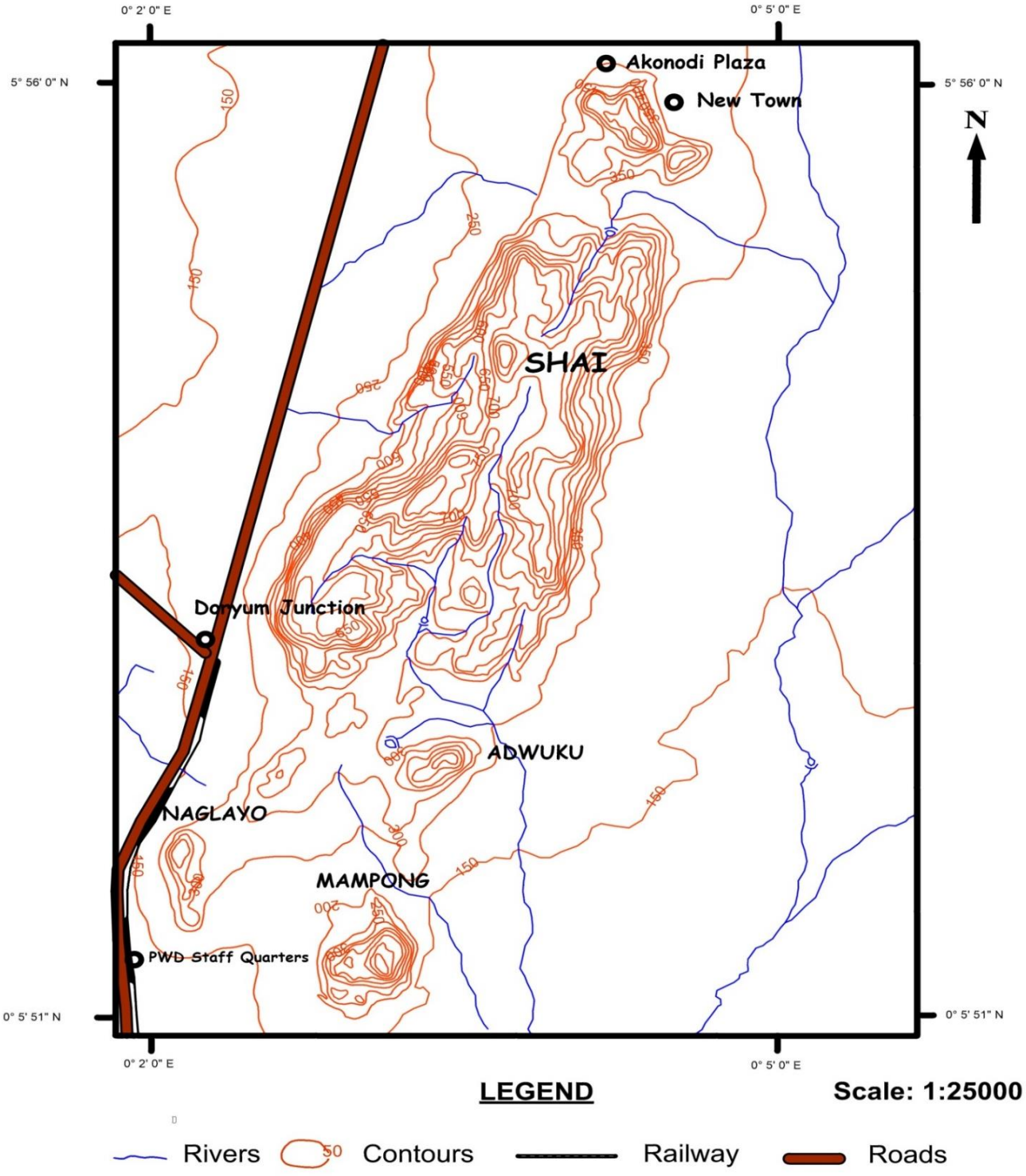

Figure 1.2: Topographical Map of the study area.

University of Ghana http://ugspace.ug.edu.gh

1.3.1 Accessibility

The study area can be accessed by road through the Tema – Akosombo highway. Notable towns are Dzopaanya, Dedenya, Mampong and Kissehkope and surrounding areas. The Tema to Ho road is a first class road which passes through the study area at the Southwestern corner through the study area to the northeastern part. It has also other roads footpaths leading to various villages in the study area. Through the footpaths and roads, the field mapping exercise was successful.

1.3.2 Physical Features

The study area is a SW-NE trending range of hills and inselbergs which are the most obvious physical feature on the base map. The Shai Hills vary in width from 65 to 95 km. Waterways and dams are also conspicuous physical features in the area. The waterways flow in the valleys between the rocks and join others to form dams.

1.3.3 Climate

The study falls within the wet semi equatorial climatic region (Dickson and Benneh, 1988). The mean annual rainfall is between 125 and 200 cm. The rainfall pattern of the study area is of a double maxima type where two rainy seasons occur in a year. The first rainy season is from May to June and the second rainy season is from September to October. Heaviest rainfall mainly occurs in June. The mean annual temperature is 26.6^{o}C (Dickson and Benneh, 1988). Average relative humidity is about (75-80%) during the two rainy seasons and the lowest (70-80%) during the rest of the year (Dickson and Benneh, 1988).

University of Ghana http://ugspace.ug.edu.gh

1.3.4 Vegetation

The area of study has a low cover of vegetation cover but due to the Shai Hills forest reserve there is a quiet dense forest which is kept as a resource. The areas east of the Shai Hills and the north eastern part of the field of study have very low and thin vegetation which could be due to clayey nature of soil and are referred to as the lowlands. Some of the highland areas have thick and impenetrable vegetation. Vegetation, where it is present, forms an important part of the physical environment and helps greatly in the definition of the recourses and character of the area (Dickson and Benneh, 1988). The forest areas are mainly highlands and exhibit semi deciduous forest type during the long dry season from November to March. The lowland is mainly the Guinea savannah (Dickson and Benneh, 1988). They are covered by low bushes and open grassland (Dickson and Benneh, 1988). The principal soil is the forest ochrosols at the highlands. A soil that is highly coloured soil from highly weathered parent mafic or felsic materials. The soil at the lowlands is the lateritic sandy soil. The nature of the soils impedes downward drainage and causes waterlogging during the wet season (Dickson and Benneh, 1988). These hills are poorly covered with soil, and their slopes are mostly covered with gneiss debris. The area is covered with dark brownish-black silt and clayey soil (Mani, 1977).

1.3.5 Relief

The area has a relief system with the highlands running gently into the lowlands. Some of the low areas are wide valleys which are characterized by waterways and dams. The highlands run as stretches of hills from the NE-SW with the highest peak around 290m

University of Ghana http://ugspace.ug.edu.gh

above sea level. The highlands mostly occur as ridges and a few isolated hills. They mostly consist of gneissic rocks. The lowlands on the other hand occur just east of the area of study then downwards towards the south with the lowest altitude around 50m above sea level. The lowlands have relatively flat topography with quite a number of waterways running across in different directions but most of them are dried up.

1.3.6 Settlement, Population and Occupation

The study area is sparsely populated when compared to urban cities. Major towns and communities include Doryumu, Dzopaanya, Dedenya and Mampong. The people of these communities speak the Krobo language and Ga-Adangme. There also some Fulanis herdsmen who live in the study areas with a main occupation of cattle farming. The people in the semi-urban areas live in modern semi-detached homes while the people in the smaller communities live in mud houses and wooden buildings. The major occupations of the people in these communities are farming, cattle rearing and trading. Stone quarrying is also an occupation of the inhabitants.

1.4 Structure of the Thesis

The Thesis work has six (6) chapters with each chapter addressing a main heading. Chapter one introduces the field of research. It also deals with the location, and socioeconomic activities of the research area. The objectives, importance and the problems the research seeks to address are also mentioned. Chapter two gives a general overview of the national and local geological setting of the study area. This chapter also deals with the major types of formations found in Ghana. Chapter three deals with the materials and the methods used in

University of Ghana http://ugspace.ug.edu.gh

collecting and analyzing data. Chapter four and five presents the results obtained and discusses the results presented in the various maps obtained. Chapter six presents conclusions from the study.

University of Ghana http://ugspace.ug.edu.gh

CHAPTER TWO

2.0 REGIONAL GEOLOGY AND GEOLOGICAL SETTING

The assembly of NW Gondwana from various cratonic fragments postulated to be derived from the breakup of Rodinia supercontinent (Hoffman 1991) resulted in Pan-African (Neoproterozoic) orogens including the 2000 km long Trans-Saharan orogen (Caby 1987; Trompette, 1994) located on the eastern margin of the West African craton (WAC). The southeastern segment of the Trans-Saharan belt exposed in southeastern Ghana and adjoining parts of Togo and Benin comprises the Dahomeyide orogen (Affaton et al.1991; Castaing et al. 1993; Attoh et al. 1997).

According to Attoh et al. (1997), the principal tectonic elements of the Dahomeyide orogen are:

(1) the deformed edge of the West African craton (WAC) with its cover rocks consisting of craton verging nappes and thrust sheets bounded by ductile shear zones that is the external units made of up the Buem structural unit, The Togo structural unit and the Kara gneisses.

(2) the suture zone representing the eastern boundary of the autochthonous West African Craton (WAC).

(3) exotic rocks that form the granitoid gneiss complexes east of the suture zone. That is the internal units.

The Pan-African Dahomeyide orogen in West Africa is interpreted to have formed by the collision of exotic blocks with the passive continental margin of the West African craton

University of Ghana http://ugspace.ug.edu.gh

(Caby, 1987; Affaton et al., 1991; Agbossoumonde et al., 2004; Attoh and Morgan, 2004). The western zone is the external nappes domain, which corresponds to the Buem and Togo/Atacora monocyclic metasedimentary units. The eastern zone is the internal units nappes domain that formed the composite basement of the Benin Nigeria Shield (Nude et al., 2009). Intermediate nappes domain is a narrow and structurally complicated zone called the Suture zone which is made up of ultramafic to mafic rocks together with high grade metasediment (Nude et al., 2009).

The terrane is a convergence tectonic closure and sutured collision boundary zone that occurs along the easten margin of the West African Craton. It trends inland northeast-wards from the Gulf of Guinea through southeastern Ghana, the Republics of Togo and Burkina Faso to Mali (Kutu et al., 2014).

2.1 Buem Structural Units

The Buem consists of two lithologic assemblages, volcanic and sedimentary. The volcanic assemblage is made up of pillow basalt, agglomerate, hawaiite and trachyte. The sedimentary assemblage, which encloses the volcanics, consists of red shales, feldspathic to quartz arenite, conglomerate, tillite, jasper and minor limestone. Whereas the volcanics were deposited in a submarine environment, the sediments appear to be shallow water to subaerial in origin (Jones, 1990). Kesse (1985) states that the rocks are strongly folded whiles Jones (1990) describes the Buem as an eastward dipping homoclinal sequence.

University of Ghana http://ugspace.ug.edu.gh

2.2 Togo Structural Unit

The Togo Structural Unit is found to the east of the Buem unit. The north east trending Togo or Akwapimian hills trend from west of Accra to the Republic of Togo and Benin. According to Kesse (1985), Togo unit can be divided into two:

I. Togo units of the main Akwapim, Awudome-Amedzofe range.

II. Togo units with Dahomeyan on both margins.

The main Akwapim, Awudome-Amedzofe range further consists of:

I. interbedded schists and phyllites, usually sericitic or chlorite schist making the upper schist.

II. massive quartzites, chert, quartz schists forming the upper quartzite units.

III. interbedded schists and phyllites usually sericitic or chloritic, locally conglomerate forming the lower schist.

The western margin of the Akwapimian range consist of quartz schists, quartz sericite schist and locally massive quartzites. Togo units are being surrounded by Dahomeyan units. These are eastern scarps and considered as outliers. They are found in Abutia, Kabakaba, Kluma hills, Ziavi and those north east up to Kpedze. They are made up of phyllites, flaggy and cataclastic quartzites marked by folding, cross faulting and shearing and generally well foliated. Quartzites are dominant in the south but phyllites are prominent towards the north (Kesse, 1985). They display penetrative structures in the quartzites and quartz mica schists with prominent lineation typified by fold rocks. Recumbent folds with rotated hinges to the north and south south-east indicates transport directions (Kesse, 1985).

University of Ghana http://ugspace.ug.edu.gh

The geology of the Togo unit has been described by Kitson (1928) and Junner (1940). The main lithologies within the Togo unit are quartzites, schists, phyllites and phyllonites. Minor amounts of shale and siliceous limestone occur within the Togo unit. Often rocks in the thrust zones are strongly sheared resulting in brecciation as well as flattening of quartz grains and mylonitization.

Generally, the quartzites and the phyllites within the Togo unit are intensely deformed, and mostly occur as craton verging recumbent folds with regionally pervasive sub-horizontal foliation. Regarding the age of the Togo unit, Attoh et al. (1997) reported $^{40}Ar/^{39}Ar$ dates from muscovite in the quartzites in Ghana to be 579.4 ± 0.8 Ma.

2.3 Dahomeyan Structural Unit

The Dahomeyan structural unit of southeastern Ghana belongs to the Pan-African terrain, also called the Dahomeyides (Bessoles and Trompette, 1980; Attoh, 1990). The geology of the area has been described by Holm (1974), and Kesse (1985). These workers described the Dahomeyan in Ghana as consisting generally of two belts of felsic gneiss that alternate with two belts of mafic gneiss. These belts are up to 30 km wide and can be traced from Fete in the west of Accra to Agu in the Republic of Togo and beyond. The regional strike is northeast with moderate dips to the southeast. Others such as Grant (1969) and Holm (1974) considered the Dahomeyan as a reworked Archean basement of the late Precambrian Pan-African orogen and having records of polycyclic deformation.

University of Ghana http://ugspace.ug.edu.gh

Recent works by Attoh (1990, 1998); Attoh et al. (1991, and 1997) and Agbossoumonde et al. (2004) consider the Dahomeyan structural unit as consisting of various structural units based on age and tectonics. The principal litho-tectonic units identified are:

(i) quartzo-feldspathic and augen-gneisses referred to locally as the Ho gneisses

(ii) a suture zone of distinct mafic and ultramafic rocks, and

(iii) a granitoid gneiss-migmatite assemblages east of the suture zone.

The Ho gneisses represent the deformed edge of the West African Craton and includes augen gneisses and mylonitic gneisses most of which are hornblende-rich and often sheared and at some localities (Attoh et al., 1996). Doleritic and dioritic intrusives are common along contact zones with the Togo cover rocks and may represent late stage magmatism associated with the Pan- African orogen. The Ho gneiss recorded ages of 2176 ± 44 Ma on whole rock Rb-Sr isochron (Agyei et al., 1986).

The suture zone, east of the Ho gneisses and marks the boundary between the autochthonous West African Craton and the exotic rocks of the Dahomeyan lithotectonic units. Rocks of the suture zone are high pressure granulite and eclogite facies assemblages of garnet-hornblende-pyroxene gneiss referred to locally as Shai-Hills gneiss, in addition to pyroxenites and metanorites (Attoh and Nude 2008). U-Pb analyses of zircon from the high pressure granulites gave an age of 610 ± 2 Ma (Attoh et al., 1991) which was interpreted as the time of peak granulite metamorphism. In southeastern Ghana, the HP mafic granulites have been referred to as Shai Hills gneiss (Attoh et al., 1997), and are tectonically juxtaposed with the alkaline gneiss complex in the suture zone (Attoh and Nude 2008).

University of Ghana http://ugspace.ug.edu.gh

Hirdes and Davis (2002) reported U-Pb analyses of zircon from the same high pressure garnet granulite unit, the youngest age recorded their analysis is 603 ± 5 Ma which is close to the time of peak metamorphism. Similar age of 613 ± 1 Ma from zircon Evaporation ($^{207}Pb/^{206}Pb$) was published by Affaton et al. (2000) for the suture zone rocks in northern Togo. Hornblende separates from the mafic granulites yielded $^{40}Ar/^{39}Ar$ ages between 587 and 567 Ma, interpreted as the time of exhumation of the nappes (Attoh et al., 1997). Taken together, these ages confirm high pressure metamorphism of the suture zone rocks around 603-613 Ma and exhumation through the hornblende ages around 580-570 Ma (Attoh et al., 2007).

To the coterminous east of the Shai Hills and in tectonic contact with the suture zone rocks are felsic gneisses and migmatites (Attoh et al., 1996). K-Ar dates from biotite in the migmatite gave an age of 452-506 Ma (Agyei et al., 1986). It thus appears that migmatization in this area may have been associated with the late stages of the Pan-African orogen.

University of Ghana http://ugspace.ug.edu.gh

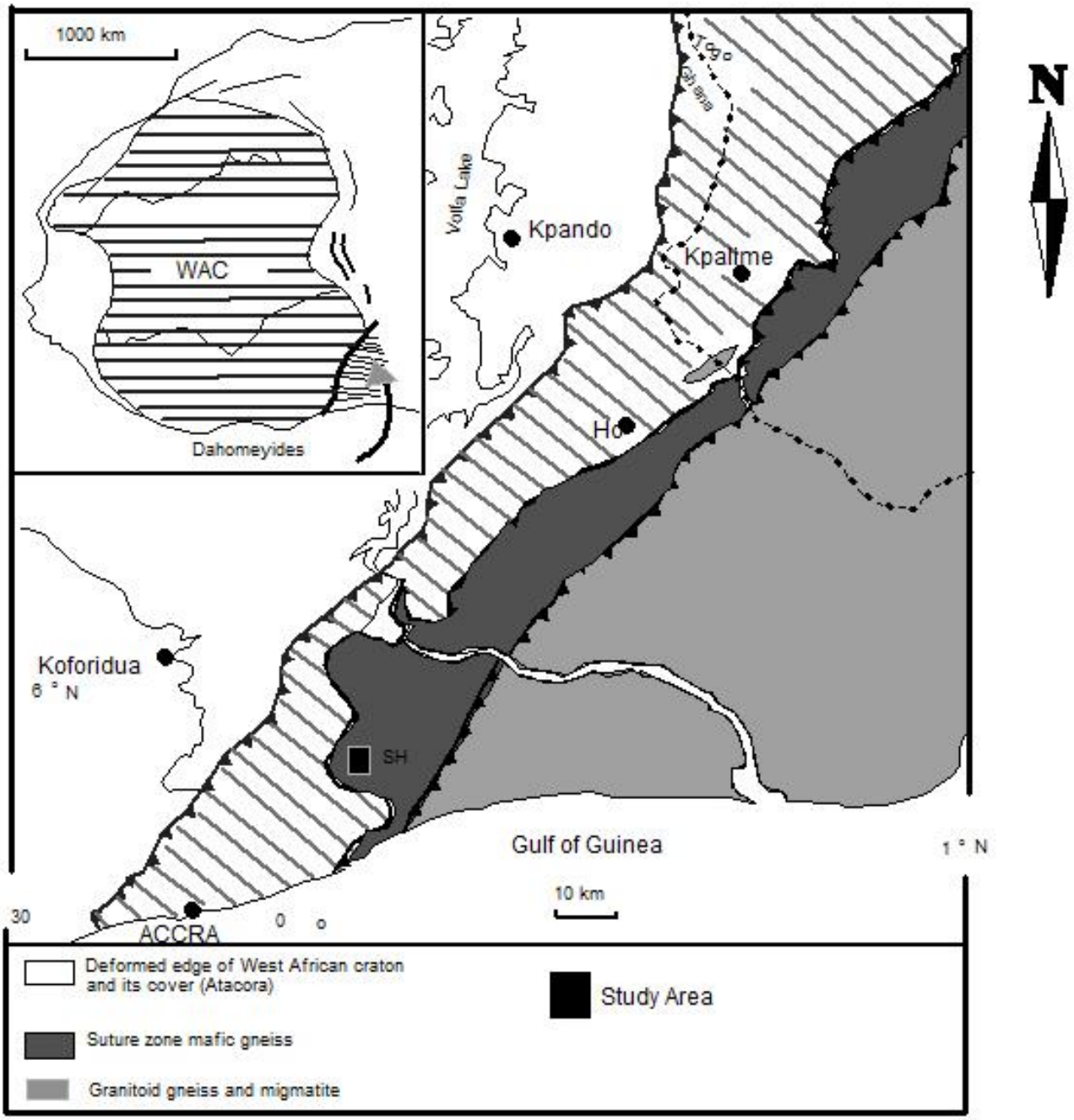

Figure 2.1: Tectonic map of the Dahomeyides of southeastern Ghana (after Attoh, 1998) showing the location of the study area.

University of Ghana http://ugspace.ug.edu.gh

2.4 Previous Work

Previous work has been done extensively by Knorring and Kennedy (1958), Attoh and Morgan (2004), Attoh and Nude (2008) and Kutu et. al., (2014). According to Attoh and Nude (2008), the association of carbonatite and ultrahigh-pressure (UHP) metamorphic rocks in the Dahomeyide suture zone of southeastern Ghana is unique among the Neoproterozoic orogens that surround the West African craton (WAC). Carbonatite occurs in an alkaline complex that decorates the sole thrust of the suture zone and is characterized by high concentrations of incompatible trace elements such as light rare earth elements (LREE), Sr and Ba.

Within the suture zone deformed alkaline rocks, including carbonatites, together with mafic granulites form an imbricate stack of thrust panels that involve 2.1 Ga rocks of the West African Craton (WAC) basement (Attoh and Nude, 2008). The dominant rocks units of the suture zone are mafic granulites in which garnet megacrysts preserve a diagnostic microstructure of Ultra High Pressure (UHP) metamorphism; consisting of a crystallographically controlled array of exsolved rutile rods in garnet. Metamorphic Pressures estimated from Ti concentrations in the inferred precursor garnet indicate pressure greater than 3 GPa, which requires subduction (and exhumation) of the suture zone rocks to and from mantle depths during collisional orogeny on the West African Craton (WAC) margin. Available age constraints on carbonatite magmatism suggest that continental rifting, leading to the formation of the passive West African Craton (WAC) margin c. 700 Ma, occurred c. 100 Ma before intrusion of carbonatite, which was preceded by HP and UHP metamorphism at 610+5 Ma (Attoh and Nude, 2008).

University of Ghana http://ugspace.ug.edu.gh

According to Kutu et al. (2014), the two most abundant and prominent rocks present in the suture zone are the mafic garnet gneiss and amphibolite. These rocks are associated with minor occurrences of dolerite, nepheline gneiss, carbonitite, alkali gneiss, quartzite and quartz muscovite schist with metamorphic grade ranging from amphibolite to granulite facies. The mafic garnet gneisses are strongly sheared deformed and recrystallized with mafic garnet gneiss doubly metamorphosed, well consolidated and competent (Kutu et al., 2014).

According to Kutu et. al. (2014), the amphibolite is characterized by tremolite actinolite amphiboles, plagioclase feldspar and minor quartz and iron oxides. The garnet gneiss is also characterized by quartz, feldspars, hornblende, hypersthene-dominated pyroxenes, pyrope-almandine garnets some with rutile inclusions, minor micas and scapolite. Deformation of the terrane and rocks was intense, and by compressional thrusting and shearing. The direction of tectonic transport from southeast to northwest in a craton-ward vergence on subparallel thrust planes (Kutu et al., 2014).

The amphibolite and garnet gneiss have undergone temperature and pressure changes in the solid state, and transformed from the parent igneous basaltic protolith into the metamorphosed and deformed amphibolite and polymetamorphosed garnet gneiss respectively. The metamorphic grade ranges from amphibolite to granulite facies. The terrane has undergone at least two phases of metamorphism, from the amphibolite facies change from basalt to amphibolite and granulite facies change from the amphibolite to the hornblende-garnet gneiss (Kutu et al, 2014).

University of Ghana http://ugspace.ug.edu.gh

According to Tairou and Affaton (2012), the suture zone includes rock types indicating Pan-African crustal thickening and comprising various granulites, pyroxenites and eclogitoids, associated with their heteromorphic equivalents and rare chromitites and metasediments. The Pan-African tectogenesis is composed of five phases defined as Dn, Dn + 1, Dn + 2, Dn + 3 and Dn + 4 (Tairou and Affaton, 2012). The Dn phase corresponds to the long process culminating in the collision between the active eastern margin, or the Benino-Nigerian plate, and the passive Western margin belonging to the West-African Craton. This collisional episode is materialized by a Sn foliation that is obliterated by the subsequent phases in the polycyclic basement and suture zone nappes with the Dn + 1 phase represents the main episode in Dahomeyide structuring leading to nappe and slice individualization and their west stacking. This tangential phase is materialized by the Sn + 1 regional foliation and by mineral or stretching Ln + 1 lineation. The Dn + 2 to Dn + 4 post nappe episodes successively rework the Sn + 1 foliation. They resulted in Pn + 2 folds, with submeridian to NE-SW axes, Pn + 3 antiforms and synforms, with NE-SW axes, and Pn + 4 virgations, with NE-SW to ENE-WSW axes (Tairou and Affaton, 2012).

The overall structure of the suture zone is interpreted to have resulted from early east–west compression, which produced the north–south imbricate thrust slices followed by NNW-directed thrusting in the orogen (Attoh et al., 1997).

University of Ghana http://ugspace.ug.edu.gh

CHAPTER THREE

3.0 METHODOLOGY

The research was carried out in three main stages were employed: The Pre field stage, field stage and then post field stage. Samples were taken from rock exposures and from outcrops for petrographic and structural studies, thin sections prepared at the Earth Science Department, University of Ghana were examined using a Petrological microscope.

3.1 Desk Study and Literature Survey

The base map of the study area was first acquired and the coordinates were located on the geological map of Ghana to know the precise geological terrene which it is located. A literature searches to know the formations in the study area which included information on petrology, mineralogy, structures and field relationship and general geology standard text was carried out. This provided the necessary background knowledge that would facilitate field investigation. Literature review actually lasted throughout the whole period of this research.

The stage involved reviewing of previous literature on the area, conducting of research about the general geography and previous work in the study area. An important exercise carried during the desk study was the reproduction of the topographical base map of the area by enlargement. The enlargement of 1:25000 was done from the original topographic maps with sheet numbers 0500A1 and map scale of 1: 50000 obtained from the Ghana Survey Department.

University of Ghana http://ugspace.ug.edu.gh

3.2 Tools and Equipment

Standard geological field tools were used during the mapping exercise. Among these tools was a standard geological compass and Global positioning system (GPS) which was mainly used for finding direction, self-location and self-orientations and the measurement of attitudes of structures. Other tools used include geological hammer for breaking and chipping rocks, tape measure for taking measurement of outcrops, digital camera for taking pictures of outcrops, cutlass for creating paths in inaccessible areas and for clearing weeds around hidden outcrops, and a geological field gear including a pair of safety boots for ensuring safety in the field.

3.3 Field Methods and Sampling

Several field methods were used during the entire period of mapping. Field methods such as a reconnaissance survey, setting up a base camp, choosing of relevant reference points, self-location, self-orientation, self-positioning, Global positioning system (GPS) -and-compass traversing, outcrop description and sampling were all carried out to facilitate a smooth and successful mapping of the study area.

Fresh, representative and orientated rock samples were taken from the field and to the laboratory for subsequent analyses (i.e., petrographic and geochemical analyses). The samples from the field were further sorted, grouped and carefully selected for thin section preparations

University of Ghana http://ugspace.ug.edu.gh

3.3.1 Reconnaissance Survey

On the field, a reconnaissance survey was conducted early in the study area especially in places close to the base camp in order to become fairly acquainted with the area. This exercise was done in two days. During the exercise I walked in and around the community in which the base camp was located observing the general topography, climate and vegetation. I also familiarized myself with local people to inform them about my mission in their locality; by this, vital information was obtained about the accessibility and cultural practices of the area.

3.3.2 Mapping Procedures

The main mapping procedures constitute the major part of the whole field work. The mapping procedures used included the Global positioning system (GPS)-and-Compass traversing technique, outcrop description techniques and plotting of field data. However, since the geological compass was used in almost all the mapping procedures it had to be first corrected to produce accurate.

3.3.2.1 Compass Correction

The geological compass used for the survey was corrected using the required compass correction information provided on the topographic base map of the area. This information included the magnetic declination data which includes the value of the deviation of the magnetic north from the grid north and the value of the annual declination as well as the date of production of the map. With this information the magnetic declination of the area with

University of Ghana http://ugspace.ug.edu.gh

respect to the base map was calculated and the compass was thus corrected accordingly by shifting the adjusting screw. The geological compass was adjusted to align the magnetic north with the grid north to ensure accuracy.

3.3.2.2 Traversing

The main survey method used on the field was the Global positioning system (GPS) and Compass traversing method. With the help of the base map, GPS and corrected geological compass I established suitable reference points in each of the divisions. In each of the divisions systematic traversing was done to locate and identify rock outcrops. With the help of the base map, the GPS and compass as the primary guide, I traversed the study area using all the available accessible routes. However, in the places where there were no accessible routes to potential outcrop locations, paths were created with the help of the cutlasses. Traversing was mostly done along footpaths, road cuts and river channels, and often in closed loops across strike from a known location towards a prominent feature along a particular bearing. The geological compass was used to find the bearing any time there was a change in direction during the traversing.

3.3.2.3 Outcrop description techniques.

At every outcrop site or station, standard petrographic field description techniques were used to describe and classify the rocks. The dimensions of mesoscopic outcrops were taken with the help of the tape measure. Attitudes of structures including the strike and dip of foliations and joints were measured with compass, whilst the hammer was used to chip of oriented samples for further petrographical analyses. These samples were labeled and the measured

University of Ghana http://ugspace.ug.edu.gh

attitude values written on them where necessary. Large enough representative samples were taken of the rocks to cover mineralogical and structural features of the outcrops; mostly they were about 5 Kg. All measurements were recorded in the field notebook at the outcrop station before proceeding to new outcrops. This was done to ensure the authenticity and reliability of the data taken from the field. Sketches of spectacular features of the outcrops were also made in the field notebooks, whilst the cameras were used to take photographs of other vital features of the outcrops.

3.3.2.4 Data Plotting

After every field session, the data collected were adequately reviewed, analyzed and plotted on the appropriate overlays. The field traversing data were plotted on the traverse map, the outcrop data on the outcrop map and structural data were plotted on the structural map. The labels and the characteristics of the samples obtained were also compared with what were recorded in the notebooks to ensure accuracy and consistency.

3.4 Post Field Procedures

Post field procedures involved preparations of rocks samples for further petrological and microstructural analysis as well as the analysis of field data and further plotting and geochemical analysis on the sample taken.

University of Ghana http://ugspace.ug.edu.gh

3.4.1 Thin section Preparation

Thin sections were prepared from thirty-Five (35) selected rock samples at the Earth Science Department, University of Ghana. The selected samples were first cut into thin slices of about 3 mm thick. Samples that were not hard enough to provide the required slices were impregnated with cohesive cement to harden them before they were cut. Cutting was mostly done across mineral grains in order to obtain enough information from the thin sections. For each rock sample at least two slices were cut, in order to obtain two thin sections from each sample. Next, the surfaces of the rock slices were polished with abrasives and mounted on thin wet glass surfaces. One side of the glass slides was also polished to obtain a smooth surface before the mounting was carried out. The surface was cleaned and made perfectly flat and free of grooves and pits. A thin layer of Canada balsam was spread over the surface of the rock slice and the glass slide and evaporated to a preferred hardness. Rock slice and glass slide were removed quickly and the balsam coated surfaces were put in contact. The slice and slide were pressed together to remove bubbles and allow the mount to cool. Thickness of the thin section made was 0.03 mm.

The rock texture in the prepared thin sections was studied under the petrographic microscope. Photomicrographs were taken of the minerals and micro-structures in the thin section. Through thin section analyses invisible minerals in hand specimen were identified and quantitative measurements of percentage mineral content were made usingpoint counting. Rocks names were assigned to the rock samples based on hand specimen and petrographic results.

University of Ghana http://ugspace.ug.edu.gh

3.4.2 Geochemical Analysis

Based on the results from the petrographic study, twenty-five (25) fresh, relatively unaltered and representative samples were selected and sent to the ALS laboratory, Vancouver-Canada for their whole rock major and trace elements (including REEs) analyses. Major and trace elements analyses were carried out by inductively coupled plasma atomic emission spectrometry (ICP-AES) and multi elements fusion inductively coupled plasma mass spectrometry (ICP-MS) respectively. Loss of ignition was determined at 1000 ^{0}C. For the major elements analyses, a mixture of about 0.200g of prepared sample and lithium metaborate was fused in a furnace at 1025^{0}C. The resulted melt was then cooled and dissolved in an acid mixture. The acid mixture contained nitric, hydrochloric and hydrofluoric acids. The solution was then analysed by ICP-AES for the major element composition. The trace element analyses were performed observing the protocols as done for the major element analyses. However, here the prepared sample weighed 0.100 g and the analysis was done by the ICP-MS. The base metals were analysed using ICP-AES. A 0.25 g prepared sample was digested with perchloric, nitric, hydrochloric and hydrofluoric acids. Dilute hydrochloric acid was then added to the residue and the solution was analysed by the ICP-AES. Results obtained were corrected for spectral interferences (ALS laboratory). Precision is better than 2%.

University of Ghana http://ugspace.ug.edu.gh

3.4.3 Map Digitization, Stereographic projections and Cross Section Drawing.

The various maps obtained from the field were digitized with computer software (e.g. Map Info and Arc GIS). This was done in order to help in the construction of a composite geological map of the area. With the complete geological map of the area a cross-section was drawn through all the lithologies showing their distribution and relationships with the various geological structures. Stereographic plots were made using the Stereopro to determine the general behavior of structures in the area.

University of Ghana http://ugspace.ug.edu.gh

CHAPTER FOUR

4.0 RESULTS

4.1 Field Relation and Petrography

Outcrops within the study area were mainly mafic garnet gneisses with NE strike and gentle dip to the east. The rocks appear to have experienced intense deformation and shearing.

The mafic garnet gneisses (Fig 4.1) are divided into pyroxene garnet gneisses and garnet hornblende gneisses based on their mineral compositions. The pyroxene garnet gneisses are the most dominant. The pyroxene garnet gneisses outcrop mainly in the Naglayo Hill and Shai forest reserve area. The hornblende garnet gneisses outcrop mainly at the Mawum and Eastern quarries at the Mampong Hill.

These mafic garnet gneisses are associated with pyroxenite, pyroxene bearing amphibolites and a fault rock. The pyroxenite occurs as older materials thrusted within mafic garnet gneisses. They are observed throughout the hills in the study area. Some form boudins within the gneisses. A fault rock was found within a fault at the PW Quarries in the Naglayo hill. The pyroxene bearing amphibolite was observed at the Eastern Quarries at the Mampong Hill. They are tectonically welded within the mafic garnet gneisses.

University of Ghana http://ugspace.ug.edu.gh

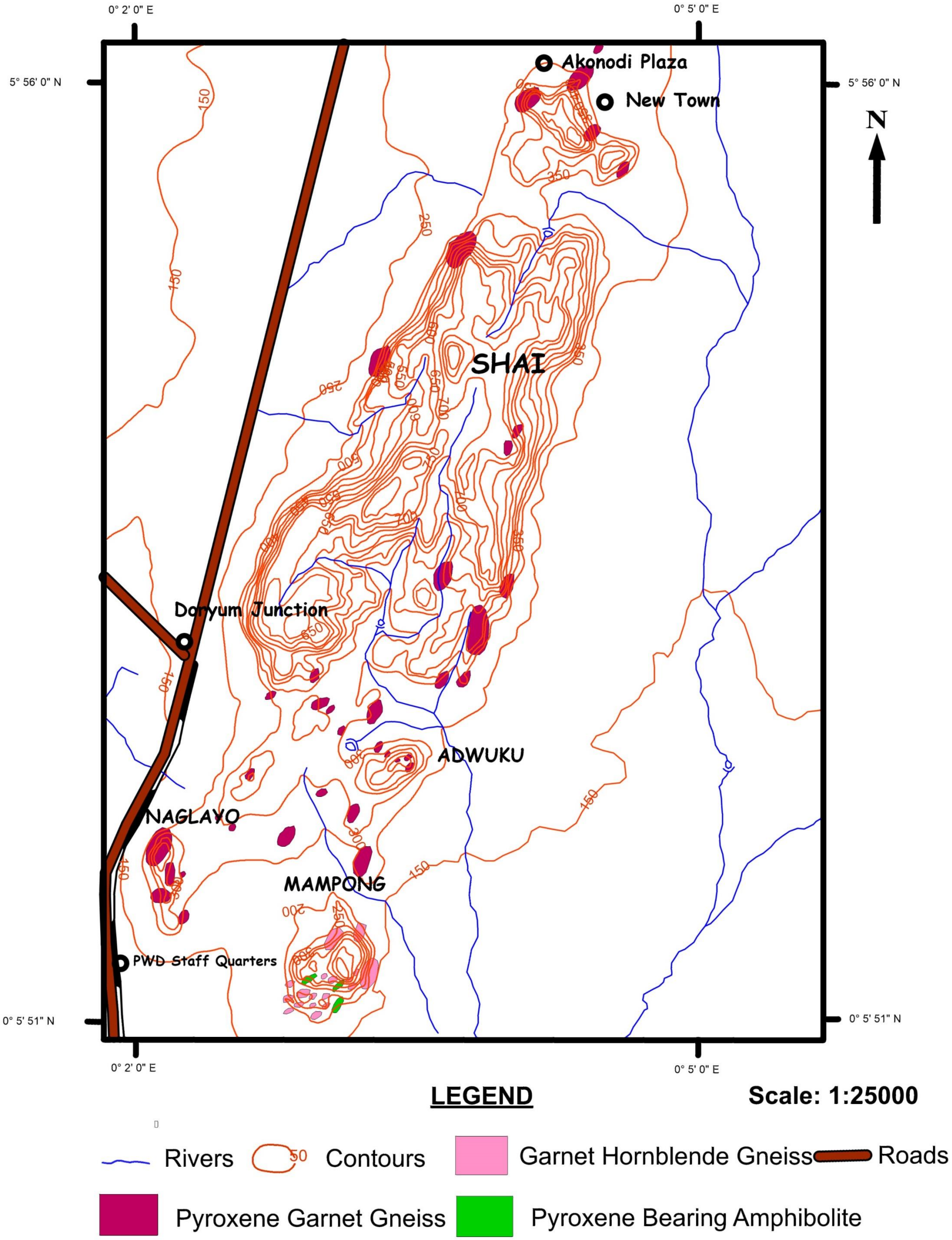

Figure 4.1: Outcrop map of the study Area.

University of Ghana http://ugspace.ug.edu.gh

4.1.1 Mafic Garnet Gneisses

The mafic garnet gneisses generally occur as inselbergs and scattered outcrops and represented the most dominant lithology across the study area. These inselbergs are the Mampong, Naglayo and the Shai Hills which are trending North-South. Several quarries in the study area provide access to fresh outcrops for detailed studies and sampling.

These mafic garnet gneisses are medium to coarse grained and are generally greyish, and sometimes reddish, with garnetiferous facies or true garnetites. The mafic gneisses exhibit gneissic banding. The rocks have alternating white and dark bands (Fig 4.2a). The garnet crystals are millimetric to centimetric and probably of several generations (Fig 4.2c). Their great abundance is the outstanding characteristic of these gneisses. The predominant minerals in these gneisses are amphiboles, quartz, plagioclase feldspar, pyroxenes, garnet and some opaque minerals. They contain shreds of pyroxenites and pyroxenite boudins. The mafic layers present in the rocks are rich in pyroxene and hornblende whilst the felsic layers are rich in feldspar and quartz. At some places, some garnet bands are observed in the mafic garnet gneisses.

University of Ghana http://ugspace.ug.edu.gh

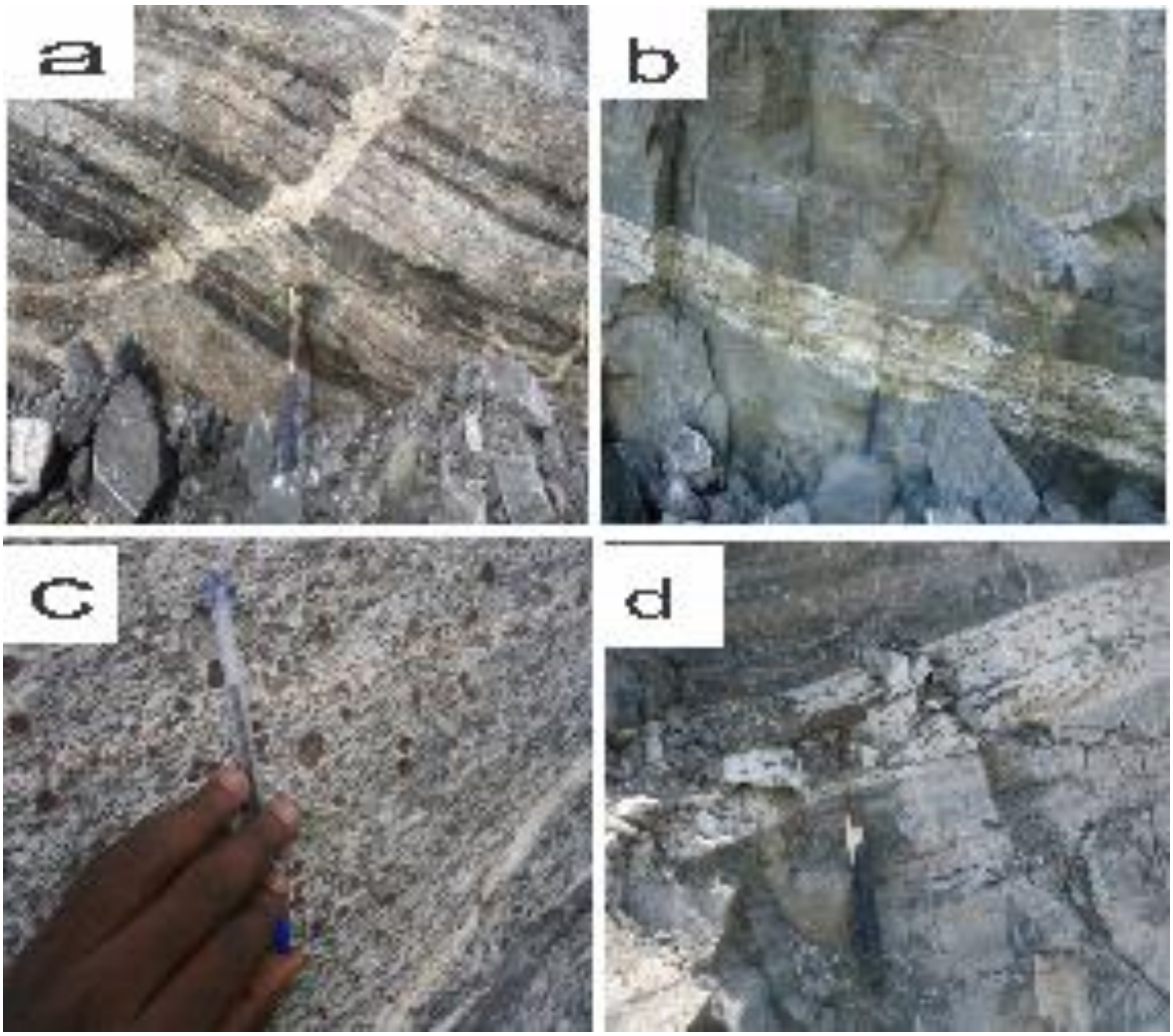

Figure 4.2: Field photographs showing (a) subhorizontal layers of mafic and felsic bands in mafic garnet gneiss; at Eastern Quarries, Mampong Hill (b) Compositional felsic bands in the mafic garnet gneiss at Mampong Hill (c) Porphyroblastic garnet of different sizes at PW Quarries, Naglayo Hills (d) Alternating bands of mafic, felsic and garnet bands in the mafic garnet gneiss at the West Coast Quarries, Naglayo Hills.

University of Ghana http://ugspace.ug.edu.gh

The rocks generally trend in the northeast-southwest direction. The mafic garnet gneisses are more strongly deformed, sheared and recrystallized. There are prominent discontinuous layerings which consist of garnet rich and hornblende-rich zones in some locality which give the rock a streaky appearance and are interpreted to be shear induced. The alternating parallel to sub-parallel dark and white (quartzo-feldspathic) layers or bands centimeters to meter thick are prominent in the area and well exposed as a results of the quarrying activities in the area. The white silica rich layers are made up of feldspars most predominantly plagioclase, quartz and hornblendes form compositional banding and together with and the mafic layers define the foliations S_1 planes.

The hornblende porphyroclasts within the compositional bands are well-developed and stretched into sigma and delta-type tails (Fig 4.3a). Some of the compositional bands are folded into ptygmatic folds (Fig 4.3c). These folded compositional bands occur in all sizes and orientations to the tectonic layering; some prominent once which attain a thickness of 0.5 m and together with the thin bands, which are only a few millimetres thick, are estimated to make up to 10% of the rock by volume (Burke, 1959). Pressure shadows are mostly observed around large garnet porphyroblasts (Fig 4.3d). Some of these garnet porphyroblasts are wrapped around by the S_1 external foliation. A halo of feldspar is mostly observed around large garnet porphyroblasts. In some localities, some of the pyroxenite layers are well sheared and stretched in the mafic garnet gneisses as a result of shearing (Fig 4.4a).

The Hornblende porphyroclasts with well-developed sigma and delta type tails within the thick bands, together with asymmetrical pressure shadows around garnet porphyroblasts and

University of Ghana http://ugspace.ug.edu.gh

sheared pyroxenite layer form spectacular sets of kinematic indicators. There are several brittle vertical to subvertical normal faults and fractures (Fig 4.4b). A fault rock comprising a 0.5–3.0 m thick zone of dark green, chlorite-rich breccia is observed at the PW Quarries (Fig 4.4c).

University of Ghana http://ugspace.ug.edu.gh

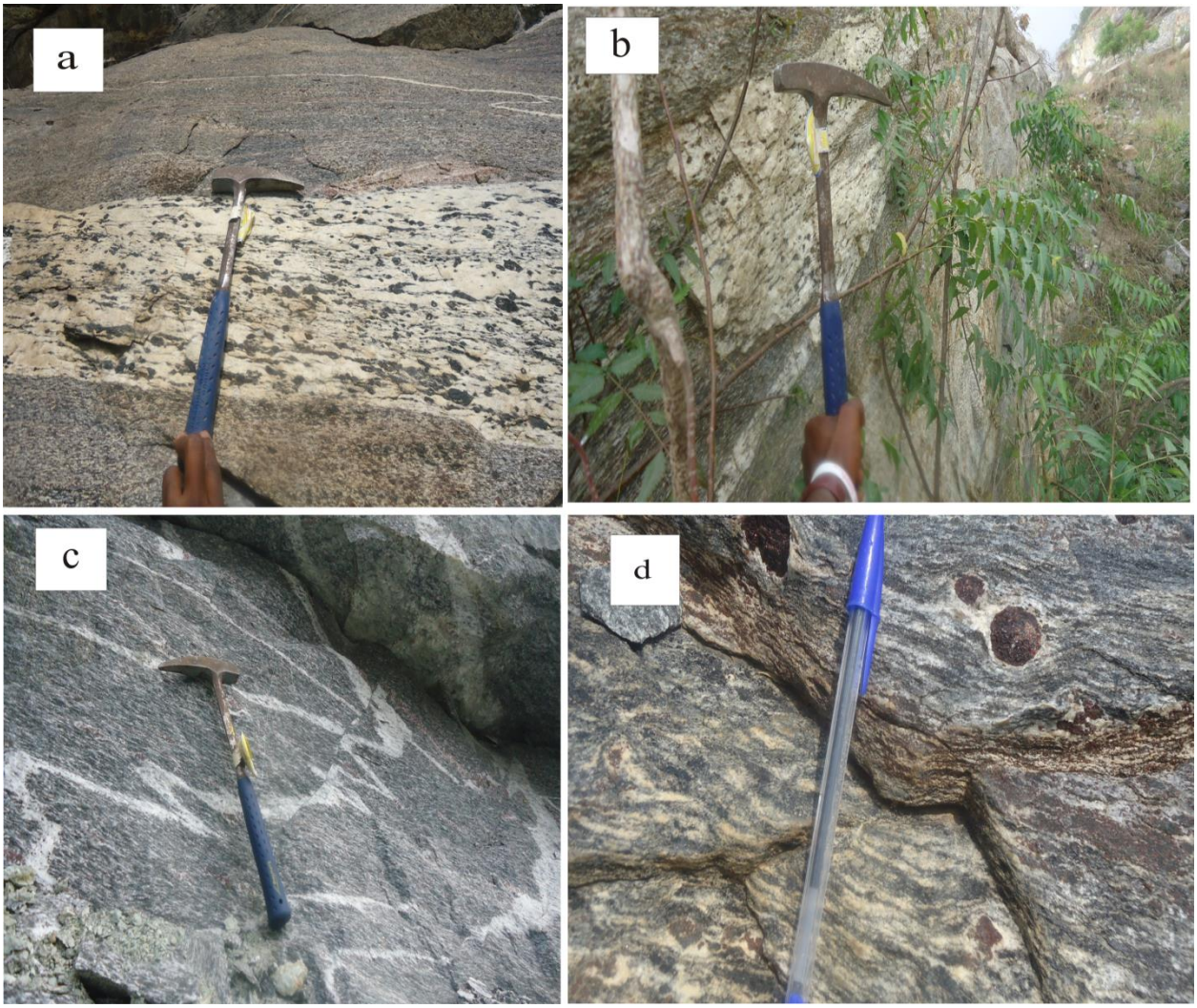

Figure 4.3: Field Photographs showing (a) compositional bands with stretched hornblendes (b) Compositional bands folded into ptygmatic fold (c) Ptygmatic folds (d) Pressure Shadow formed at the edges of porphyroblastic garnet minerals.

University of Ghana http://ugspace.ug.edu.gh

Figure 4.4: Field photographs showing (a) stretched pyroxenite within the mafic garnet gneisses at the Shai Hill Game Reserve (b) brittle fault at the PW Quarries; Naglayo Hill (c) brittle fault zone observed at PW Quarries at Naglayo Hill (d) Joints found at the Shai Hill game reserve.

University of Ghana http://ugspace.ug.edu.gh

Under the microscope, the mafic garnet gneisses are medium to coarse grained and show recrystallized texture. The minerals observed are mainly; garnet, pyroxene, plagioclase, hornblende, quartz, ilmenite and rutile. In these rocks, the porphyroblasts are represented by millimetric sections of garnet, and clinopyroxene clearly oriented in granoblastic to granonematoblastic groundmass of plagioclase and quartz (Fig 4.5a and b). The main facies of the mafic garnet gneisses include lenticular clinopyroxene porphyroblasts, garnet porphyroblast and plagioclase.

Clinopyroxene

The clinopyroxene minerals display deformed cleavage microfractures, undulose extinction and large rims or overgrowths of green hornblende (Fig 4.6). The clinopyroxenes under plane polarized light is pale green in colour, has low relief and shows subtle greenish pleochroism. The minerals are highly fractured and mostly appear broken. Some clinopyroxenes have inclusions of hornblende and ilmenite. Furthermore, some of the clinopyroxenes have rims of hornblende and some with rims of chlorite (Fig 4.6a). Inclusions of clinopyroxenes are observed in poikiloblastic euhedral garnet crystals (Fig 4.8b). A corona texture of clinopyroxene surrounds porphyroblastic garnet (Fig 4.8f). The clinopyroxene porphyroblasts are been wrapped by S_1 foliation.

Garnet

Garnets are abundant, both as tiny crystals scattered throughout and as larger porphyroblasts. The garnet porphyroblast vary in shape and size. Garnet grains have brownish absorption colors but goes dark with no extinction under crossed polars. The

University of Ghana http://ugspace.ug.edu.gh

shapes of the garnet are anhedral to euhedral. The garnet porphyroblasts mainly display sieve structure or poikiloblastic texture owing to the inclusions of hornblende, clinopyroxenes, ilmenite and rutile. This feature is very well displayed by the garnet porphyroblasts in the thin section (Fig 4.5d) and (Fig 4.8b).

Some of the garnet are highly deformed and are related to multiple posterior tectonic phases in the mafic garnet gneisses. According to the shape of the garnet, their relationship with the S_1 foliations and their inclusions, at least two generations of garnet can be defined. The first garnet is the pre kinematic garnet, followed by and syn to post kinematic garnets. The pre kinematic garnet type are most deformed and surrounded by the S_1 foliation (Fig 4.8a). Some have inclusions of hornblende and ilmenite. They are highly deformed, broken with anhedral shape. One of these garnets displays a corona texture around it. The syn kinematic garnet is the most abundant garnet in the mafic garnet gneisses. The syn kinematic garnets have inclusion of clinopyroxenes, hornblende, rutile and plagioclase (Fig 4.8b). The syn kinematic garnets are relatively less deformed and are most abundant in the mafic garnet gneisses and have euhedral to subhedral shapes. Some garnet megacrysts (diameter of about >1cm) contain rutile ex-solution rods (Fig 4.8c). Rutile ex-solution rods are lamellar or rod-like intergrowths of rutile arranged in a somewhat triangular pattern in garnet.

University of Ghana http://ugspace.ug.edu.gh

Plagioclase

Plagioclase and quartz constitute the leucocratic and granoblastic groundmass in these mafic garnet gneisses. The plagioclase is andesine plagioclase. Some of the plagioclase grains are more or less porphyroblast. They are deformed with bent twinning. They display polysynthetic flexural twins and spectacularly abnormal extinction (Fig 4.9b). Most of the plagioclases are associated with quartz materializing the S_1 foliations. The plagioclases are colourless, show low relief and exhibit polysynthetic twinning.

Quartz

The quartz crystals are colorless under plane polarized light and lack cleavages. They show sutured boundaries, exhibit undulose extinction and are associated with plagioclase forming granoblastic textures. The quartz crystals often define the gneissic banding (S_1).

Hornblende

Hornblende under plane polarized light is distinctly coloured and display strong yellowish to greenish pleochroism. However, it assumes a dark greenish brown color. Some hornblende shows cleavage in two directions typical of amphibole cleavage of $120^0/60^o$ intersection. Hornblende crystals observed are mostly anhedral. Inclusions of the hornblendes occur in the garnet porphyroblast (Fig 4.5c). Some of the hornblende form rims around pyroxenes and garnet (Fig 4.6). Some dark reddish brown hornblende is well represented in S_1 foliation and defines the L_1 mineral lineations (Fig 4.9a).

University of Ghana http://ugspace.ug.edu.gh

Chlorite and Epidote

Fibrous pale green chlorites also occur in the mafic garnet gneisses around some clinopyroxenes and garnets porphyroblast. Also some plagioclase minerals seem to alter into epidote which exhibit faint yellow taint under plane polars.

Accessory Minerals

Ilmenite occurs quite frequently as xenomorphic clusters or opaque inclusions garnet porphyroblasts. Rutiles also occur as exsolution rods in the garnet porphroblast (Fig 4.8c). Ilmenite and rutile occur as accessory minerals in these rocks.

University of Ghana http://ugspace.ug.edu.gh

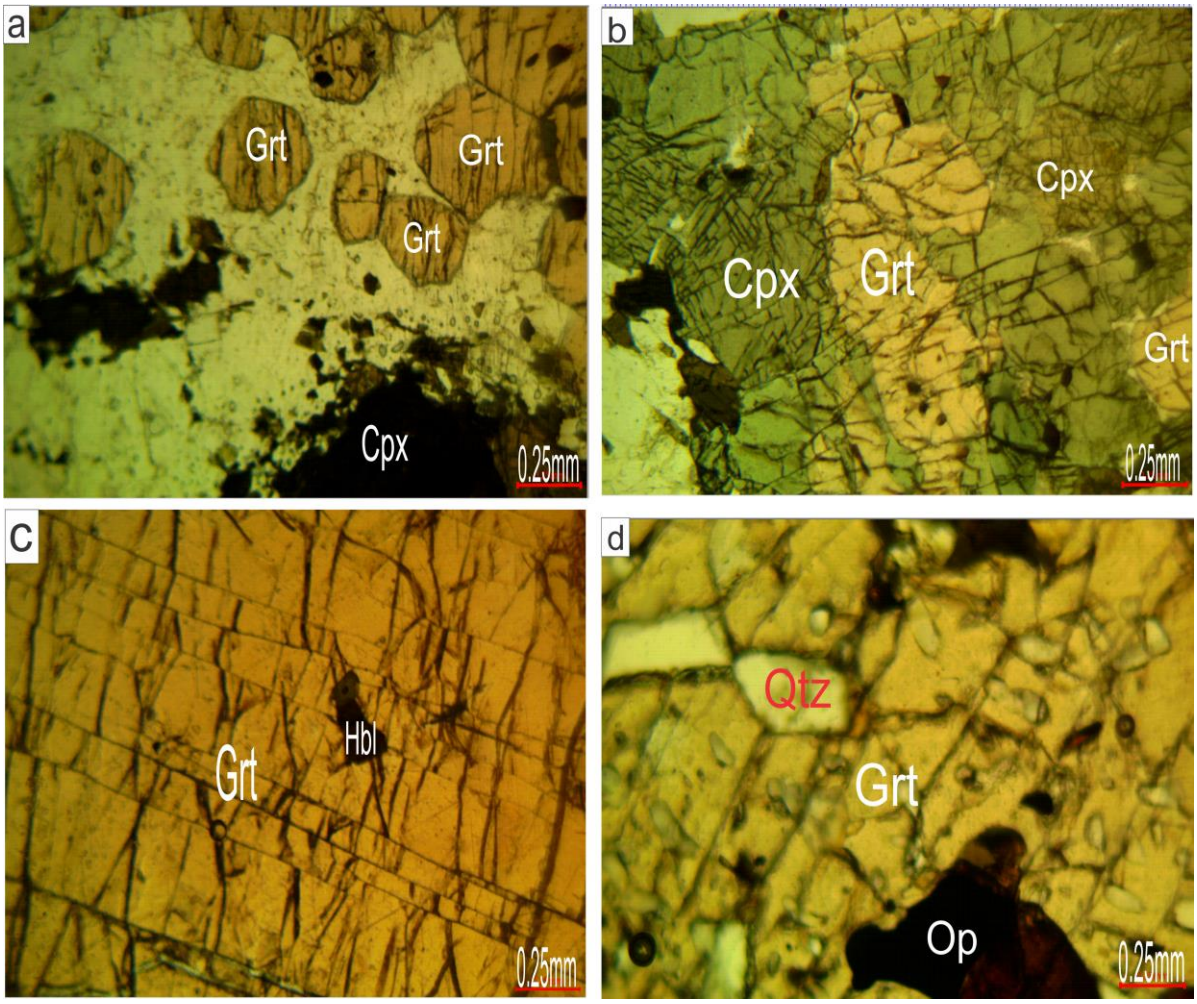

Figure 4.5: (a) Photomicrograph showing garnet minerals. Plane polarized light (Ppl) (b) Photomicrograph showing garnet and clinopyroxene porphyroblast (Ppl) (c) Garnet porhyroblast with hornblende inclusion (Ppl) (d) Poikiloblastic texture of garnet with inclusions of quartz and opaque minerals (Ppl). Garnet (Grt), Plagioclase (Pl), Microcline (Mc), Pyroxene (Px), Clinopyroxene (Cpx), Orthopyroxene (Opx), Hornblende (Hbl), Quartz (Qtz), Chlorite (Chl), Opaque mineral (Op).

University of Ghana http://ugspace.ug.edu.gh

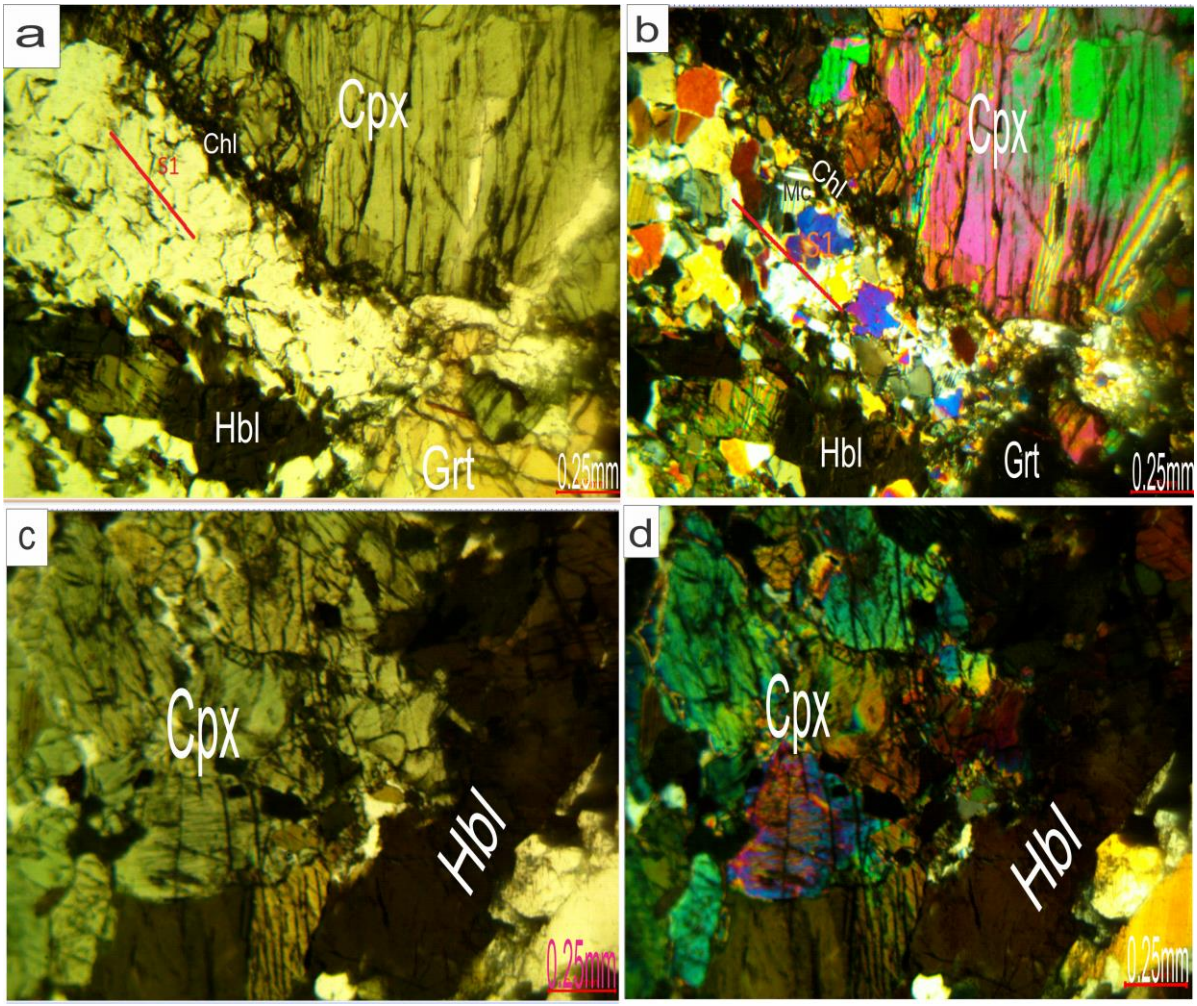

Figure 4.6: (a) Photomicrograph showing Clinopyroxene porphyroblast with rims of chlorite with the S_1 foliation around it. (Ppl). (b) Photomicrograph showing Clinopyroxene porphyroblast with rims of chlorite. (Xpl). (c) Hornblende rims around broken Clinopyroxene (Ppl) (d) Hornblende rims around broken Clinopyroxene (Xpl). Same Abbreviations are used.

University of Ghana http://ugspace.ug.edu.gh

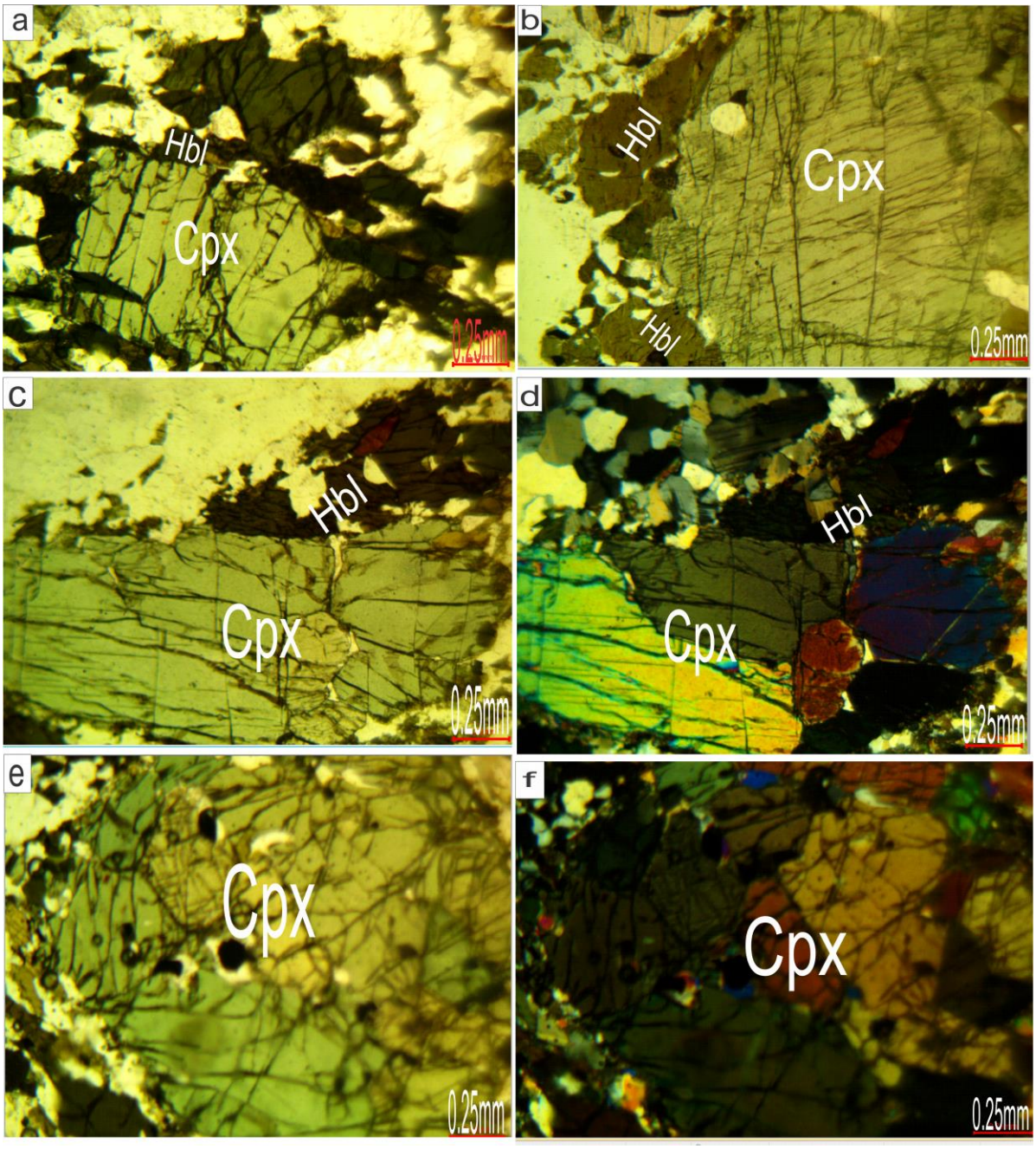

Figure 4.7: (a) and (b) Photomicrographs are showing porphyroblastic Clinopyroxene with rims of hornblende intracrystalline fractures. (Ppl) (c) and (e) Broken and cracked Clinopyroxene porphyroblast (Ppl) (d) and (f) Broken Clinopyroxene porphyroblast. (Xpl). Same Abbreviations are used.

University of Ghana http://ugspace.ug.edu.gh

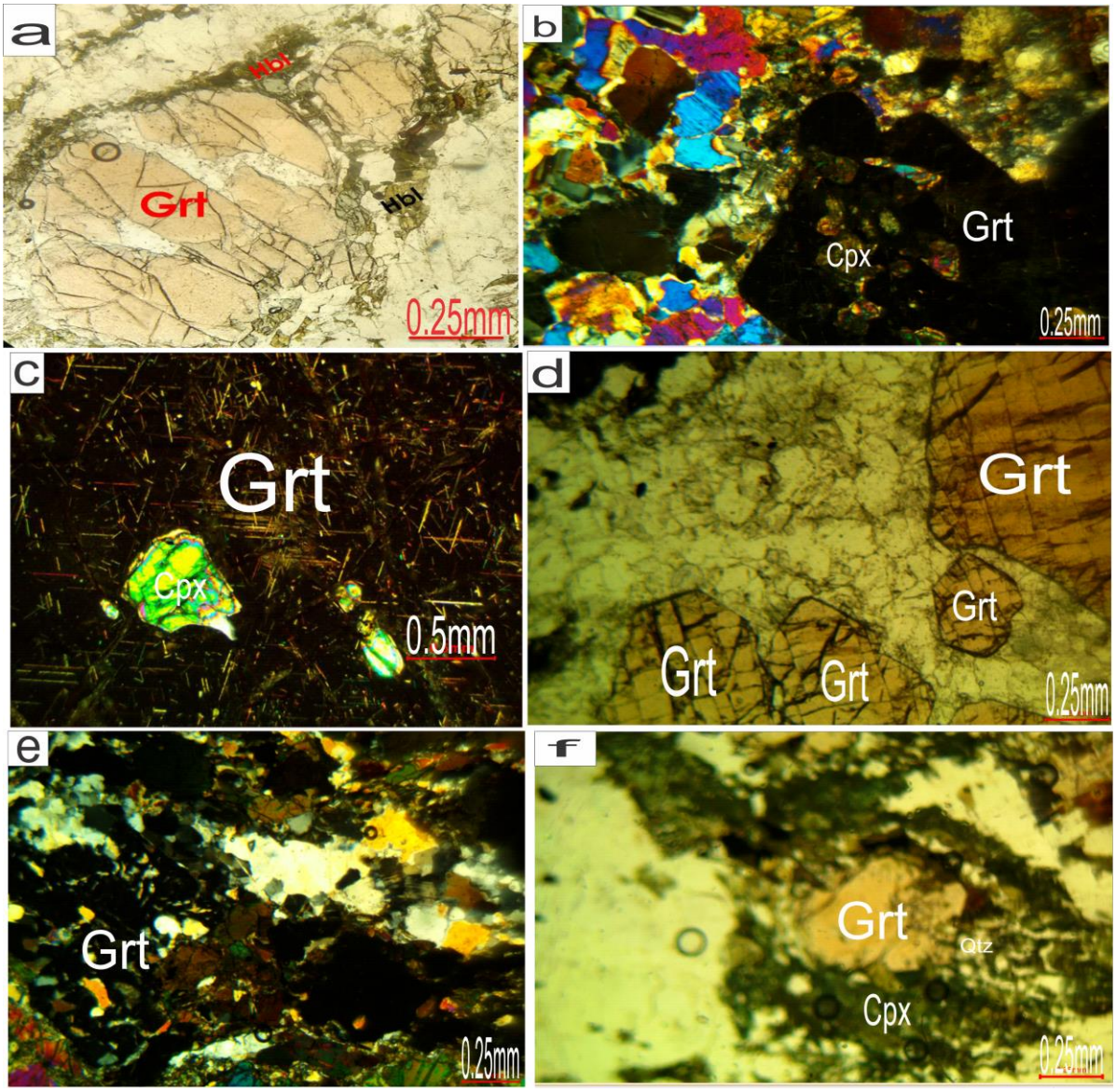

Figure 4.8: (a) Photomicrogragh showing deformed pre kinematic garnet porphyroblast with rims of hornblende and S_1 foliation wrapping around it. (Ppl). (b) Syn kinematic garnet with inclusion of Clinopyroxenes. (Xpl). (c) Garnet with rutile exsolution (Xpl). (d) Syn kinematic garnets (Ppl). (e) Garnet porphroblast with inclusions of quartz and plagioclase (Xpl). (f) Corona texture of Clinopyroxenes and quartz around garnet porphyroblast (Ppl). Same Abbreviations are used.

University of Ghana http://ugspace.ug.edu.gh

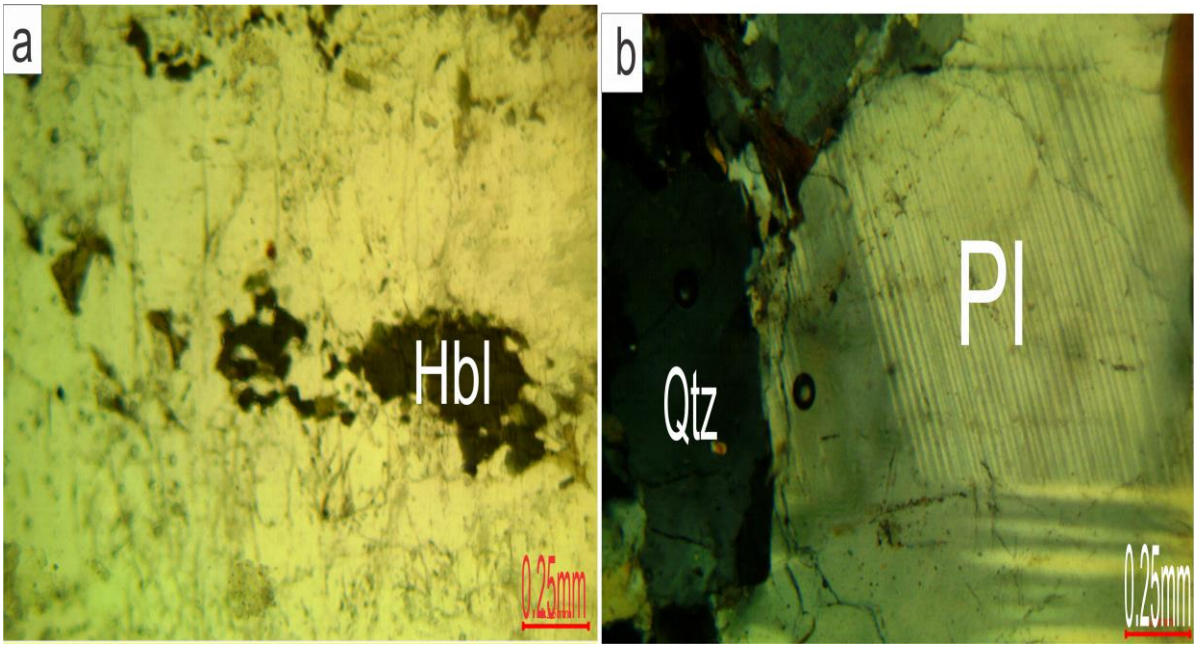

Figure 4.9: (a) Photomicrograph showing L_1 mineral lineation in the S_1 foliation. (b) Photomicrograph showing deformed polysynthetic twining in plagioclase and deformed quartz. (Ppl). Same Abbreviations are used.

The mafic garnet gneisses are distinguished into pyroxene garnet gneisses and garnet hornblende gneisses based on the modal composition of the studied samples.

University of Ghana http://ugspace.ug.edu.gh

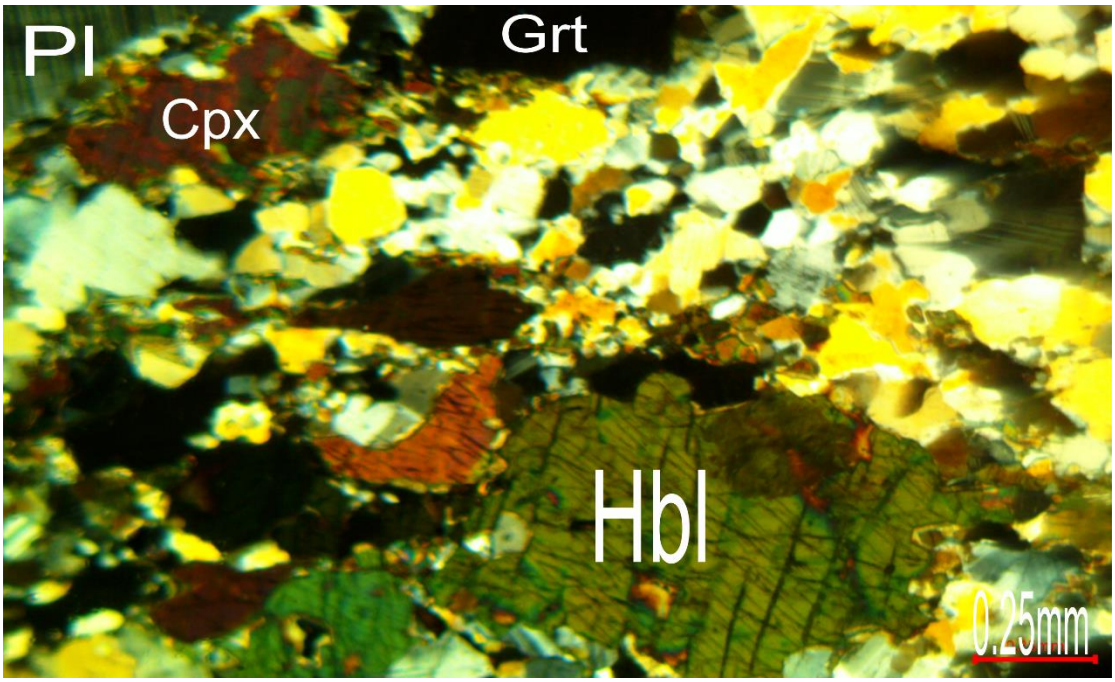

Figure 4.10: Photomicrograph showing garnet hornblende gneiss. (Xpl) Same Abbreviations are used.

Table 1: Average modal composition (vol %) of minerals in the garnet hornblende gneiss.

Mineral	Modal composition
Hornblende	30
Plagioclase	25
Garnet	15
Clinopyroxene	13
Quartz	7
Chlorite	4
Epidote	3
Accessory mineral (Ilmenite and rutile)	5

University of Ghana http://ugspace.ug.edu.gh

The pyroxene garnet gneisses are most abundant in the study area. They have the same minerals composition but different modal composition as the hornblende garnet gneisses.

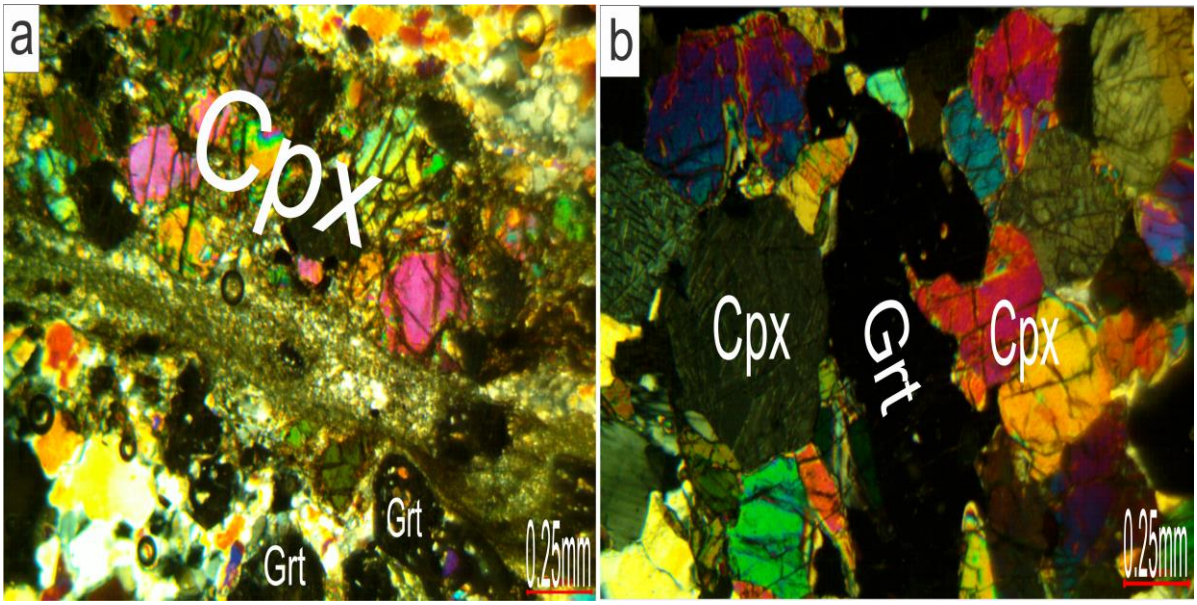

Figure 4.11: Photomicrographs of pyroxene garnet gneiss. (Xpl). Same Abbreviations are used.

University of Ghana http://ugspace.ug.edu.gh

Table 2: Average modal composition (vol%) of minerals in the pyroxene garnet gneiss.

Mineral	Modal composition
Hornblende	10
Plagioclase	22
Garnet	30
Clinopyroxene	20
Quartz	6
Chlorite	4
Epidote	3
Accessory minerals (Ilmenite and rutile)	5

4.1.2 Pyroxene Bearing Amphibolite

The pyroxene bearing amphibolites are found at the base of the mafic garnet gneisses at Eastern Quarries at the Mampong Hill. These rocks are tectonically welded with the mafic garnet gneisses. They are strongly deformed and sheared together with mafic garnet gneisses. They look massive at the base of the mafic garnet gneisses and gradually transpose into the foliations plane of the mafic garnet gneisses. The contact between the two rocks is gradational. The amphibolite is a dark grey coloured, medium-grained rock, essentially composed of dark greenish-black hornblende and feldspar with some garnet.

University of Ghana http://ugspace.ug.edu.gh

Figure 4.12: Field photograph of pyroxene bearing amphibolite.

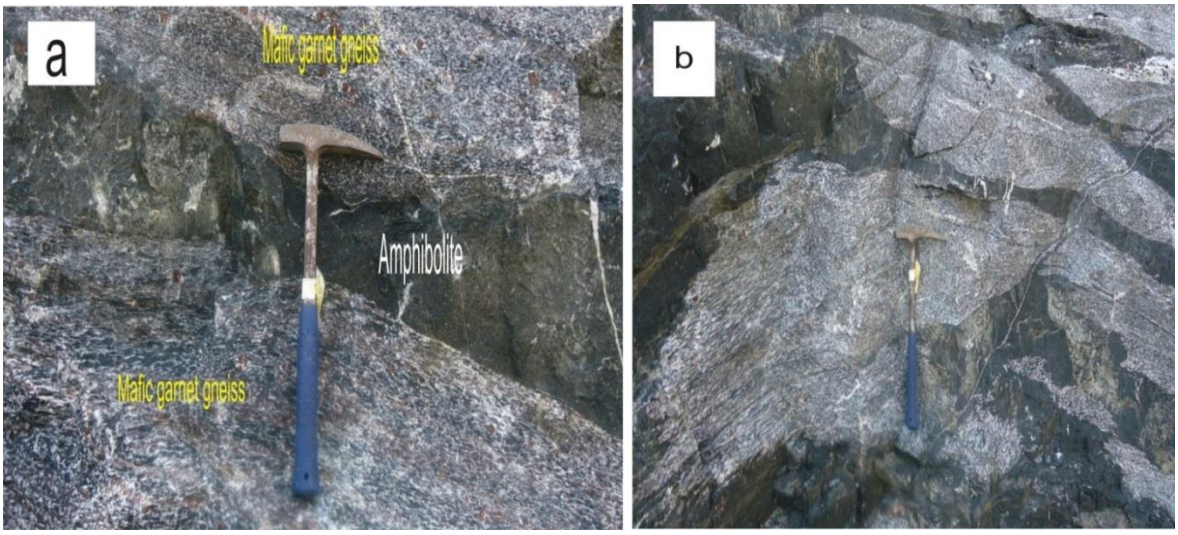

Figure 4.13: Field photograph of amphibolite tectonically welded into host mafic garnet gneiss at Eastern quarries, Mampong Hill. (b) Gradational contact between the amphibolite and the mafic garnet garnet gneiss.

University of Ghana http://ugspace.ug.edu.gh

Under the petrographic microscope, minerals observed are amphiboles, pyroxenes, garnet, plagioclase and quartz. The amphiboles are distinctively coloured. They exhibit deep green absorption colors with some exhibiting a typical $60^o/120^o$ amphibole cleavage. They show deep green to light green pleochroism. The amphiboles are anhedral in shape. The plagioclases are colorless under plane polar. Some grains show multiple twinning which may indicate deformation during recrystallization. The pyroxenes exhibit yellowish green absorptions colors which undergo pleochroism to green upon rotation of the stage. These pyroxenes are clinopyroxenes. They are anhedral to subhedral in shape. A few garnet grains are observed in the thin section. The garnets have subhedral shape. The garnet crystal display sieve structure or poikiloblastic texture with inclusions of hornblende. Few quartz minerals are also observed. The grains of quartz are colorless and shows sutured boundaries. They undergo undulose extinction under cross polars when the stage is rotated. The mineral assemblage of the pyroxene bearing amphibolite indicates amphibolite facies at higher temperature and pressure.

University of Ghana http://ugspace.ug.edu.gh

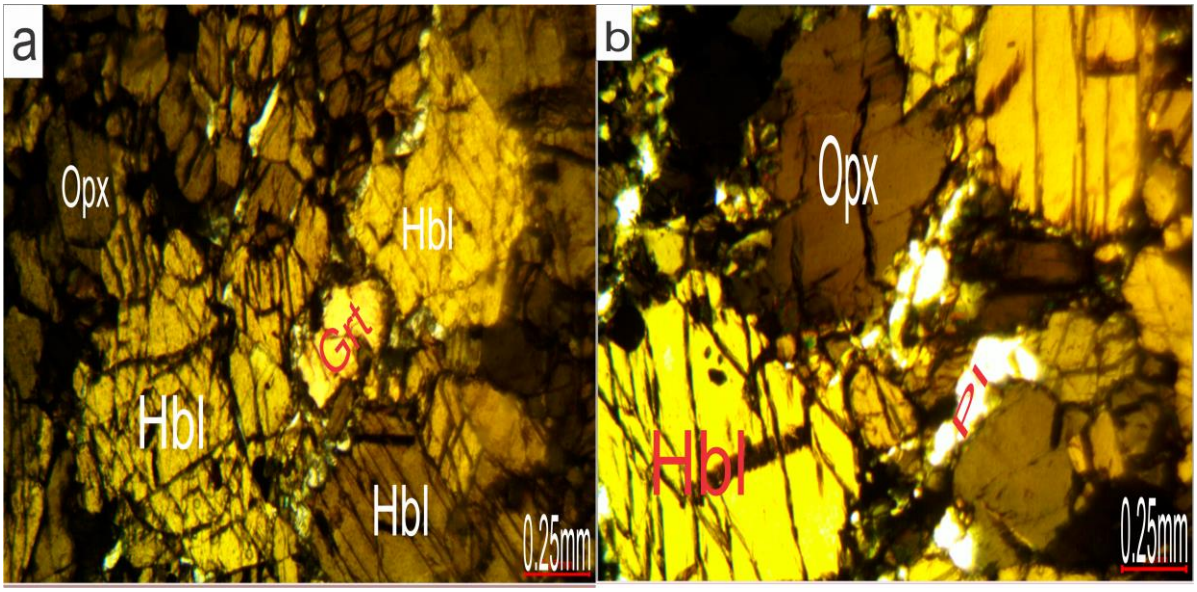

Figure 4.14: Photomicrographs of pyroxene bearing amphibolite. (Ppl). Same Abbreviations are used.

University of Ghana http://ugspace.ug.edu.gh

Table 3: Average modal composition (vol %) of minerals in pyroxene bearing Amphibolite.

Mineral	Modal composition
Amphibole (hornblende)	55
Pyroxene	20
Plagioclase	15
Garnet	5
Quartz	3
Opaque mineral	2

4.1.3 Pyroxenite

The pyroxenites associated with mafic garnet gneisses are seen as older materials thrusted into gneisses. Some form boudins in the gneisses. The pyroxenites rocks are thrusted into the mafic garnet gneisses. They consist of dark pyroxene minerals. Some form boudins in the mafic garnet gneisses at some localities. These pyroxenites are also tectonically deformed together with the mafic garnet gneisses.

University of Ghana http://ugspace.ug.edu.gh

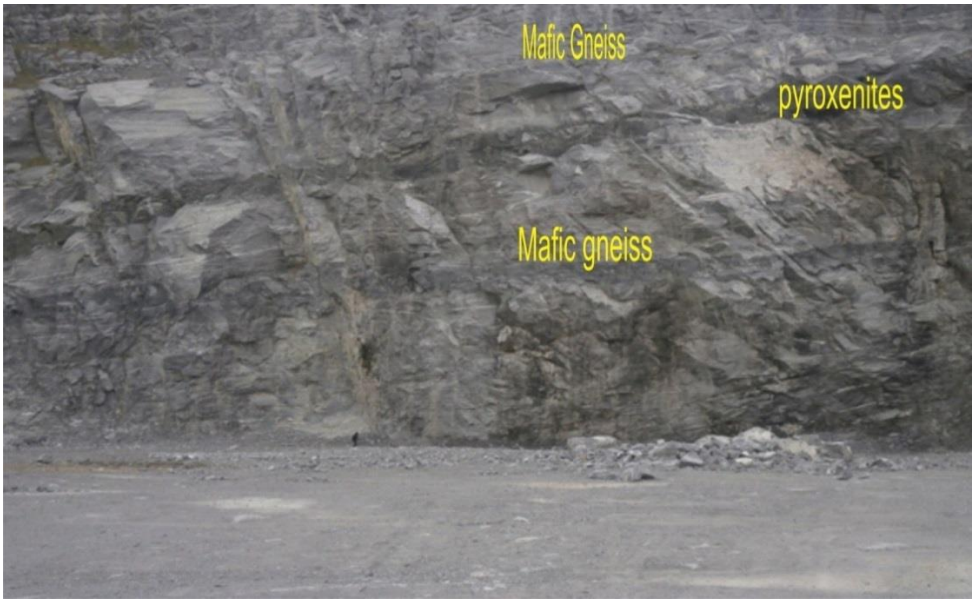

Figure 4.15: Field photograph showing pyroxenite thrusted into the mafic garnet gneiss at Eastern Quarries. Mampong Hill.

Figure 4.16: Field photograph showing pyroxenites boudins in the mafic garnet gneiss at PW Quarries. Naglayo hill.

University of Ghana http://ugspace.ug.edu.gh

The pyroxenites under the microscope display granoblastic and quite equant textures. They are made up of variable proportions of orthopyroxenes and clinopyroxenes. These minerals display deformed cleavages. They are highly fractured with intracrystalline fractures. The clinopyroxenes are pale green and shows pleochroism. The exhibit pale green to deep green upon rotation of the stage under plane polars. The orthopyroxenes exhibit pale green to pink pleochrosim.

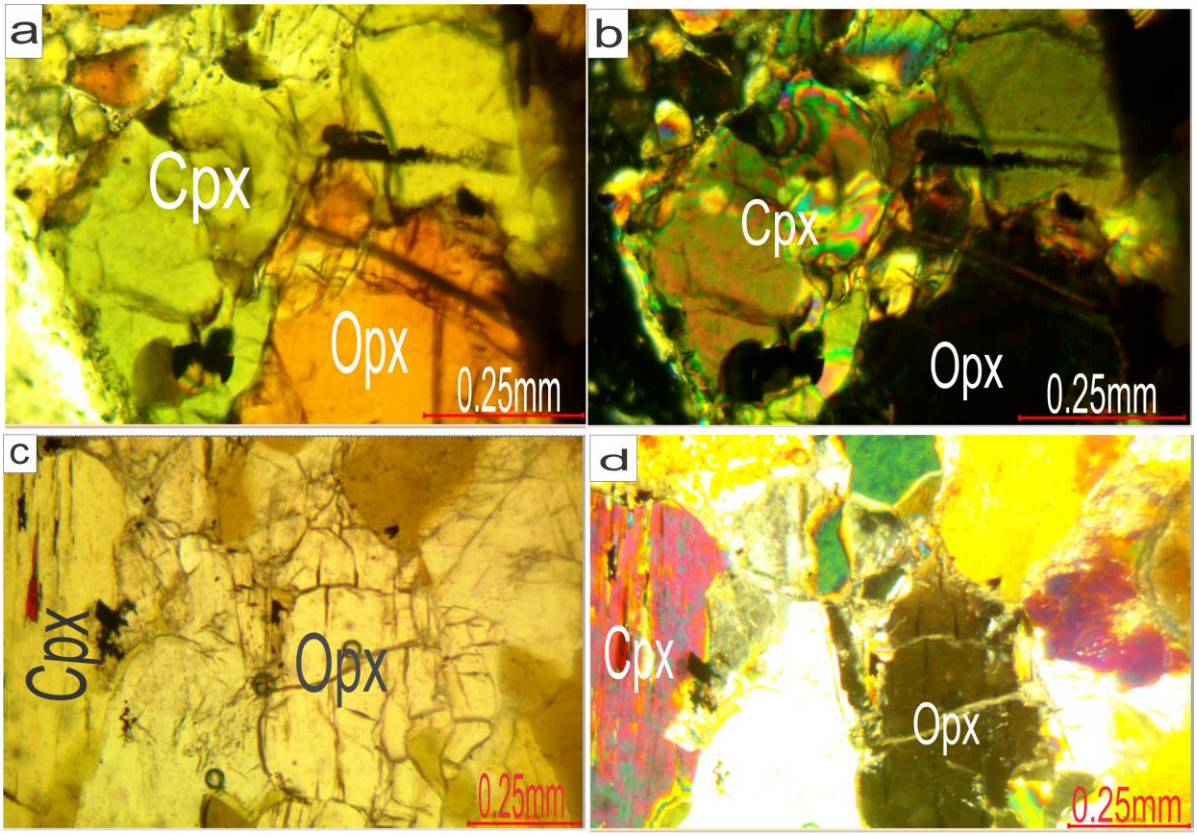

Figure 4.17: (a) and (c) Photomicrographs showing Clinopyroxene (Cpx) and Orthopyroxene (Opx) in the pyroxenite. (Ppl). (b) and (d) Photomicrographs showing Clinopyroxene (Cpx) and Orthopyroxene (Opx) in the pyroxenite. (Xpl). Same Abbreviations are used.

University of Ghana http://ugspace.ug.edu.gh

Table 4: Average modal composition (vol%) of minerals in pyroxenite.

Mineral	Modal composition
Pyroxene	95
Opaque minerals	5

4.1.4 Fault Breccia

The brecciated rock is found within the mafic garnet gneisses at the PW Quarries, Naglayo Hill in the study area. They are found in a brittle fault zone in the area (Fig. 4.4c). The fault rocks comprise a 0.5–3.0 m thick zone of dark green, chlorite-rich breccia is observed at the PW Quarries. The rocks represent a crushed garnet mafic gneisses during a brittle deformational event in the area. Clast of quartz minerals of variable shapes and sizes are observed within the matrix in the rock. The fault zone had strike of $N310^0W$ with dip 40^0SW.

Under the microscope, the rock exhibited clasts of quartz within broken fine grains of pyroxenes and chlorite matrix. These quartz clasts are anhedral to subhedral in shape. They exhibited undulose extinction. The matrix is made up of fine and crushed grains of pyroxenes with some chlorites. The rock exhibits a mortar texture where porphyroclast of quartz are surrounded by crushed matrix.

University of Ghana http://ugspace.ug.edu.gh

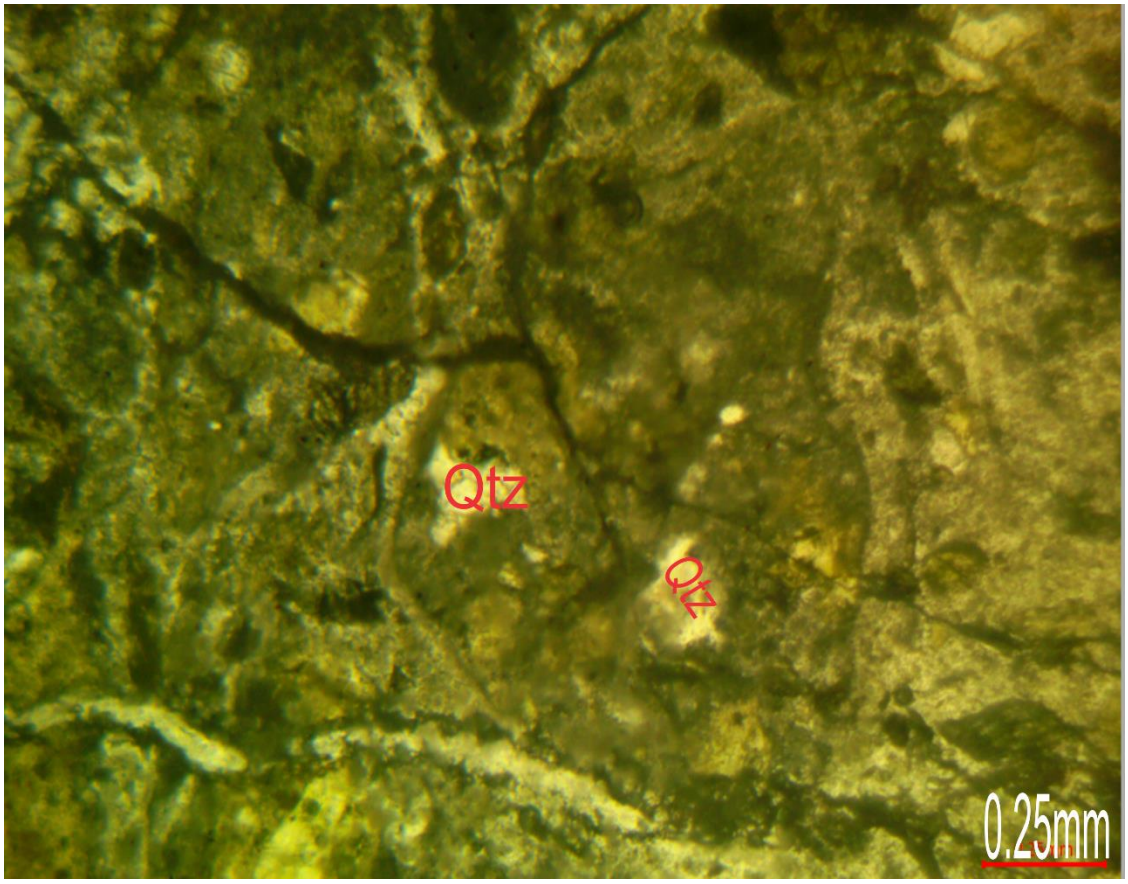

Figure 4.18: Photomicrograph of the Fault Breccia. (Ppl). Same Abbreviations are used.

Table 5: Average modal composition (vol%) of minerals in fault breccia.

Mineral	**Modal composition**
Quartz	20
Matrix	80

University of Ghana http://ugspace.ug.edu.gh

4.2 Deformations, Structures and Kinematics

The exposure of outcrops in the study area provided detailed information on the structural setting on the study area. The structures have been statistically analyzed and their probable causes and relations have been established. The area has undergone several regimes of tectonic and metamorphic events; thus, the rocks show numerous deformational structures. The mafic garnet gneisses together with the related rocks in the study area are tectonically sheared. They have undergone several regimes of metamorphic and deformational events that have caused the rocks to undergo significant textural and structural changes resulting in the development of tectonic structures with kinematic indicators. The structures include bands and foliations, folds, faults, boudins, mineral lineations.

4.2.1 Gneissic Bands and Foliations.

The foliations in the mafic garnet gneiss are well represented by the gneissic bands found in the rocks. The alternating gneissic bands in the rock are well exposed as a result of the quarries activities in the study. They were formed probably during the D_1 deformational event and produced S_1 foliations fabric. These structures occur as repetitive layering or alternating dark and light minerals caused by shearing forces or differential pressure acting on a rock mass. The gneissic bands generally formed by the reorganisation of the original rock's chemical constituents into layers within which particularly minerals are concentrated. Foliations are more pronounced in the mafic garnet gneisses. The felsic compositional band is composed of plagioclase feldspar, quartz and hornblende. The hornblende mineral defines L_1 mineral lineation during the D_1 deformation. At certain place garnet bands are also

University of Ghana http://ugspace.ug.edu.gh

observed which are sub parallel to the alternating light and dark bands. The foliations have a NE–SW (average at N20E) foliation trend with gentle dips of average of 15^{o} toward SE. Few exceptions show NNW strike (Table 6). The general north easterly strike indicates NW to SE simple or non-coaxial shearing during the D_1 deformation. The S_1 foliations are well exposed in the mafic garnet gneisses.

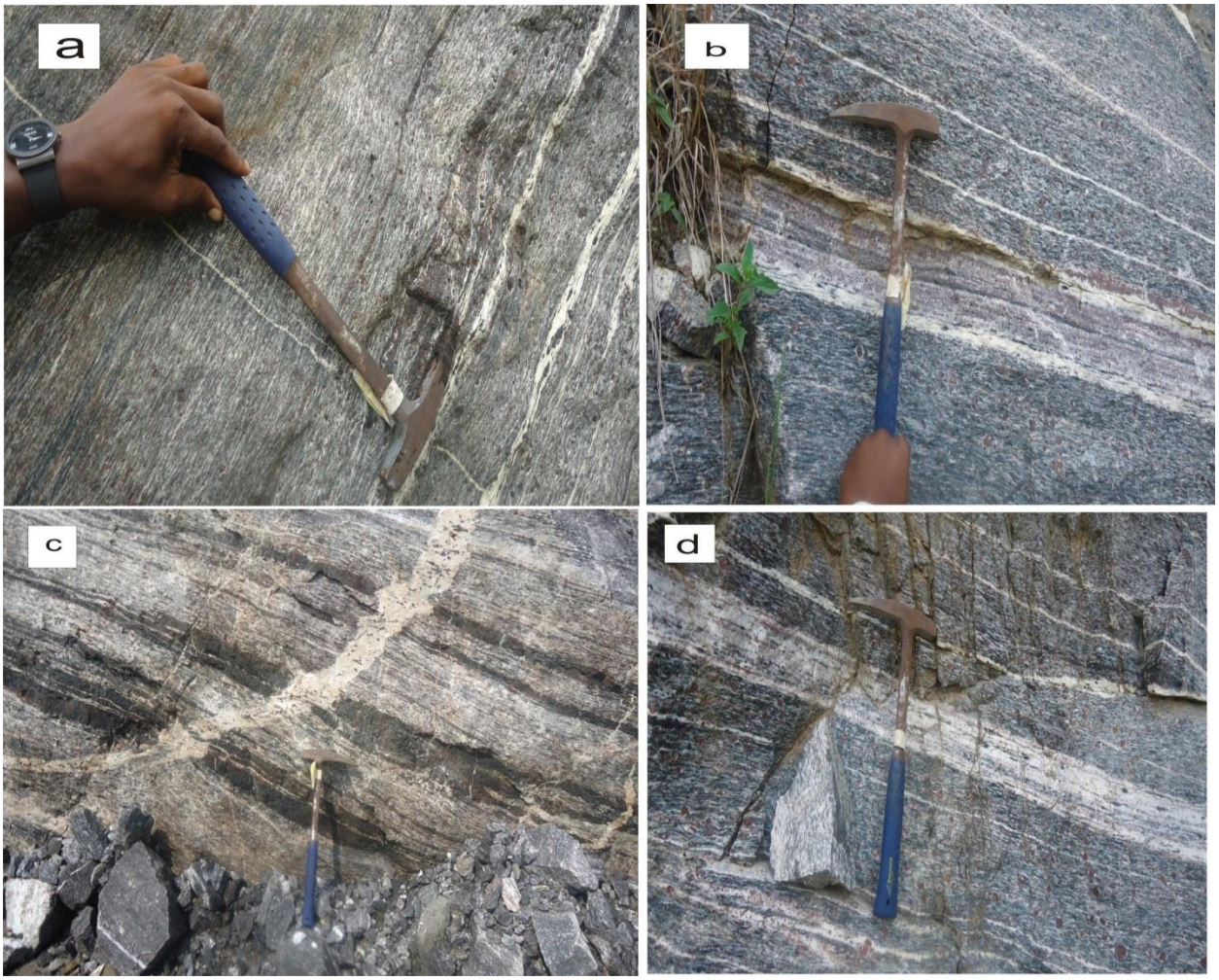

Figure 4.19: Field photographs showing gneissic banding and foliations in the mafic garnet gneisses. Shai hills.

University of Ghana http://ugspace.ug.edu.gh

Table 6: Structural attitude (degree) of foliation planes.

Strike	Dip	Dip Direction
20	15	124
15	20	120
28	15	100
20	20	110
16	20	130
40	15	126
340	15	30
350	20	40

From the poles plots (Fig 4.20a) it shows that the foliation in the mafic garnet gneisses have predominantly southeasterly dip direction with gentle to moderate dips. The plane to pole (Fig 4.20b) indicates that the rock mainly dips to southeastern direction with average dip been moderate thus about 15^{o}. The contoured poles density plot (Fig 4.21) indicates majority of the poles are concentrated closer to the center, which show that the foliations in the area are of gentle dip.

University of Ghana http://ugspace.ug.edu.gh

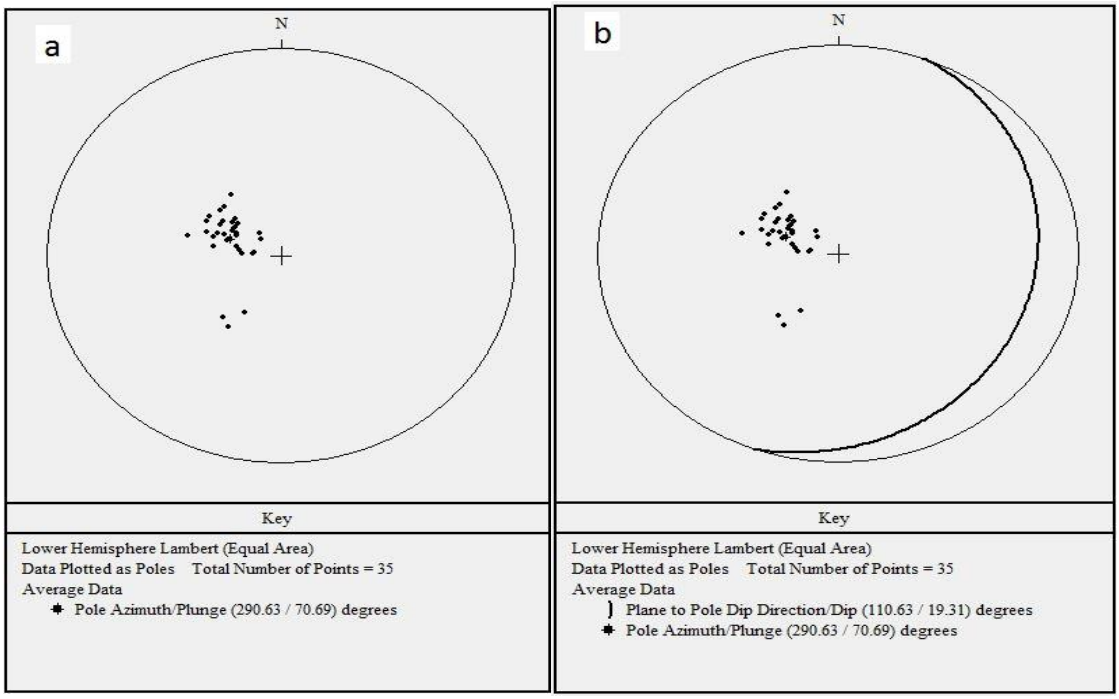

Figure 4.20: (a) Poles plot of foliations in mafic garnet gneisses (b) Poles plot with plane to poles plot in the mafic garnet gneiss.

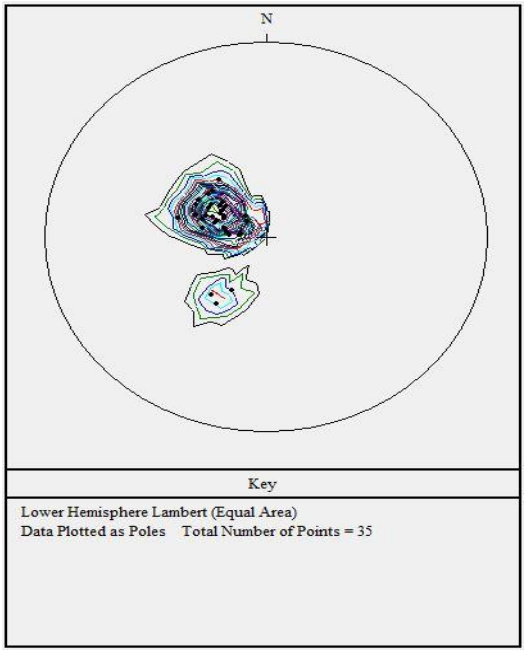

Figure 4.21: Contoured poles-density plot of foliations in mafic garnet gneisses.

University of Ghana http://ugspace.ug.edu.gh

4.2.2 Mineral lineation.

The mineral lineations are well represented by hornblende within the compositional felsic bands in the mafic garnet gneisses. The L_1 hornblende minerals are developed into sigma (σ) and delta (δ) giving indications of simple shearing probably during during the D_1 deformation stage. This structure also gives shear sense indications during the D_1 deformation of the mafic gneisses. These hornblende minerals are stretched within the quartzofeldspathic compositional bands. The stretching lineation observed on the foliation planes shows a NE–SW trend direction with gentle plunge (average of about 20^0) towards the NE or SW (Table 7)

Figure 4.22: Stretched hornblende within compositional banding in the mafic garnet gneiss.

University of Ghana http://ugspace.ug.edu.gh

Table 7: Structural attitude (degree) of mineral lineation.

Trend	Plunge
215	20
200	15
208	30
200	20
206	24
20	16
34	18
212	15

The poles plots (Fig 4.23) indicate NE–SW trends of the L_1 mineral lineation which gently plunges. It gently plunges to the SW with some plunging gently to NE.

University of Ghana http://ugspace.ug.edu.gh

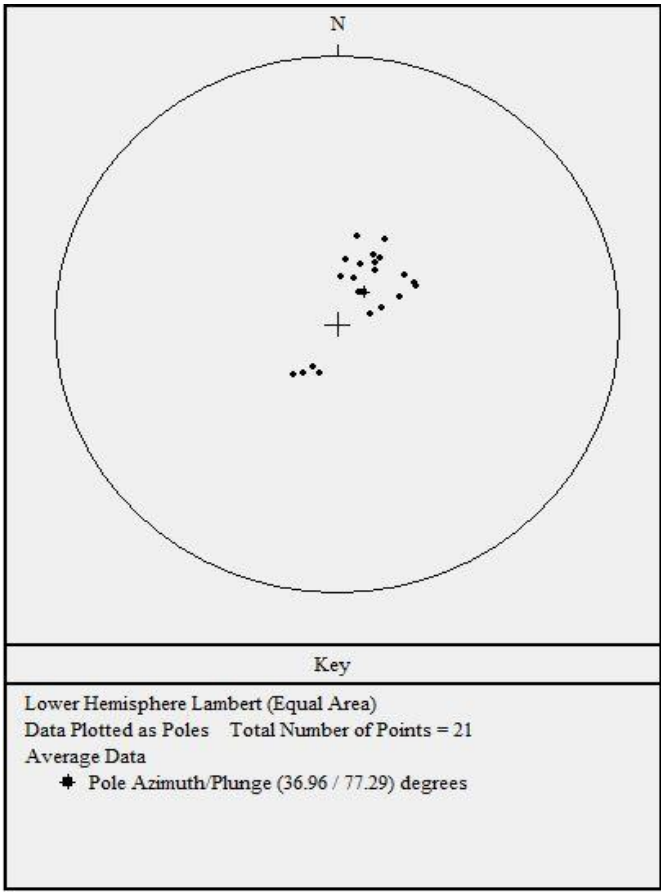

Figure 4.23: Shows Poles plot of lineations in mafic garnet gneisses.

Shear sense indicators during the D_1 are mainly dextral, represented by:

- Sheared pyroxenite boudin rock within the mafic garnet gneiss (Fig 4.24)
- Stretched hornblende mineral lineations into sigma and delta structures (Fig 4.22).
- Clockwise rotation of garnets minerals. (Fig 4.25)

University of Ghana http://ugspace.ug.edu.gh

Figure 4.24: Photograph showing dextral sense of shearing by sheared pyroxenite boudin in the mafic garnet gneiss during D_1 deformation at Shai Forest reserve.

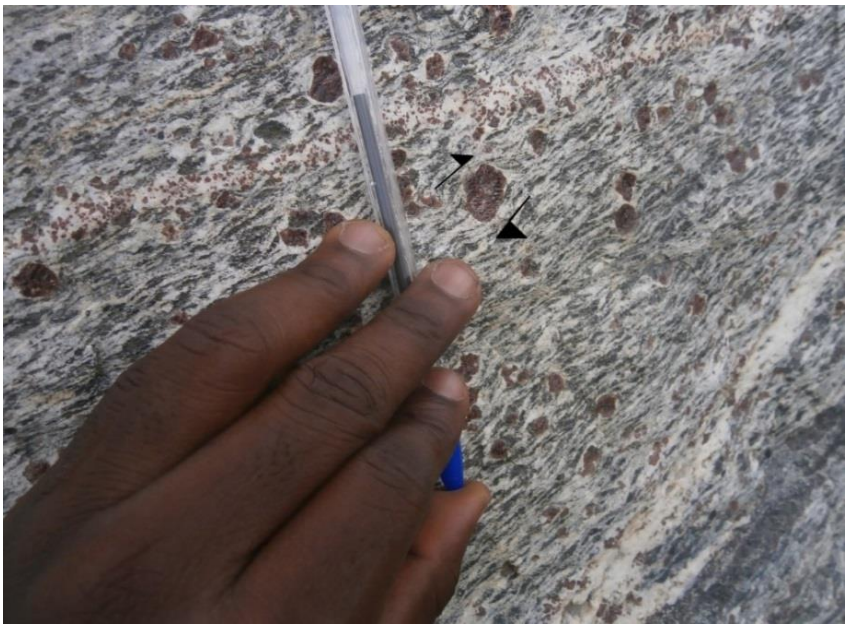

Figure 4.25: Photograph showing dextral sense by clockwise rotation of garnet in the mafic garnet gneiss during D_1 deformation at PW Quarries, Naglayo Hill.

University of Ghana http://ugspace.ug.edu.gh

4.2.3 Ptygmatic Folds

In the mafic garnet gneisses, the compositional banding is folded into ptygmatic folds. These folds probably might have been formed during D_2 deformational phase in the mafic garnet gneisses. They postdate D_1 deformation. These folds are observable almost throughout mafic garnet gneisses. These D_2 ptygmatic folds cross cut foliation (Fig 4.19c and Fig 4.3c). Upon axial measurements of these folds, it was observed that they are of different orientations. Some have NE/SW trend and others with NW/SE trends with average of 25^o plunge (Table 8). They crosscut the S_1 foliations which show that they are younger than the foliations or postdate the S_1 foliations.

Table 8: Structural attitude (degree) of Ptygmatic fold axis.

Trend	Plunge
200	30
210	20
214	25
212	22
200	30
190	24
124	40
120	25

University of Ghana http://ugspace.ug.edu.gh

From the stereographic poles plot below, these folds are of different direction. They trend SW/NE and SE/NW with average plunge of 15^0 SW and SE respectively.

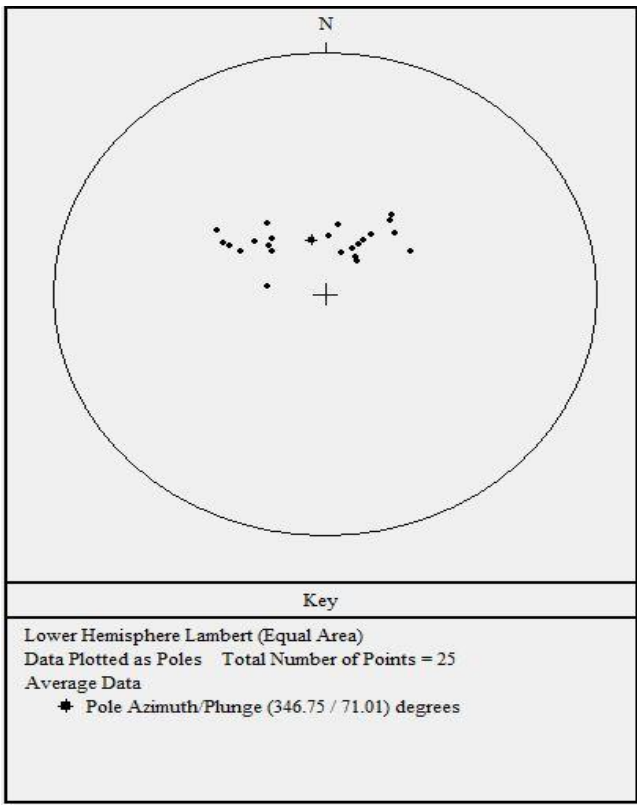

Figure 4.26: Poles plot of fold axis of ptymatic folds.

University of Ghana http://ugspace.ug.edu.gh

4.2.4 Faults

The subvertical faults found through the mafic garnet gneisses represent the D_3 deformations in the area. These brittle faults cut through the S_1 foliation and the D_2 folding. This indicates that the faults are younger event in the mafic garnet gneisses. These faults seen mainly in the area are normal faulting where the hanging wall have move down relatively to the footwall as a result of extension during decompression. These normal dip slip faults have moderate dips with two different direction of dip. These faults dip SW and strike NW/SE with some having a NW dip direction and NE/SW strike (Table 9). These faults have maximum displacement of about 30 cm.

Figure 4.27: Field photograph showing normal faults in the mafic garnet gneiss at PW Quarries, Mampong Hill.

University of Ghana http://ugspace.ug.edu.gh

Table 9: Structural attitude (degree) of faults planes in the area.

Strike	Dip	Dip Direction
312	40	215
302	42	200
350	40	208
310	34	240
322	44	232
70	38	300
72	40	312
50	32	320

University of Ghana http://ugspace.ug.edu.gh

From the stereographic pole plots, it can inferred that there are indicates two dip directions of the fault planes with most dipping SW and having moderate dips average of about 35^0 to 40^0 (Fig 4.28).

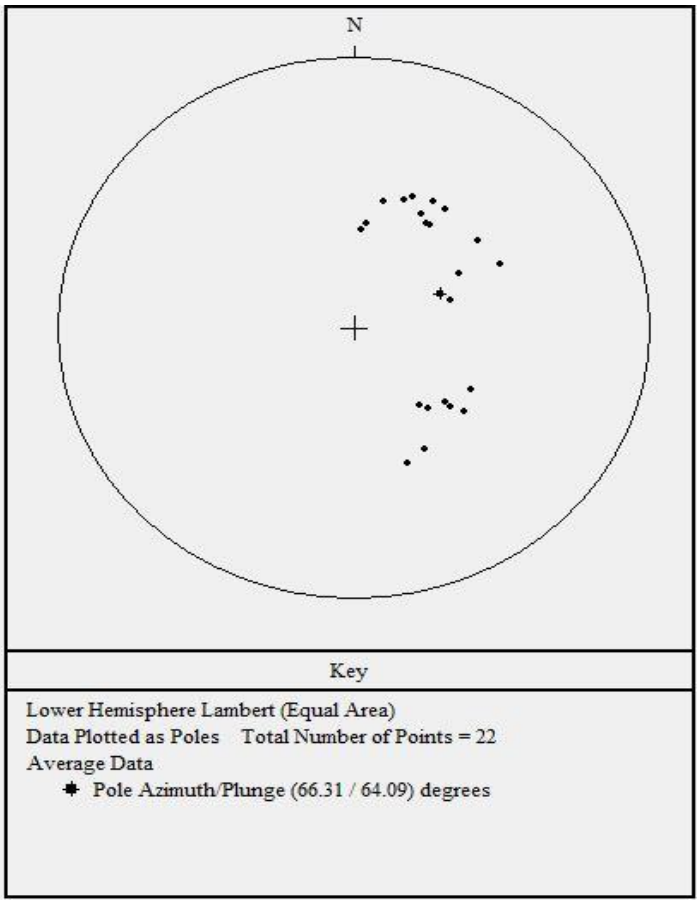

Figure 4.28: Poles plot of faults in the mafic garnet gneisses.

University of Ghana http://ugspace.ug.edu.gh

These subvertical faults postdate the ductile deformations and cuts through the main foliations, the ptygmatic folds. The above structures represent a ductile–brittle continuum of extensional deformation of the mafic garnet gneiss during decreasing temperatures and pressures during exhumation. The thrusted rigid older materials (pyroxenite) within the mafic garnet gneiss are fractured and exhibit dextral displaced grains but have overall sinistral sense of shearing during D_3 deformation (Fig 4.29).

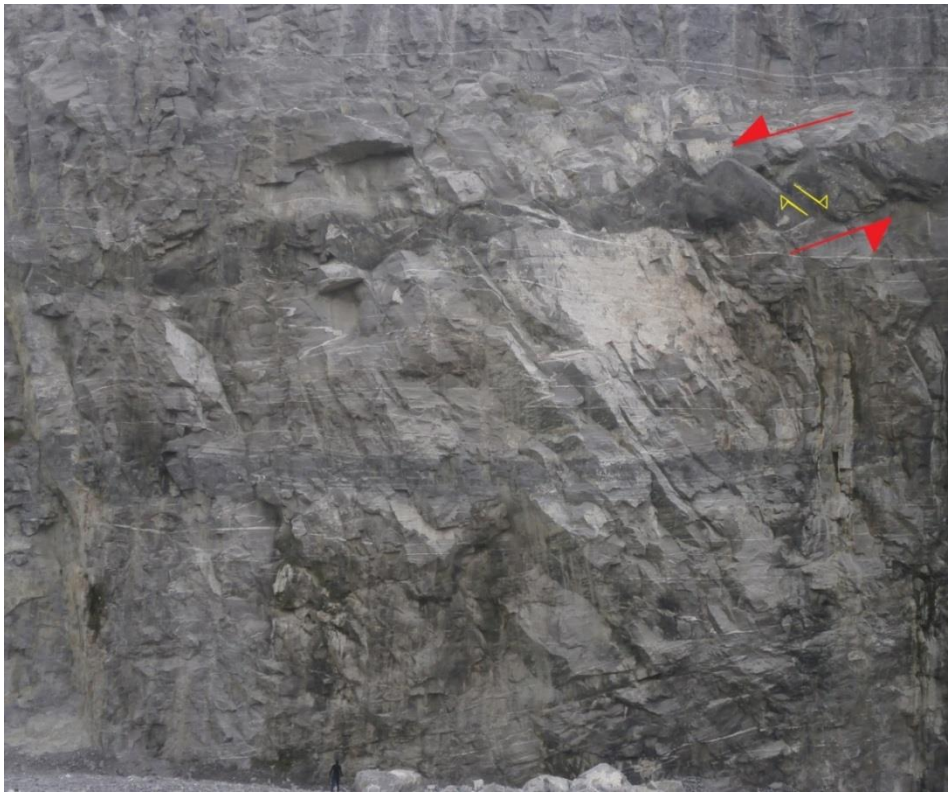

Figure 4.29: Photograph showing overall sinistral sense of shear during the D_3 deformations.

University of Ghana http://ugspace.ug.edu.gh

4.2.5 Joints

Joints are fractures or cracks in a rock body which show no appreciable level of openings. These joints also postdate the foliations and ptygamtic folds in the rocks. They are usually found in the mafic gneisses (Fig 4.4d). Joints form at shallow depths in the crust where rocks break in a brittle way and are pulled slightly apart by tensional stresses during extension.

4.2.6 Boudins

Pyroxenite boudins were found within the mafic garnet gneisses. These are older pyroxenite materials that were thrusted in to the mafic garnet gneisses during the main D_1 deformation. The boudins form as a response to layer parallel extension or layer perpendicular flattening of the stiff pyroxenite materials. They stretch as a result of ductile contrast of less competent participating layers or rocks (Fig 4.16).

University of Ghana http://ugspace.ug.edu.gh

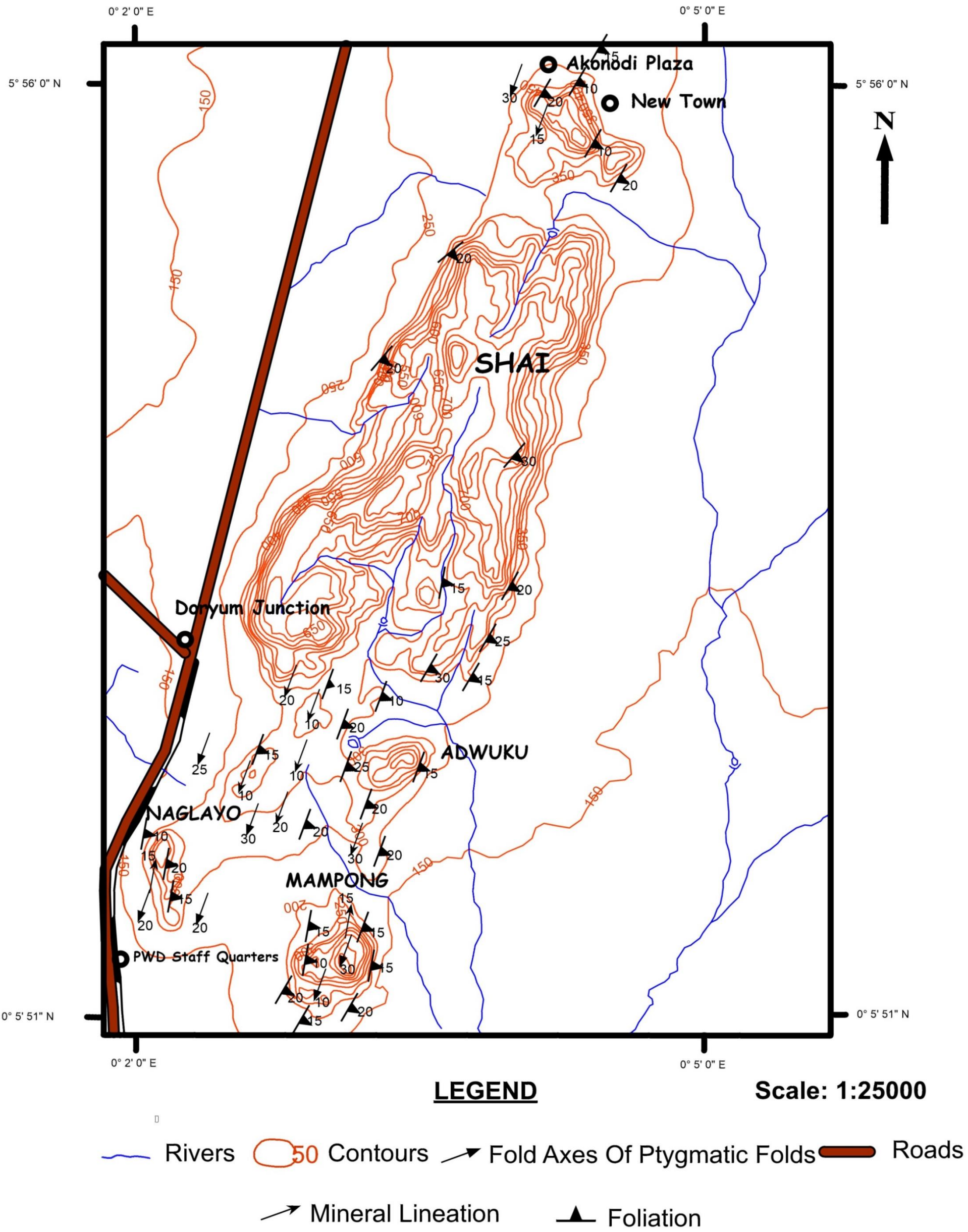

Figure 4.30: Structural map of the study area.

University of Ghana http://ugspace.ug.edu.gh

4.3 Major and Trace Element Geochemistry

The whole rocks major and trace element compositions of 23 rock samples from the study are presented in Table 10, Table 11 and Table 12. Two (2) samples of pyroxene bearing amphibolite, one (1) fault breccia, one (1) pyroxenite rock sample and nineteen (19) mafic garnet gneisses rock samples of which seven (7) samples are garnet hornblende gneisses and twelve (12) are pyroxene garnet gneiss rock samples.

4.3.1 Major Element Geochemistry

4.3.1.1 Pyroxene Garnet Gneisses

The concentration of SiO_2 ranges from 49.5 to 57.2 wt.%. The rocks have high Al_2O_3 content of 18.35 to 23.8 wt%. TiO_2 of 0.56 to 1.09 wt.%. Fe_2O_3t from 2.06 to 10.25 wt.%, CaO content of 7.44 to 9.06 wt.%, MgO of 1.18 to 6.65 wt.%, Na_2O content of 4.1 to 6.68 wt.%, K_2O of 0.26 to 0.56 wt%, CrO_3 of 0.01 to 0.02wt%, MnO from 0.01 to 0.19, P_2O_5 of 0.06 to 0.26 wt.%, SrO from 0.08-0.18 wt.%, BaO from 0.01 – 0.03 wt.% (Table 10). The Mg# ranges from 50.63 to 60.30%. Samples with higher Mg# have relatively lower Al_2O_3 content. Some of the samples have TiO_2 >1.0 wt%. These basaltic rocks are depleted in K_2O (K_2O of 0.26-0.56 wt.%,), but relatively higher Na_2O content of 4.1-6.68 wt.%. These rocks have high composition of aluminium (high-alumina), Low-K tholeiitic basalt (Table 10).

University of Ghana http://ugspace.ug.edu.gh

4.3.1.2 Garnet Hornblende Gneisses.

The garnet hornblende gneisses have similar major elements concentrations just as the pyroxene garnet gneisses (Table 11). The SiO_2 ranges from 47.7 to 51.1wt%. These rocks just as the pyroxene garnet gneisses are characterized by high alumina content from 17.9 to 20.3 wt%. Fe_2O_3 from 8.64 to 11.9 wt.%, CaO of 8.11 to 9.65 wt.%, MgO ranges from 4.67 to 6.75wt.%, Na_2O 4.02 to 4.97 wt.%, low K_2O from 0.33 to 0.48 wt.%, Cr_2O_3 0.01 to 0.02 wt.%, TiO_2 0.89 to 1.76 wt.%, MnO 0.08 to 0.15 wt.%, P_2O_5 of 0.15wt%, SrO from 0.07 to 0.1wt%, BaO 0.01 to 0.02. The Mg# ranges from 50.72 to 57.99 (Table 11).

4.3.1.3 Fault Breccia.

The fault breccia which is found in a fault zone in the pyroxene bearing gneisses at PW Quarries also has the similar characteristics as the host rock. One sample of the fault rock was analysed. The result (Table 12) shows that the breccia is characterized by SiO_2 of 50.1 wt.%, high alumina content of 17.35 wt.%, Fe_2O_3 of 6.99 wt.%, high CaO content of 19.05 wt.%, MgO content of 2.88 wt.%, Na_2O of content of 0.11wt.%, low K_2O content of 0.04 wt.%, Cr_2O_3 of 0.01wt.%, TiO_2 of 0.58 wt.%, MnO of 0.09 wt.%, P_2O_5 of 0.08wt.%, SrO of 0.15wt.%, BaO of 0.01wt%, The Mg# of 49.94.

4.3.1.4 Pyroxene bearing Amphibolite.

Two samples were analysed. These rocks are characterized by low silica content (Table 12). The SiO_2 contents are 41 and 40.6 wt.% which are representative of ultrabasic rock. They were 14.1 and 14.35 wt.% alumina content relative lower compared to the mafic garnet

University of Ghana http://ugspace.ug.edu.gh

gneisses. They have higher Fe_2O_3t content with 14.65 and 14.8 wt.% concentration with also high content of CaO content of 11.4 and 11.35wt.%. The MgO content is high 11.2 wt.% and 10.9 wt.%. Relatively low Na_2O content of 2.76 and 2.73 wt.%. K_2O of 0.59 and 0.58 wt.%, Cr_2O_3 is 0.03 and 0.02 wt.%, TiO_2 is 2.62 and 2.91 wt.%, MnO of 0.13 and 0.13 wt.%, P_2O_5 is 0.83 and 0.87wt.%, SrO is 0.02 and 0.02wt.%, BaO of 0.01 and 0.01 wt.%. It has higher magnesium number (Mg#) than the mafic garnet gneisses. The Magnessium number (Mg#) of these rocks are 60.23 and 59.33%.

4.3.1.5 Pyroxenite.

The pyroxenite has SiO_2 content of 51 wt.%. It has very low 7.19 alumina content relative lower. They have higher Fe_2O_3t content with 16.75 wt.% concentration. The CaO content is 8.03 wt.%. The MgO content is high (14.1 wt.%). Very low Na_2O content of 1.31wt.%. K_2O content of 0.21wt.%, Cr_2O_3 content of 0.05 wt.%, TiO_2 content of 1.19 wt.%, MnO content of 0.27 wt.%, P_2O_5 content of 0.14 wt.%, SrO content of 0.02 wt.%, BaO content of 0.01 wt%. The Magnessium number Mg# for the rock is 62.51% (Table 12).

University of Ghana http://ugspace.ug.edu.gh

Table 10: Major and trace elements composition of the pyroxene garnet gneiss.

Sample	S11	S15	S16A	S20	S24	N58A	N58h	N58f	N62A	N63	N67	N68
Major Elements (wt%)												
SiO_2	54.4	53.3	49.9	53.7	54.7	49.5	52.6	51.2	54.7	54.6	57.2	53.4
TiO_2	0.95	1.07	1.02	0.97	1.09	1.06	0.97	1.08	0.56	0.88	1.25	1.03
Al_2O_3	19.05	18.35	19.9	18.7	18.55	19.45	19.15	19.65	18.4	17.95	23.8	18.8
Fe_2O_3	7.5	8.65	9.7	7.99	9.08	10.25	8.73	8.84	7.46	8.1	2.06	8.18
MnO	0.1	0.12	0.15	0.11	0.14	0.19	0.12	0.1	0.12	0.12	0.01	0.09
MgO	4.33	5.04	5.61	4.93	4.7	6.65	6.15	6.48	5.72	5.64	1.18	4.98
CaO	7.92	8.27	8.77	8.27	7.91	8.75	8.6	9.06	8.2	8.07	7.44	8.29
Na_2O	5.1	4.74	4.37	4.76	4.14	4.1	4.57	4.46	4.29	4.31	6.68	5.29
K_2O	0.56	0.37	0.26	0.49	0.51	0.29	0.35	0.32	0.51	0.53	0.3	0.53
P_2O_5	0.23	0.26	0.18	0.25	0.26	0.18	0.11	0.12	0.06	0.16	0.19	0.22
Cr_2O_3	0.01	0.01	0.01	0.01	0.01	0.02	0.02	0.02	0.02	0.02	0.01	0.01
SrO	0.09	0.09	0.09	0.09	0.08	0.08	0.09	0.09	0.08	0.08	0.18	0.09
BaO	0.03	0.02	0.01	0.02	0.03	0.01	0.01	0.01	0.02	0.02	0.01	0.02
LOI	0.33	0.2	0.24	0.36	0.22	0.47	0.48	0.38	0.34	0.37	0.27	0.33
Total	100.6	100.49	100.21	100.65	101.42	101	101.95	101.81	100.48	100.85	100.57	101.26
Mg#	53.35	53.58	53.40	55.00	50.63	56.24	58.26	59.22	60.3	57.97	53.16	54.67
Trace elements (ppm)												
Cs	0.04	0.03	0.01	0.08	0.04	0.04	0.01	0.02	0.01	0.01	0.02	0.02
Ba	256	170	92.3	194	227	76.2	111	87.8	197	188	106	211
Rb	3.2	1.7	0.6	6	3.2	1	1	1	1.9	2.3	1	1.4
Sr	709	717	747	774	636	688	729	781	681	639	1495	771
Y	9.7	12.6	11.3	9.8	12.2	13	7.7	6.9	7.5	9.1	1.3	11
Zr	50	39	24	34	59	25	33	33	32	42	17	45
Nb	2.5	2.6	2.1	5.4	3.7	2.4	1.5	1.8	0.9	2	7.5	1.9
Hf	1.3	1.2	0.8	1.1	1.6	0.8	1	0.9	0.9	1.3	0.4	1.1
Ta	0.1	0.2	0.1	0.2	0.2	0.1	0.1	0.1	0.1	0.1	0.4	0.1
Pb	10	2	2	2	2	2	2	2	2	2	2	2
P	1003.86	1134.8	785.63	1091.15	1134.8	785.63	480.11	523.75	261.88	698.34	829.27	960.21
Ti	5695.25	6414.65	6114.90	5815.15	6534.55	6354.70	5815.15	6474.60	3357.20	5275.60	7493.75	6174.85
Th	0.19	0.05	0.05	0.18	0.25	0.05	0.1	0.05	0.12	0.2	0.05	0.07
U	0.1	0.05	0.05	0.05	0.22	0.05	0.05	0.05	0.08	0.09	0.05	0.05
K	4648.73	3071.48	2158.34	4067.64	4233.66	2407.38	2905.46	2656.42	4233.68	4399.69	2490.39	4399.69
Sc	16	20	21	17	21	23	18	19	18	18	3	18
V	195	237	242	221	231	221	230	242	175	220	90	222
Cr	70	90	120	80	60	140	130	150	150	140	10	90
Co	27	30	31	28	29	34	30	37	30	29	7	30
Ni	45	54	46	48	29	78	75	90	63	67	6	50
Cu	44	39	9	21	36	17	4	2	6	21	1	22
Zn	81	88	84	80	87	92	97	102	78	79	19	103
La	8.4	8	3.5	7.1	9.2	3.6	5.2	3.1	4.8	6.5	2.1	7.5
Ce	18.8	19.6	9.3	16.7	20.6	9.8	12.8	8.9	10.1	14.2	4.7	18.7
Pr	2.58	3	1.56	2.44	2.96	1.63	1.97	1.55	1.4	1.99	0.69	3.09
Nd	12.2	14.4	8.9	11.4	13.5	9.2	10.2	9.1	6.7	9.5	3.5	14.7
Sm	2.47	3.25	2.5	2.59	3.01	2.61	2.33	2.53	1.64	2.38	0.77	3.24
Eu	1.1	1.24	1	0.99	1.18	1	0.94	0.98	0.82	0.92	0.35	1.26
Gd	2.47	3.25	2.85	2.6	3.22	2.45	2.17	2.19	1.6	2.18	0.63	3.13
Tb	0.34	0.41	0.39	0.33	0.43	0.37	0.3	0.27	0.22	0.3	0.07	0.39
Dy	1.81	2.36	1.98	1.88	2.36	2.37	1.66	1.51	1.35	1.74	0.24	2.19
Ho	0.38	0.48	0.42	0.35	0.43	0.47	0.31	0.23	0.27	0.34	0.04	0.38
Er	1.02	1.47	1.23	1.13	1.3	1.57	0.95	0.7	0.95	1.01	0.12	1.15
Tm	0.16	0.2	0.2	0.15	0.19	0.26	0.13	0.12	0.13	0.14	0.01	0.18
Yb	0.96	1.04	1.04	0.94	1.06	1.54	0.77	0.67	0.73	0.88	0.05	1
Lu	0.14	0.18	0.16	0.14	0.18	0.22	0.11	0.09	0.12	0.14	0.01	0.13

University of Ghana http://ugspace.ug.edu.gh

Table 11: Major and trace elements composition of garnet hornblende gneiss.

Sample	M2	M5A	M5B	M3	M4A	M4B	M6C
Major Elements (wt%)							
SiO_2	51.1	49.6	49.4	47.7	50.1	51.8	50.8
TiO_2	1.34	0.89	1.2	1.76	1.49	1.17	1.24
Al_2O_3	19.65	19	19.3	17.9	18.15	20.3	18.75
Fe_2O_3	9.26	9.68	9.83	11.9	9.65	8.62	8.64
MnO	0.14	0.14	0.12	0.15	0.08	0.13	0.1
CaO	8.49	8.68	8.69	9.65	9.11	8.11	9.24
MgO	4.81	6.56	6.34	6.75	5.58	4.67	6.02
Na_2O	4.97	4.43	4.56	4.02	4.8	4.95	4.66
K_2O	0.33	0.35	0.41	0.33	0.48	0.34	0.4
P_2O_5	0.41	0.15	0.3	0.49	0.43	0.4	0.22
Cr_2O_3	0.01	0.02	0.02	0.02	0.01	0.01	0.02
SrO	0.09	0.09	0.09	0.07	0.08	0.1	0.09
BaO	0.01	0.01	0.01	0.01	0.02	0.01	0.01
LOI	0.2	0.55	0.34	0.53	0.38	0.25	0.54
Total	100.81	100.15	100.61	101.28	100.36	100.86	100.73
Mg#	50.72	57.31	56.1	52.91	53.4	51.77	57.99
Trace elements(ppm)							
Cs	0.01	0.01	0.01	0.02	0.01	0.01	0.02
Ba	113.5	90.5	101.5	66.1	144	115.5	106
Rb	0.6	1.3	1	0.8	1.9	0.7	1.2
Sr	807	721	765	584	755	876	784
Y	18.4	12.3	12.1	22.1	12.9	14.7	12.5
Zr	113	24	40	147	60	48	33
Nb	6.2	1.4	1.9	5	1.3	4.2	2
Hf	2.8	0.8	1.2	3.5	1.5	1.3	1.1
Ta	0.4	0.1	0.1	0.2	0.1	0.3	0.1
Pb	2	2	2	2	2	2	2
P	1789.49	654.69	1309.38	2138.65	1876.79	1745.84	960.21
Ti	8033.3	5335.55	7194	10551.2	8932.55	7014.15	7433.8
Th	0.09	0.05	0.1	0.23	0.09	0.14	0.18
U	0.08	0.05	0.05	0.11	0.07	0.07	0.1
K	2739.43	89.57	89.57	89.57	179.13	89.57	89.57
Sc	22	22	21	28	21	18	21
V	258	246	288	379	334	240	265
Cr	90	150	140	140	100	70	150
Co	29	35	35	41	34	31	33
Ni	44	80	76	72	53	48	70
Cu	288	11	2	186	59	132	15
Zn	90	100	104	128	118	91	100
La	5.7	2.8	3.3	10.3	6.1	6	5.3
Ce	15.1	7.8	9.5	28.9	18	16	14.3
Pr	2.53	1.48	1.84	4.87	3.19	2.64	2.58
Nd	13.1	9.2	10.6	25.2	17.6	14	13.7
Sm	3.58	2.51	3.11	5.76	4.62	3.57	3.82
Eu	1.13	0.92	1.04	1.58	1.29	1.18	1.16
Gd	4	2.71	3.16	5.79	3.95	3.78	3.49
Tb	0.58	0.39	0.44	0.76	0.46	0.48	0.46
Dy	3.44	2.5	2.54	4.3	2.94	2.97	2.58
Ho	0.65	0.4	0.46	0.82	0.48	0.51	0.44
Er	1.93	1.35	1.3	2.47	1.33	1.63	1.3
Tm	0.32	0.19	0.17	0.36	0.2	0.24	0.17
Yb	1.86	1.18	1.24	2.1	1.13	1.3	1.16
Lu	0.25	0.21	0.16	0.3	0.15	0.21	0.14

University of Ghana http://ugspace.ug.edu.gh

Table 12: Major and trace elements composition.

	Pyroxene bearing Amphibolite		Fault Breccia	Pyroxenite
Sample	M5C	M5D	N58d	N58g
Major Elements (wt%)				
SiO_2	41	40.6	50.1	51
TiO_2	2.62	2.91	0.58	1.19
Al_2O_3	14.1	14.35	17.35	7.19
Fe_2O_3	14.65	14.8	6.99	16.75
MnO	0.13	0.13	0.09	0.27
MgO	11.2	10.9	2.88	14.1
CaO	11.4	11.35	19.05	8.03
Na_2O	2.76	2.73	0.11	1.31
K_2O	0.59	0.58	0.04	0.21
P_2O_5	0.83	0.87	0.08	0.14
Cr_2O_3	0.03	0.02	0.01	0.05
SrO	0.02	0.02	0.15	0.02
BaO	0.01	0.01	0.01	0.01
LOI	0.59	0.52	3.46	0
Total	99.93	99.79	100.89	100.27
Mg#	60.23	59.33	44.94	62.51
Trace elements (ppm)				
Cs	0.01	0.01	0.06	0.05
Ba	81.5	75.4	8.3	61.4
Rb	1.5	1	0.5	1.9
Sr	181	186	1275	180
Y	15	14.3	6	16.6
Zr	57	54	19	56
Nb	6.6	10	3.7	1.8
Hf	1.8	1.9	0.6	1.7
Ta	0.3	0.5	0.1	0.1
Pb	2	2	9	2
P	3622.62	3797.2	349.17	611.04
Ti	15706.9	17445.45	3477.1	7134.05
Th	0.09	0.05	0.05	0.21
U	0.05	0.06	0.05	0.07
K	4897.77	4814.75	332.052	1743.27
Sc	38	40	15	49
V	644	604	262	394
Cr	210	190	110	370
Co	63	64	16	71
Ni	132	123	51	189
Cu	81	9	1	16
Zn	169	178	32	179
La	5.5	5.3	1.9	3.8
Ce	18	17.7	4.8	11.3
Pr	3.33	3.38	0.83	1.95
Nd	18.8	18.8	4.2	11.2
Sm	4.78	5.2	1.05	2.94
Eu	1.41	1.6	0.58	0.74
Gd	4.69	4.81	1.45	3.53
Tb	0.6	0.62	0.17	0.53
Dy	3.35	3.08	0.99	3.19
Ho	0.59	0.57	0.21	0.69
Er	1.51	1.36	0.65	1.85
Tm	0.19	0.21	0.08	0.28
Yb	0.87	1.04	0.61	1.69
Lu	0.13	0.14	0.08	0.27

University of Ghana http://ugspace.ug.edu.gh

4.3.2 Trace Element Geochemistry

The use of trace element data to characterize rocks is predicated on the assumption that, despite evidence for mobility of many trace and major elements during metamorphism (Rudnick and Presper, 1990), the preserved trace element concentrations mimic those of the protolith (Jahn, 1990). The rare earth elements (REEs), transition metals and other trace element concentrations found in the rock have been presented in Table 10, Table 11 and Table 12.

4.3.2.1 Rare Earth Element (REE)

A chondrite-normalised rare earth element (REE) diagram of the mafic garnet gneiss and its associated rocks were plotted together with lower crust and normal MORB (N-MORB) {Fig4.31). Chondrite values are from Boynton (1984). Lower crust values from Rudinick and Fountain (1995) and N-MORB values from Sun and McDonough (1989). The pyroxene garnet gneisses have very similar characteristics to the lower crust (LC). These rocks overall display fractionated patterns with an overall negative slope. They show moderate enrichment in the light rare earth rlements (LREEs) and depletion of the heavy rare earth elements (HREEs) which is similar to the LC with $(La/Yb)_N$ values between 1.57 and 5.89 and $(Ce/Yb)_N$ values between 1.62 and 5.06). The pyroxene garnet gneisses show slight enrichment in the LREEs compared to the middle rare earth elements (MREEs) with $(La/Sm)_N$ values between 0.77 and 2.13 and $(Ce/Sm)_N$ values of 0.84 - 1.83. These $(La/Sm)_N$ ratios show slightly elevated to nearly flat LREEs and MREEs patterns. These rocks again show positive Eu anomaly which resemble the LC. The Eu anomaly (Eu/Eu*)

University of Ghana http://ugspace.ug.edu.gh

ranges from 1.14 to 1.54 (Fig 4.31a). The garnet hornblende gneisses also displayed rare earth elements (REEs) pattern very similar to the pyroxene garnet gneisses and to the once exhibited by the Lower Crust (LC). They have $(La/Yb)_N$ values between 1.59 and 3.63 and $(Ce/Yb)_N$ values between 1.70 and 4.12 with $(La/Sm)_N$ values between 0.66 and 1.12 and $(Ce/Sm)_N$ values of 0.73 - 1.21. The Eu anomaly (Eu/Eu*) range from 0.83 to 1.07 (Fig 4.31b).

The pyroxene bearing amphibolites display enrichment in the LREEs with slightly high peaks of Nd and Sm. The HREEs are depleted. They have $(La/Yb)_N$ values of 4.26 and 3.43 and $(Ce/Yb)_N$ values of 5.35 and 4.40. The pyroxene bearing amphibolites show nearly flat to negative Eu anomaly (Eu/Eu*) with values of 0.90 and 0.82. The rocks have near similar characteristics to the Lower Crust (LC) (Fig 4.32c).

The fault breccia also has the geochemical characteristics just as the mafic garnet gneisses and the Lower Crust (LC) but shows a Dy trough. The fault breccia even though exhibits similar REEs patterns as the mafic garnet gneisses and the lower crust; it is depleted in the REEs compared to the mafic garnet gneisses. It shows slight enrichment to nearly flat LREEs. HREEs are relatively slightly depleted. It has $(La/Yb)_N$ value of 2.09 and $(Ce/Yb)_N$ value of 2.03 with $(La/Sm)_N$ values of 1.13 and $(Ce/Sm)_N$ values of 1.10 with slight positive Eu Anomaly (Eu/Eu*) of 1.43 (Fig 4.32d).

University of Ghana http://ugspace.ug.edu.gh

The pyroxenite shows similar REEs patterns as the mafic garnet gneisses with slight enrichment of LREEs and nearly flat HREEs. It has $(La/Yb)_N$ value of 1.51 and $(Ce/Yb)_N$ of 1.72, with slight negative Eu anomaly (Eu/Eu*) of 0.89 (Fig 4.32d).

University of Ghana http://ugspace.ug.edu.gh

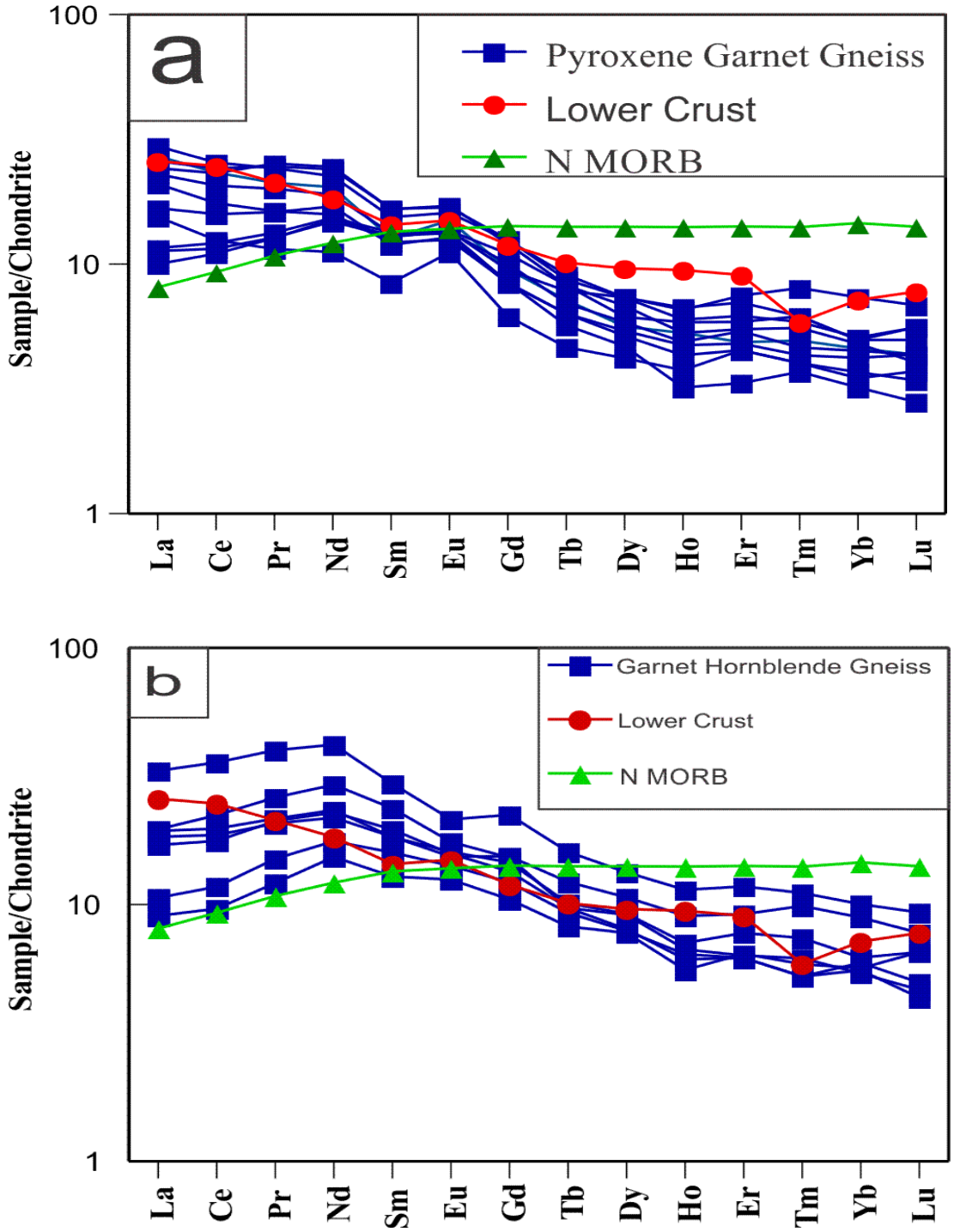

Figure 4.31: Chondrite-normalised plots of the REE composition of the rocks in the study area (a) Pyroxene garnet gneisses. (b) Garnet hornblende gneiss. With lower crust (LC) and Normal MORB (N-MORB).

University of Ghana http://ugspace.ug.edu.gh

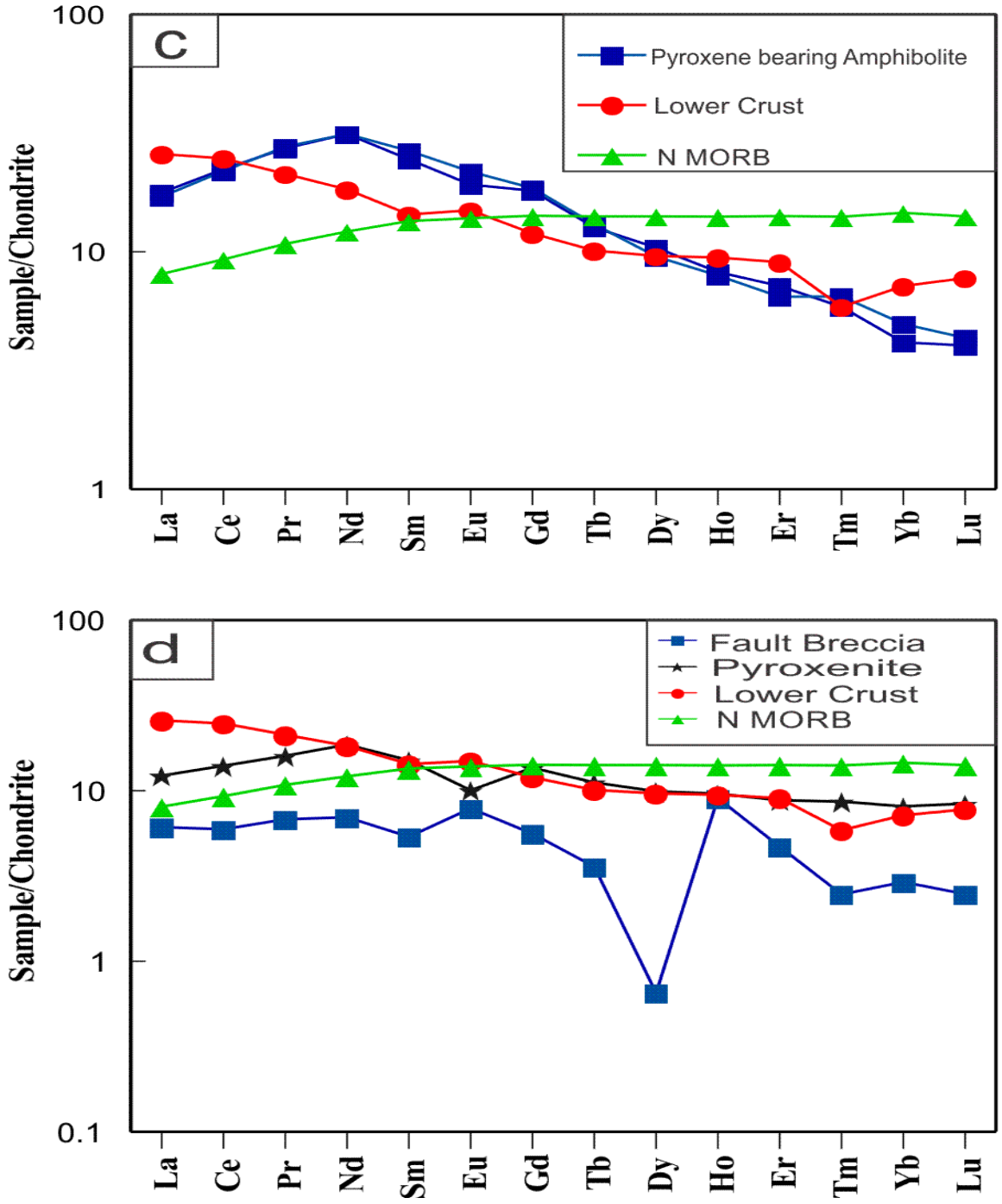

Figure 4.32: Chondrite-normalised plots of the REE composition of the rocks in the study area (c) Pyroxene bearing amphibolite (d) fault breccia and pyroxenite. With lower crust (LC) and Normal MORB (N-MORB).

University of Ghana http://ugspace.ug.edu.gh

4.3.2.2 Incompatible Trace elements

Figure 4.33 and Figure 4.34 show the incompatible trace element concentration in the rocks of the study area normalized to chondrite values from Thompson (1982) compared with Lower Crust (LC) and N-MORB. Lower Crust (LC) values are from Weaver and Tarney (1984) and N-MORB values from Saunder and Tarney 1984.

The pyroxene garnet gneisses and the garnet hornblende gneisses have similar patterns as the Lower Crust (LC). The depletion in Rb and trough by Th shown by the mafic garnet gneisses are very similar to the Lower Crust (LC). The positive peak of K is also very similar to the Lower Crust (LC). Enrichment in the Ba and Sr shown by the mafic garnet gneisses are also very similar to the Lower Crust (LC). The rocks display positive peak of Sr (Fig 4.33A and B). Generally, the mafic garnet gneisses display pattern similar to the Lower Crust (LC).

The trace element pattern depicted by pyroxene bearing amphibolite is similar to the Lower Crust (LC) and the mafic garnet gneisses, though they show slight depletion in Sr and has positive Ce anomaly. Generally, the pyroxene bearing amphibolites show more depletion in the incompatible especially Rb and Th and K (Fig 4.34C)

The fault breccia also shows more depletion of the mobile incompatible elements especially Ba, Rb, Th and K but show enrichment in Sr (Fig 4.34D). The pyroxenite also shows trace elements pattern similar to the Lower Crust (LC).

University of Ghana http://ugspace.ug.edu.gh

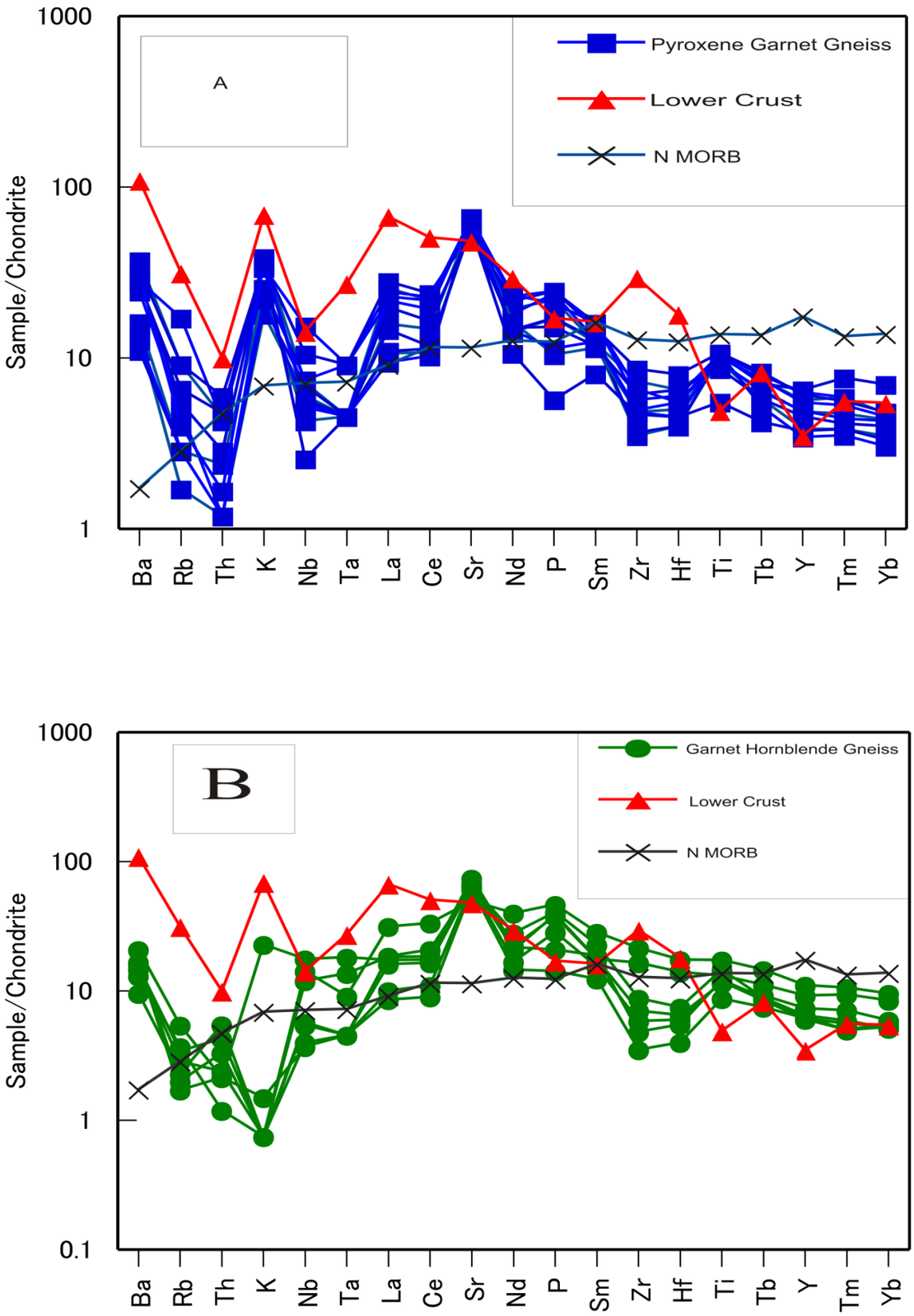

Figure 4.33: Chondrite normalized plots of the incompatible trace element composition of the rock in the study area. (A) Pyroxene garnet gneisses (B) Garnet hornblende gneisses

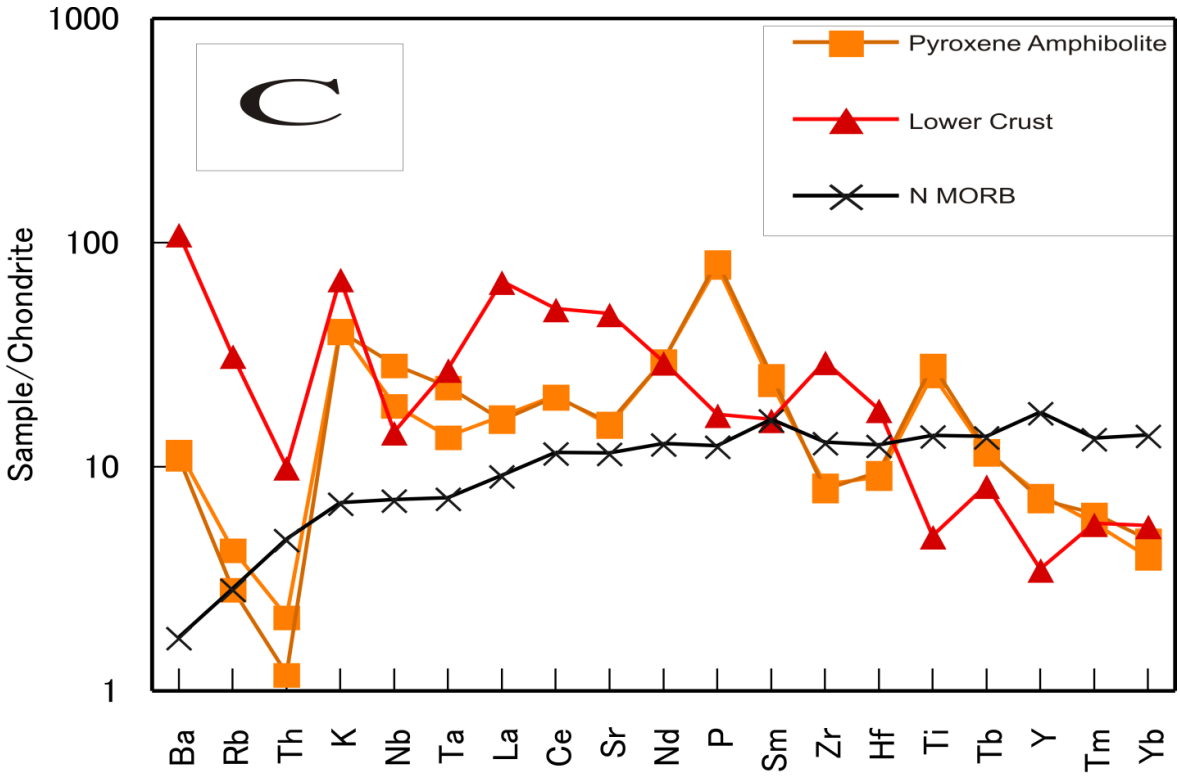

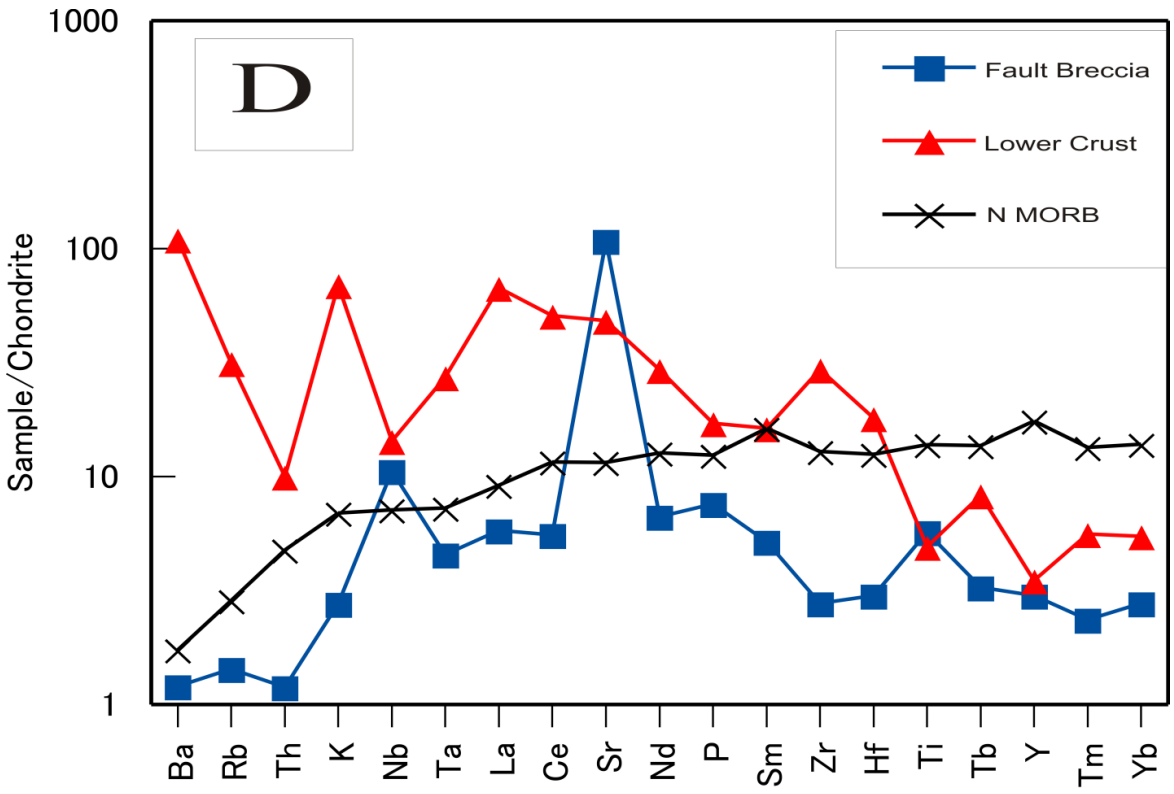

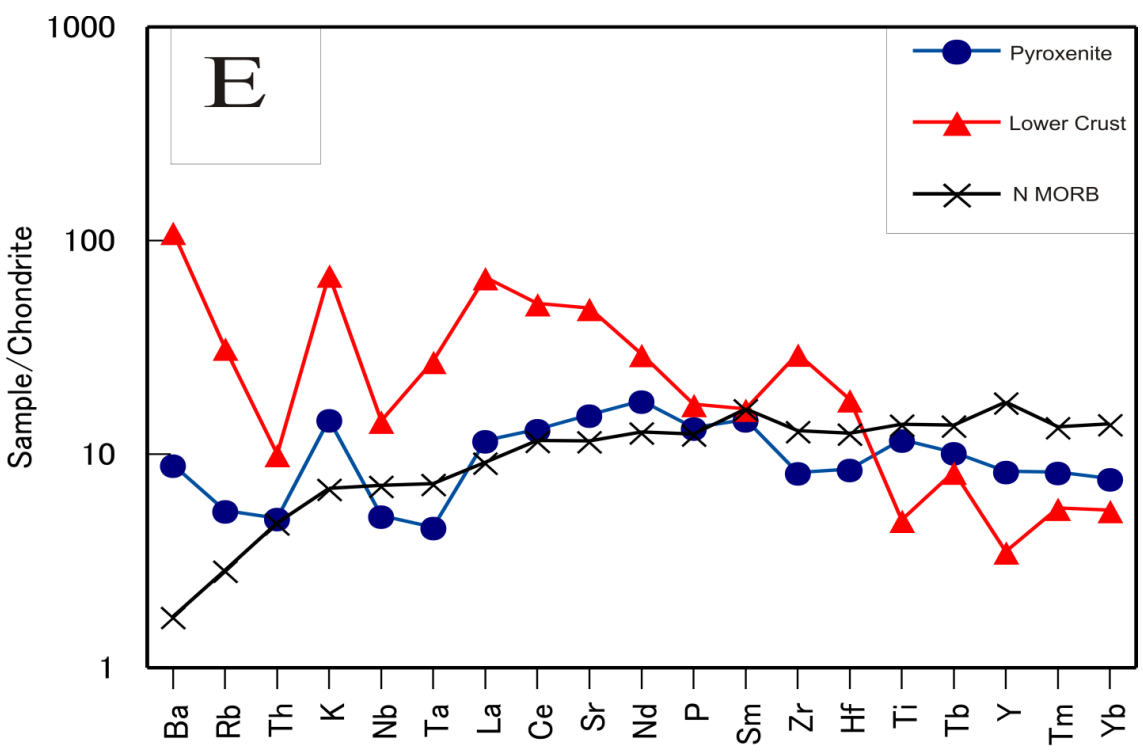

Figure 4.34: Chondrite normalized plots of the incompatible trace element composition of the rock in the study area. (C) Pyroxene bearing amphibolite (D) Fault breccia (E) Pyroxenite.

University of Ghana http://ugspace.ug.edu.gh

Figure 4.35 also shows the incompatible trace element concentration in the garnet mafic gneisses of the study area normalized to N-MORB values from Saunder and Tarney 1984 compared with Lower Crust (LC) and Island Arc Tholeiite (IAT). Lower Crust (LC) values are from Weaver and Tarney (1984) and IAT values from Attoh and Morgan (2004).

Imprints of IAT preserved in the mafic garnet gneisses are well exhibited by the pyroxene garnet gneisses. (Fig 4.35A). The pyroxene garnet gneisses exhibit almost the same pattern as the IAT with enrichment in the Large Ion Lithophile Elements (LILE) relative to N MORB and the High Field Strength Elements (HFSE) expecially Sr and Ba. The LILE behave differently from the High Field Strength Elements (HFSE) expecially Th and Yb which show nearly MORB like concentrations. The pyroxene garnet gneisses generally behave similar to the LC with the latter relatively enriched in the LILE compared to the pyroxene garnet gneisses.

The garnet hornblende gneisses also show similar pattern exhibited by the pyroxene garnet gneisses. (Fig 4.35B). The garnet hornblende gniesses exhibit almost the same pattern as the IAT though some of them exhibit depletion in K. They show very similar enrichment in the LILE just as the IAT compared to N MORB and then depletion in the HFSE which is nearly MORB like concentrations. They also behave similar to the LC with the LC relatively enriched in the LILE compared to the garnet hornblende gneisses.

Generally, the mafic garnet gneisses preserve imprints of IAT which is exhibited by close resemblance in their trace elements. Their trace elements pattern also looks similar to the LC with the LC more enriched in the LILE compared to the mafic garnet gneisses.

University of Ghana http://ugspace.ug.edu.gh

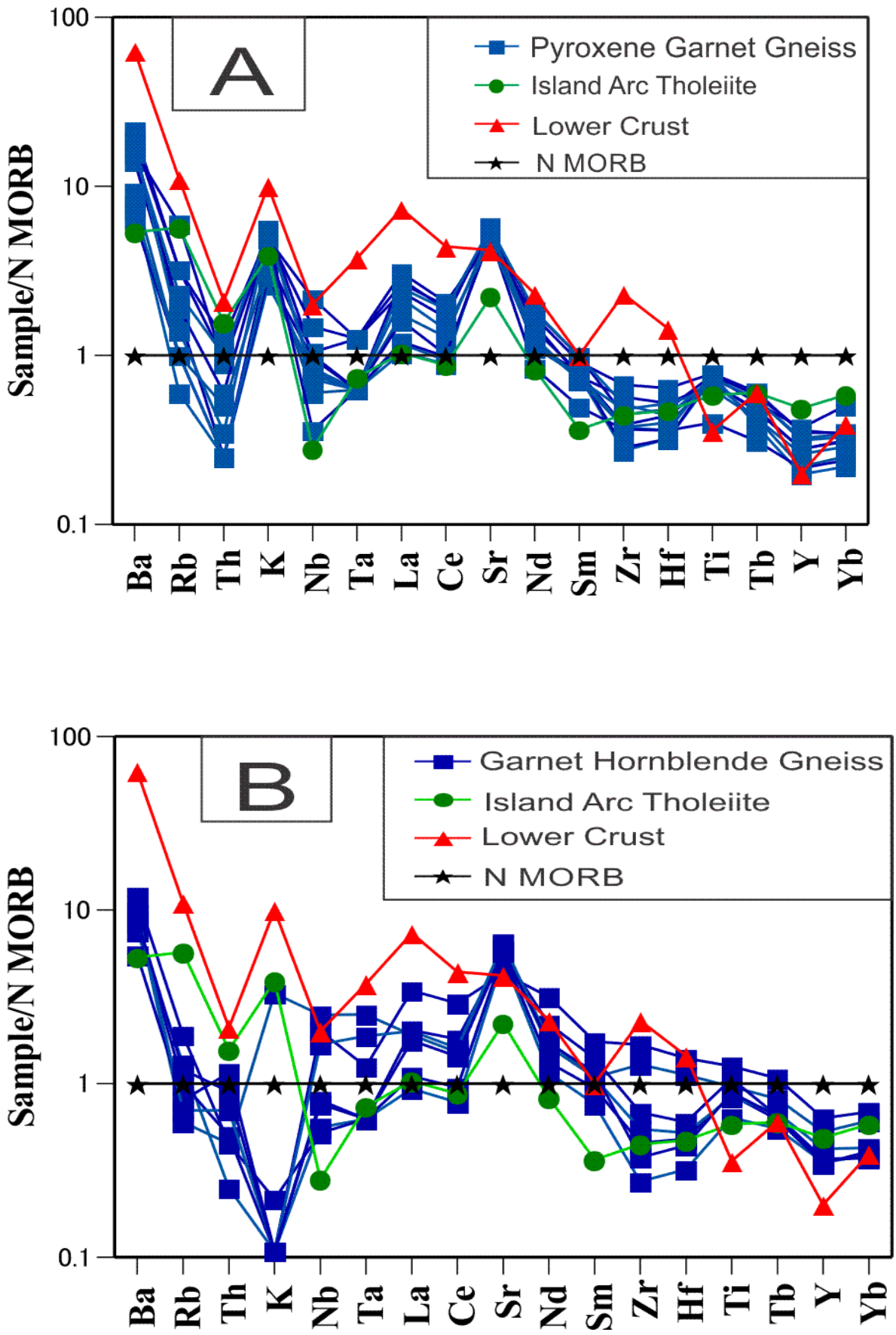

Figure 4.35: N MORB normalized plots of the incompatible trace element composition of the mafic garnet gneisses. (A) Pyroxene Garnet Gneiss (B) Garnet Hornblende Gneiss.

University of Ghana http://ugspace.ug.edu.gh

4.3.2.3 Transition elements

All the transition elements Scandium (Sc), Chromium (Cr), Titanium (Ti), Vanadium (V), Cobalt (Co), Nickel (Ni), Copper (Cu) and Zinc (Zn) are highest in the more mafic rocks. They are high in the pyroxenite and the pyroxene bearing amphibolite than the mafic garnet gneisses and the fault breccia (Tables 10 to 12).

These rocks are chondrite normalized with chondrite values from Langmuir et al. (1977). All the different rock types show similar patterns (Fig 4.36) and (Fig 4.37). They show progressive depletion from Ti to Ni. They display positive Ti anomaly and negative Cr and Ni anomaly. Anomalies in (Ni) and (Cr) concentration may reflect the role of olivine (Ni) and spinel (Cr) absence in the rock. Ti anomaly may indicate the role of Fe-Ti oxides present in the rocks.

University of Ghana http://ugspace.ug.edu.gh

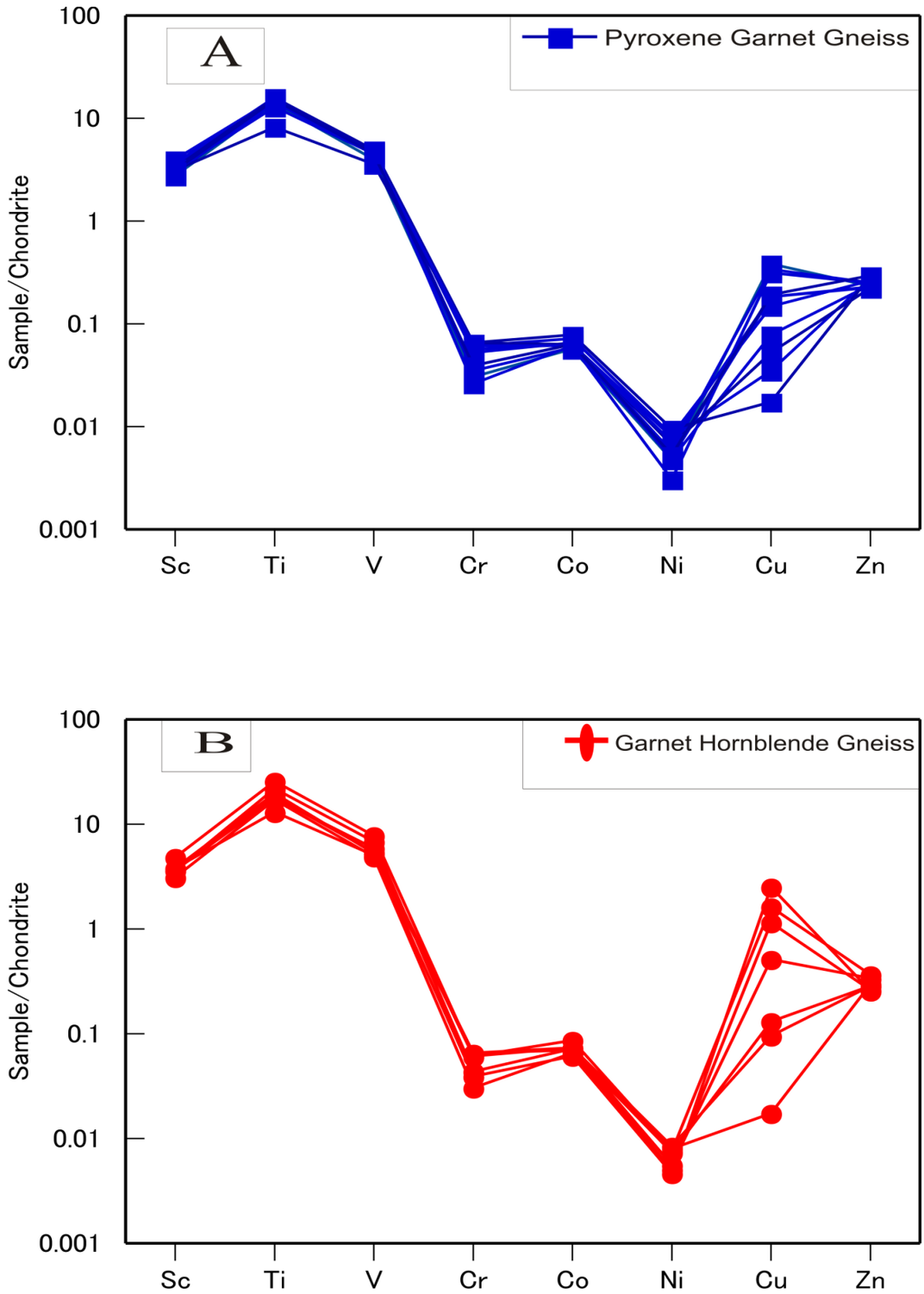

Figure 4.36: Chondrite normalized plots of transition element composition of the rocks in the study area. (A) Pyroxene garnet gneiss (B) Garnet hornblende gneiss.

University of Ghana http://ugspace.ug.edu.gh

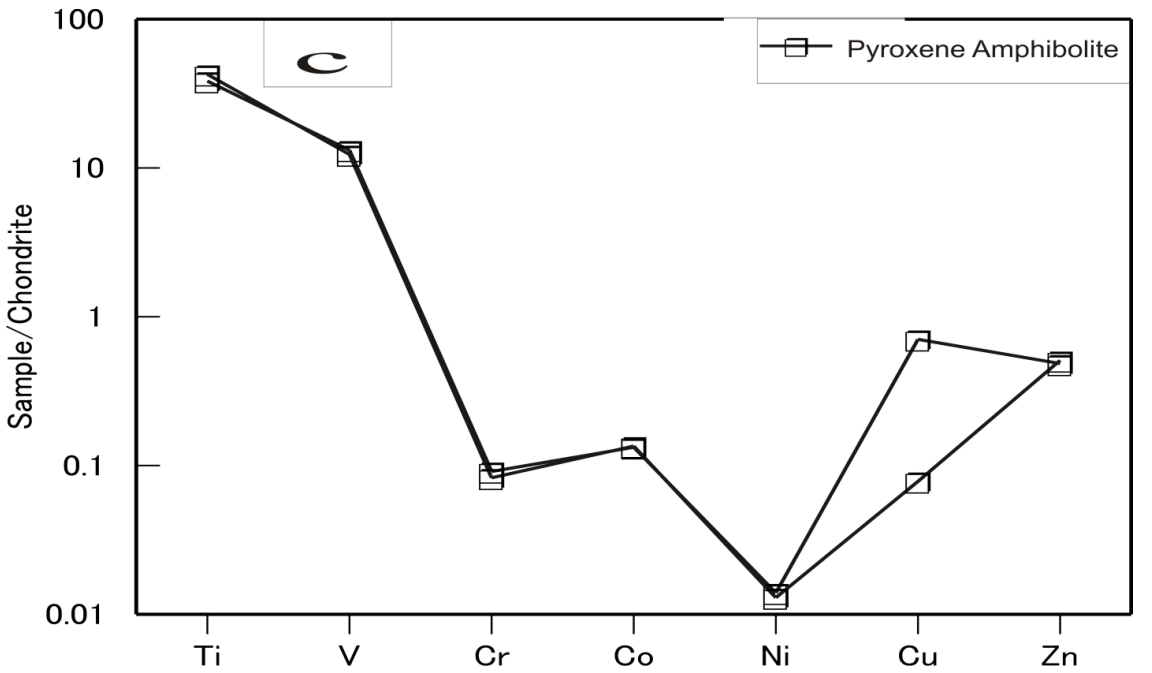

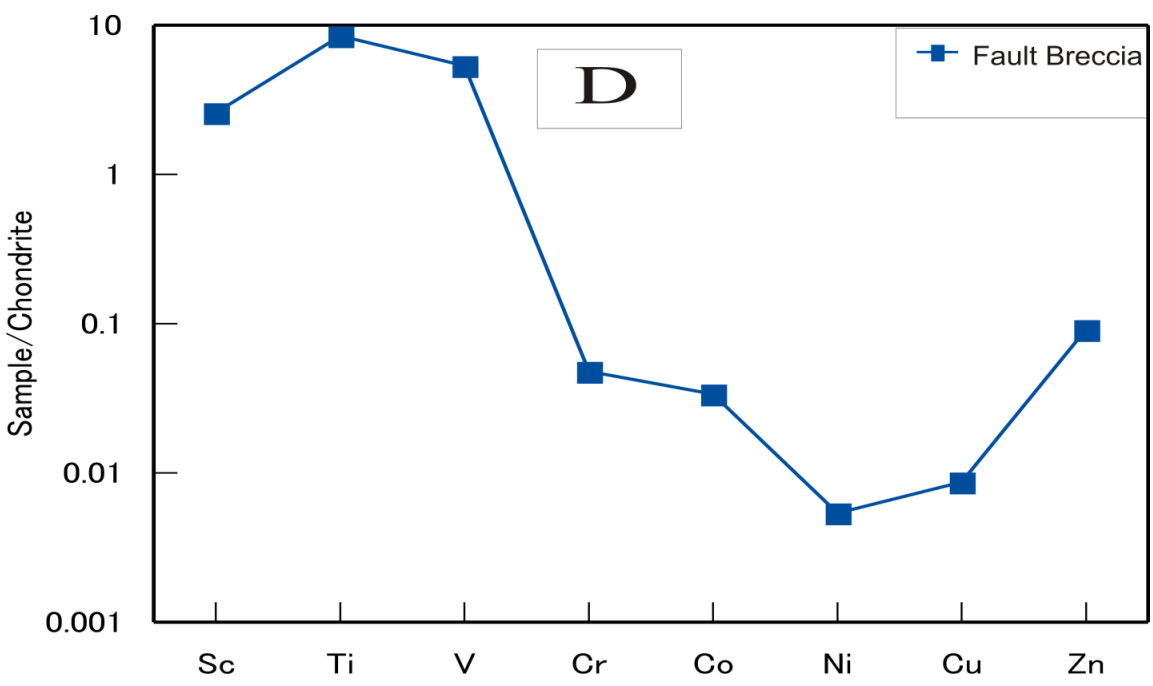

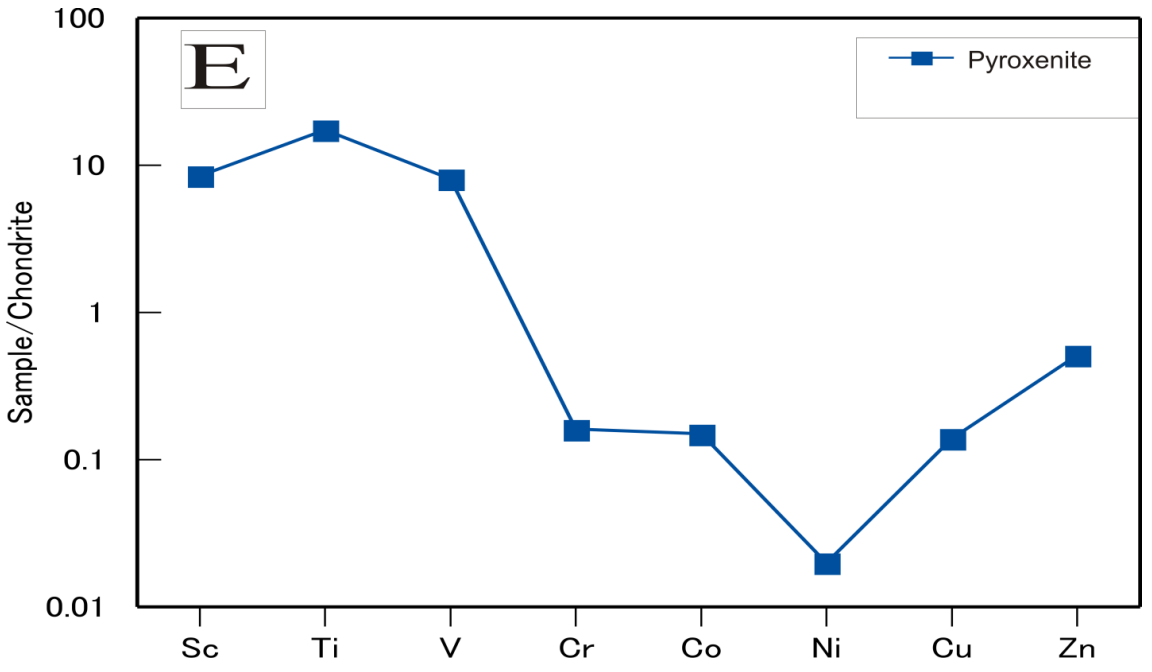

Figure 4.37: Chondrite normalized plots of transition element composition of the rocks in the study area. (C) Pyroxene bearing amphibolite (D) Fault breccia (E) Pyroxenite.

University of Ghana http://ugspace.ug.edu.gh

CHAPTER FIVE

5.0 DISCUSSIONS

According to Attoh (1990), the Dahomeyan structural unit as part of the Dahomeyide forms during the Pan African orogeny about (900-450) Ma. The suture zone consists of mainly mafic garnet gneisses. These gneisses are associated with pyroxene bearing amphibolite, pyroxenite rocks and a brecciated rock. The structures found in the gneisses are foliations, ptygmatic folds, faults, joints and fractures. From field evidences, structures, microstructures, textures and mineralogy, indicates that the mafic garnet gneisses have undergone different deformational events and have had different metamorphic episodes. Major and trace elements also suggest Island Arc Tholeiite (IAT) protolith for these rocks.

University of Ghana http://ugspace.ug.edu.gh

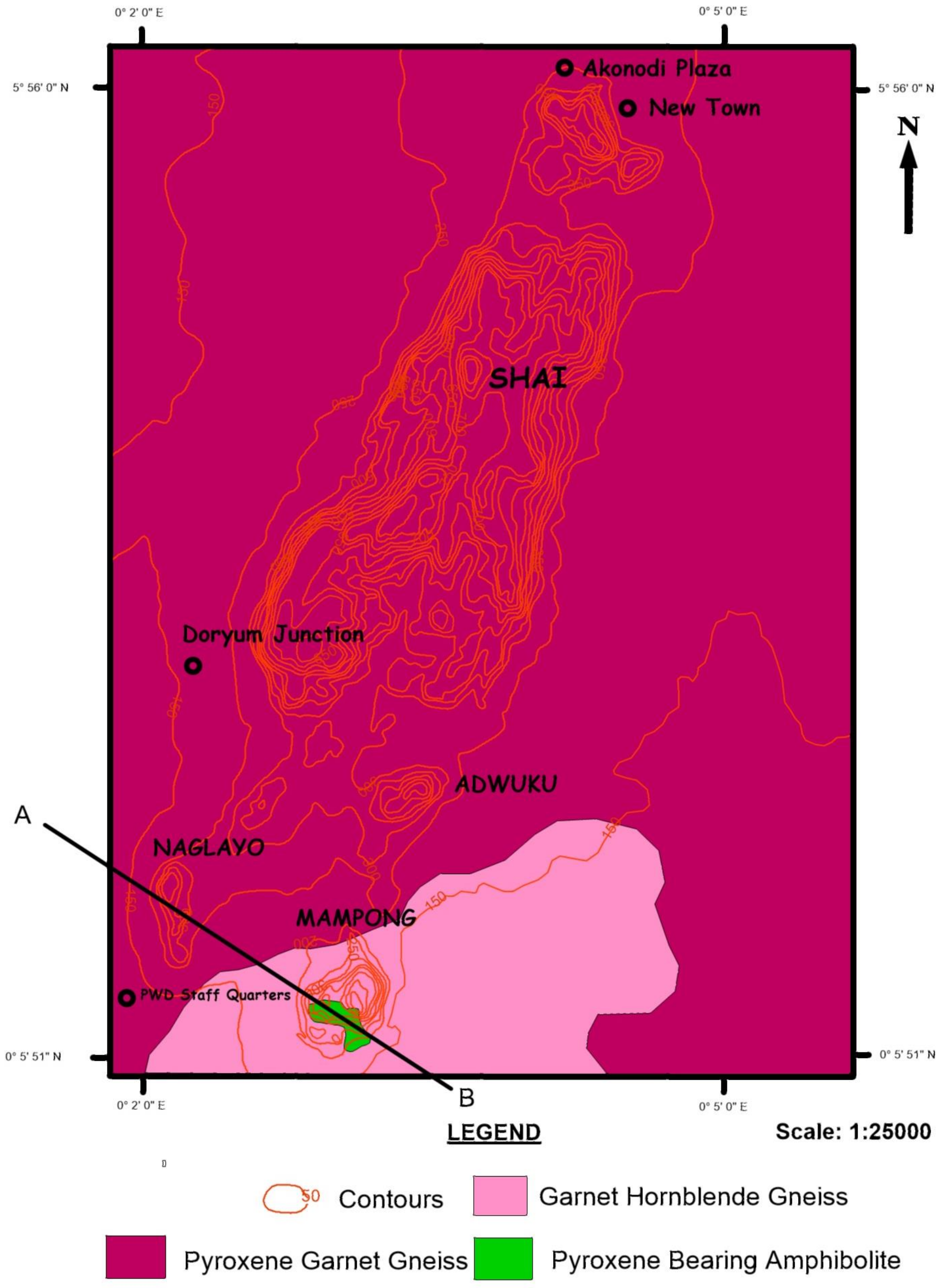

Figure 5.1: Geological map of the area.

University of Ghana http://ugspace.ug.edu.gh

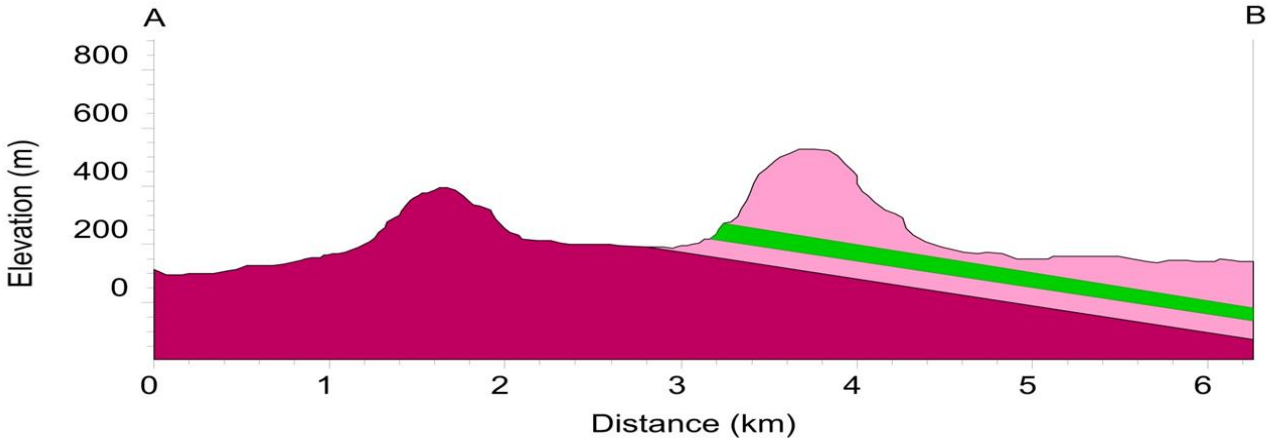

Figure 5.2: Cross section of the Study area.

University of Ghana http://ugspace.ug.edu.gh

5.1 Field Relation and Petrography

The geology of the study area is mainly characterized by the mafic garnet gneisses, with pyroxene bearing amphibolite, fault breccia and pyroxenite associations. The mafic garnet gneisses in the area are made up of the pyroxene garnet gneisses, and garnet hornblende gneisses (Fig 5.1). The pyroxene garnet gneisses and the hornblende garnet gneisses have the same composition and are distinguished using the modal composition. They together form the mafic garnet gneisses characterizing the suture zone of the Pan African belt in Ghana. The pyroxene garnet gneisses outcrop mainly at the Naglayo hill and the Shai forest reserve with the garnet hornblende gneisses outcropping at the Mampong hill. These gneisses are strongly sheared, deformed, sheared foliated and recrystallized. In the extremely sheared and deformed mafic garnet gneisses, they look homogenous with some parts quite heterogeneous, consisting of well-formed bands. This is due to planar and zonal differential shearing deformation and intense recrystallization (Kutu et al., 2014). The occurrence of high temperature and pressure metamorphic minerals such as pyroxenes and garnet indicate high intensity of metamorphism in the mafic garnet gneisses.

The mafic garnet gneisses are generally greyish and sometimes reddish as a result of the occurrences of abundant garnet in the rock. The garnet crystals are millimetric to centimetric. The different size of the garnet crystals is probably as a result of several generations of garnet minerals at different conditions. The abundance of garnet crystal in the mafic garnet gneisses indicates high metamorphic conditions of these rocks. Some garnet bands observed also suggest the intensity of metamorphism in the terrane. The streaky

University of Ghana http://ugspace.ug.edu.gh

appearance characterized by prominent discontinuous layers of garnet rich and hornblende rich zones in some localities are interpreted as shear induced (Attoh and Nude, 2008).

The gneissic white and dark bands and foliations found in these rocks also show that the mafic garnet gneisses were subjected to high degree of metamorphism. This gives indications of metamorphic differentiation during metamorphism where initially dispersed constituents segregate into layers of mafic minerals (dark compositional band) and silica rich (white compositional quartzo-feldspathic minerals) bands. This segregation happens as a result of either solution or redeposition via an aqueous phase governed by local pressure gradient, local melt segregation of minerals, diffusion controlled mineral development or segregation of minerals as a result of response to shear or stress differences (Stephens et al., 1979). Hornblende minerals developed in the quartzofeldspathic compositional band might have crystallized within the quartzofelspathic layers during the period of metamorphic segregations. These hornblendes are well sheared into sigma and delta shape probably during deformation as a result of non-coaxial shearing. Ptygmatic folds observed with the same composition in the area might have been formed as a result of partial melting of the quartzo feldspathic layers during early stages of exhumation.

Rotation of some garnet crystal and lenticular pyroxenite boudin observed in the gneisses may have formed as a result of non-coaxial or simple shearing during metamorphism. Pressure shadow of quartz observed around large garnet porphyroblast is formed during metamorphism where quartz is dissolved from the high stress (generally in the direction of the highest stress) and reprecipated in the low stress area adjacent to the porphyroblastic

University of Ghana http://ugspace.ug.edu.gh

garnet during metamorphism. Pressure shadow gives indication of direction of shearing during metamorphism. The halos of feldspar mostly observed around garnet suggest chemical reaction between garnet and pyroxene during metamorphism. The sigma and delta developed hornblende within the quartzo-feldspathic layers, together with asymmetrical pressure shadows around quartz form spectacular sets of kinematic indicators, which indicate SSW-directed thrusting of the suture zone rocks onto the West African Craton (WAC) margin (Attoh and Nude, 2008).

Under the thin section, the porphyroblastic nature of garnet, clinopyroxene and some plagioclase oriented in a granoblastic to granomatoblastic groundmass of plagioclase and quartz indicates high degree of metamorphism the rocks may have undergone. The porphyroblastic garnet and clinopyroxene minerals that are highly fractured, lenticular and mostly appear broken and are surrounded the S_1 external foliation are pre kinematic minerals; they formed prior to the formation of the S_1 foliation. The broken and highly cracked nature displayed by the clinopyroxenes indicates high degree of deformation they have undergone as a result of the later deformation experienced by the rocks. The broken nature of these minerals indicates the intensity of deformation the rocks have been subjected to. The external S_1 wrapped or compressed around the pre-kinematic porphyroblastic garnet and clinopyroxene is as a result of flattening in the matrix. The inclusions of hornblende and ilmenite in the porphyroblastic garnet and clinopyroxene show prograde metamorphism. They indicate that the hornblende and the ilmenite were formed prior to the formation of the porphyroblastic garnet and clinopyroxenes. The porphyroblastic garnet and clinopyroxenes might have enveloped the hornblende and ilmenite as they grow or evolve from them.

University of Ghana http://ugspace.ug.edu.gh

A porphyroblast can include a mineral that becomes a reactant in a later metamorphic reaction (Winter, 2001). This indicates that the hornblende inclusions may have formed the garnet and the clinopyroxenes. Furthermore, rims of hornblende and chlorite around these porphyroblast are as a result of retrograde metamorphism which there is introduction of water which alters them into low grade mineral. The corona texture of clinopyroxene surrounds porphyroblastic garnet observed in the thin section also indicates a replacement and reaction texture which did not react to completion (Winter, 2001). This may have occurred during retrogressive metamorphism in very early stages of exhumation. Replacement textures form during retrograde metamorphism (Winter, 2001).

Pre-kinematic and syn to post-kinematic garnets observed suggest different metamorphic episodes within the magic garnetiferous gneisses. This implies that the rocks were subjected to at least transitional states facies metamorphism. The pre-kinematic garnets may have formed synchronously with the pre-kinematic porphyrobalstic clinopyroxene and hence exhibit similar deformational and metamorphic features. They are broken with intracrystalline fractures, have anhedral shape and wrapped by S_1 foliation. They form prior to the formation of the later deformational and metamorphic events. The syn to post porphyroblastic garnet are less deformed relative to the pre-kinematic types and have well-formed shape compared to the prekinematic ones. They are the abundant garnet generation in the mafic garnet gneisses. Inclusions of pre-kinematic clinopyroxene in the core of these garnets indicate they formed after the clinopyroxenes had formed.

University of Ghana http://ugspace.ug.edu.gh

The presence of garnet megacrysts with ex-solved rods of rutile indicate ultrahigh pressure metamorphism as titanium is stable as a solid solution in garnet under high pressure (>3.0Gpa). This indicates that the rocks were subducted to mantle depths (Attoh and Nude 2008). Not only do the exsolution rods of rutile provide evidence of subduction and ultrahigh pressure metamorphism but they also provide evidence of exhumation and cooling as they occur when a Ti rich precursor precipitates excess Ti in response to decreasing Ti solubility during cooling or decompression (Zhang et al., 2003).

Plagioclase and quartz constitute the leucocratic and granoblastic groundmass in these mafic garnet gneisses. The plagioclase porphyroblast with bent twinning polysynthetic flexural twins and spectacularly abnormal extinction indicates deformations they have undergone by later deformational event. The yellow tint displayed by some plagioclase observed in the rocks is as a result of retrograde metamorphism of plagioclase into epidotes during late exhumation stage where there is influx of water. The undulatory extinctions displayed by quartz and plagioclase are formed as a result of strain and provide even more subtle evidence of metamorphism and deformation. They are formed probably by recovery and recrystallization during deformation. Sutured boundaries of quartz and some plagioclase also indicate recrystallization during deformations and metamorphism. Rutile is generally regarded as a characteristic constituent of basic rocks belonging to the eclogite and granulite facies (Knorring and Kennedy, 1958).

From the mineralogy of the rocks, it can be suggested that the rocks were formed from a basic or mafic protolith, possibly rocks of basaltic composition. The gneisses can therefore

University of Ghana http://ugspace.ug.edu.gh

be said to have formed from the subduction of the roots of an island arc (Attoh and Nude, 2008) to mantle depths where it was subjected to ultrahigh pressure and high pressure metamorphism and deformation by the collision between the West African Craton and exotic blocks from the east during the assemblage of NW Gondwana and subsequent exhumation.

The pyroxene bearing amphibolites are observed at the Eastern Quarries at the Mampong Hill. They are tectonically welded within the mafic garnet gneisses. These rocks are strongly deformed and sheared together with mafic garnet gneisses with gradational contact with the mafic garnet gneisses. The pyroxene bearing amphibolites are fine to medium grained dark rocks. The dark color of the rocks is as result of predominant mafic minerals present in the rocks with some plagioclase.

Under the thin section, the rock is predominantly made up of hornblende. They contain plagioclase with clinopyroxene and garnet. The presence of clinopyroxene and garnet indicates metamorphism at relatively higher temperature and pressure conditions and confirms that these rocks may have metamorphosed into the mafic garnet gneisses under higher temperature and pressure. The garnets have inclusion of hornblende and indicate prograde metamorphism. These rocks might have prograded into the mafic garnet gneisses under higher pressure and temperatures where most of the hornblende metamorphosed into garnet and clinopyroxenes and Na rich plagioclase into more Ca rich plagioclase.

The pyroxenites associated with mafic garnet gneisses may probably be older materials thrusted into gneisses. Some boudins formed from these pyroxenites indicate that these

University of Ghana http://ugspace.ug.edu.gh

pyroxenites may be older than the mafic garnet gneisses. They are thrust along the foliations in the mafic garnet gneisses. These rocks are fine to medium grained dark colored rock. These pyroxenites are also tectonically deformed together with the mafic garnet gneisses. Under thin section, the pyroxenite is made up of variable proportions of orthopyroxenes and clinopyroxenes. These mineral show highly intracrystalline fractures and mostly with anhedral shapes. This indicates deformation the pyroxenite may have undergone.

The brecciated rock found within the mafic garnet gneisses at PW quarries were formed as a result of cataclasis and crushing in fractures within the gneisses as a result of brittle deformation at relatively lower temperature and pressure. Microscopic observation of the fault breccia indicates a mortar texture of porphyroclast of quartz surrounded by crushed matrix derived by cataclasis and recrystallization. It indicates that the quartz minerals are pre-kinematic to the cataclasis.

5.2 Metamorphism

On the basis of microstructures, mineral assemblages and reaction relations between mineral phases, at least four metamorphic episodes can be established for the mafic garnet gneisses in the area. It encompasses early prograde metamorphism to peak granulite facies stage or episode and then later retrogression metamorphic stages. The early prograde metamorphism is preserved only as inclusion of prograde hornblende and ilmenite within porphyroblastic garnet and clinopyroxenes. These textural features suggest that the mafic garnet gneisses have a prograde history prior to the peak granulite metamorphism.

University of Ghana http://ugspace.ug.edu.gh

Peak metamorphism is represented by granulite facies assemblage. The granulite stage is characterized by the deformed porphyroblastic garnet (Grt), clinopyroxene (Cpx) and some plagioclase (Pl) and quartz mineral assemblages (Cpx + Grt + Pl + Qtz).

The next metamorphic stage is the hornblende-granulite stage and characterized by crystallizations of porphyroblast garnet (with inclusions of rutile exsolusion, ilmenite and earlier formed clinopyroxenes), recrystallization of plagioclase (Pl) and quartz (Qtz), development of dark reddish brown hornblende (Hbl) and corona texture of clinopyroxene (Cpx) around garnet. This stage is characterized by probable early stages of exhumation.

The crystallization of green hornblende rims around some porphyroblastic clinopyroxenes and garnet characterize retrogressive amphibolite stage during exhumation via extensional decompression. Crystallization of green fibrous chlorite around clinopyroxene and garnet, and alteration of plagioclase to epidote define retrograde greenschist facies metamorphic stage. This might have happened as a result of influx of water near the earth surface.

5.3 Deformations, Structures and Kinematics

The area has undergone several regimes of tectonic and metamorphic events, thus, most of the rocks show numerous deformational structures. Different deformational events characterize the mafic garnet gneisses in the suture zone. The structures observed in the study area are foliation and banding, ptygmatic folds, faults, fractures joints and boudins. This implies that the rocks have undergone both brittle and ductile deformational phases. Three main deformational events may have occurred in the suture from its prograde history to the later successive retrograde episodes.

University of Ghana http://ugspace.ug.edu.gh

5.3.1 D_1 Deformation

The gneissic banding observed in the gneisses indicates the gneisses were subjected to high temperature and pressure regimes that segregated the felsic and mafic minerals into bands. This gives indications of metamorphic differentiation during metamorphism where initially dispersed constituents segregate into layers of mafic minerals (dark compositional band) and silica rich (white compositional quartzo-feldspathic minerals) bands. The general trend of these structures is NE-SW direction with few having NNE-SSW direction with gentle dips towards SE. This may imply that the direction of maximum strain that formed the foliations acted perpendicularly to the general NE-SW trend. These are formed during compression with the maximum NW/SE stress causing the rocks to strain or deformed in the NE/SW direction. Deformation of the terrane and the rocks was intense and by compressional thrusting and shearing with the direction of tectonic transports from the SE to NW in a craton-ward vergence on subparallel thrust planes (Kutu et al., 2014).

The stereo plot, confirms that the foliations in the mafic garnet gneisses have predominantly southeasterly dip direction with gentle dips. The contoured poles–density plot indicated that majority of the poles are concentrated close to the center which shows that the foliations in the area is of gentle dip. These foliations are therefore S_1 fabric structures in the area.

The sigma and delta shaped hornblende within the quartzofeldspathic compositional bands represent L_1 fabric mineral lineation in the rock. They give indications of simple non coaxial shearing in the area during D_1 deformation. Structural attitudes indicated that the L_1 mineral lineations have moderate average plunge of 15^0 mainly toward SW and NE also indicating

University of Ghana http://ugspace.ug.edu.gh

that the direction of maximum shearing direction is from the NW/SE. The pole plot indicates NE/SW trend of the mineral lineations with gently plunge of NE mainly.

The older pyroxenite materials were thrusted into the mafic garnet gneisses during the main D_1 deformation. The boudins formed as a response to layer parallel extension or layer perpendicular flattening of the stiff pyroxenite materials. They stretch as a result of ductile contrast of less competent participating layers or rocks.

The gneissic bands, foliations and the mineral lineations in the rocks are characterized by D_1 deformational event. The D_1 deformational event produced the S_1 and the L_1 structural fabric in the rocks. A simple or non-coaxial shearing characterizes this deformational event. Shear sense indicators during D_1 deformational events are mainly dextral and are represented by sheared pyroxenite boudin within the mafic garnet gneiss (Fig 4.24), clockwise rotation of garnet minerals (Fig 4.25) and the stretched hornblende mineral lineation into sigma and delta structure within the felsic compositional bands (Fig 4.22). This indicates that rock have undergone a non-coaxial shearing during D_1 deformation. The foliations and mineral lineation characterizing the D_1 deformational event indicates that the deformation is a ductile deformation which occurred in high temperature regime.

5.3.2 D_2 Deformation

The ptygmatic fold observed clearly crosscut the foliations. It shows that they postdate the foliations in the rocks. The ptygmatic folds have the same composition as the felsic

University of Ghana http://ugspace.ug.edu.gh

compositional bands within the rocks. Figure 4.3b indicates a felsic compositional bands folded into ptygmatic folds. I therefore suggest most of the folding with composition as the felsic compositional bands is ptygmatic folds, formed as a result of partial melting of the felsic bands in the rocks within the rock. They might have been formed as a result of decompression during early stages of exhumation of the mafic garnet gneisses in which temperature might have remained relatively constant with decreasing pressure and addition of some volatiles. During this stage, the felsic bands with relatively lower melting point and viscous may have experienced decompressional melting, which then might have melted and begin flowing within the mafic garnet gneisses. The mafic bands may have not melted at this stage because of the higher melting point of mafic minerals. These ptygmatic folds characterize the D_2 deformational event in the area.

Upon axial measurements of folds axis, it was observed that they are of different orientations. Some have NE/SW trend and others with NW/SE trends with average of 25^o plunge. From the stereographic poles plot these folds trend SW/NE and SE/NW with average plunge of 15^0 SW and SE respectively indicating flow in different directions of the melted felsic compositional bands. Deformation at this stage is ductile deformation.

5.3.3 D_3 Deformation

The last stage of deformation D_3 is characterized by the development of brittle deformational structures. They are faults, fractures and joints. The brittle faults (Fig 4.3c) crosscut the D_1 and D_2 deformational structures. This indicates that the brittle deformational event postdate the ductile deformation in the area. It gives indications that the brittle deformations are

University of Ghana http://ugspace.ug.edu.gh

youngest among the deformation in the area. Deformation moves from ductile to brittle as a result of exhumation and subsequent retrogressive metamorphism. The changing of deformation from ductile to brittle indicates prograde metamorphism and then later retrogressive metamorphism. Deformation becomes brittle as a result of decompression and exhumation where the rocks get closer to the surface with temperature decrease. These faults seen mainly in the area are normal faulting where the hanging wall have moved down relatively to the footwall as a result of extension during decompression. This gives indication of crustal extension during exhumation.

These normal dip slip faults have moderate dips with two different direction of dip. These faults mainly dip SW and strike NW/SE with few having a NW dip direction and NE/SW strike. The predominant NW/SE strike of the faults indicates extension in the NW/SE and compression in NE/SW direction during extension. This shows that direction of maximum stress during compression experiences maximum extension during dilation or extension. From the stereographic pole plots, it can be inferred that the faults have moderate dips with average of about 35^0 to 40^0.

The thrusted rigid older materials (pyroxenite) within the mafic garnet gneiss are fractured and exhibit dextral displaced grains but have overall sinistral sense of shearing during D_3 deformation (Fig 4.29).

In summary, the Shai Hills gneisses have undergone series of deformational and metamorphic events. They have undergone prograde metamorphism as a result of the subduction to the granulitic facies which have clinopyroxenes and garnets as stable mineral

University of Ghana http://ugspace.ug.edu.gh

assemblages at high temperature and pressure. Textural evidence is the inclusions of hornblende and ilmenite, in porphyroblastic clinopyroxene and garnet. Exhumations of these rocks occurred as a result of decompression and went through to the amphibolite facies and to greenschist facies during retrograde metamorphism

5.4 Geochemistry

5.4.1 Classification

Classifications diagrams by Le Bas et al. (1986), and Cox et al. (1979), were plotted (Fig 5.3a and Fig 5.3b) for the mafic garnet gneisses in the study area. According to Le Bas et al, (1986) classification, the pyroxene garnet gneisses plot as basalts, basaltic andesites, basaltic trachy andesites and trachy andesites. The garnet hornblende gneisses plot in basalt and trachy basalt fields. The fault breccia is classified as basalt. In the Fig 5.3 b, the pyroxene garnet gneisses plot in basalt, basaltic andesite and trachy andesite field with garnet hornblende gneisses ploting in the basalt field.

University of Ghana http://ugspace.ug.edu.gh

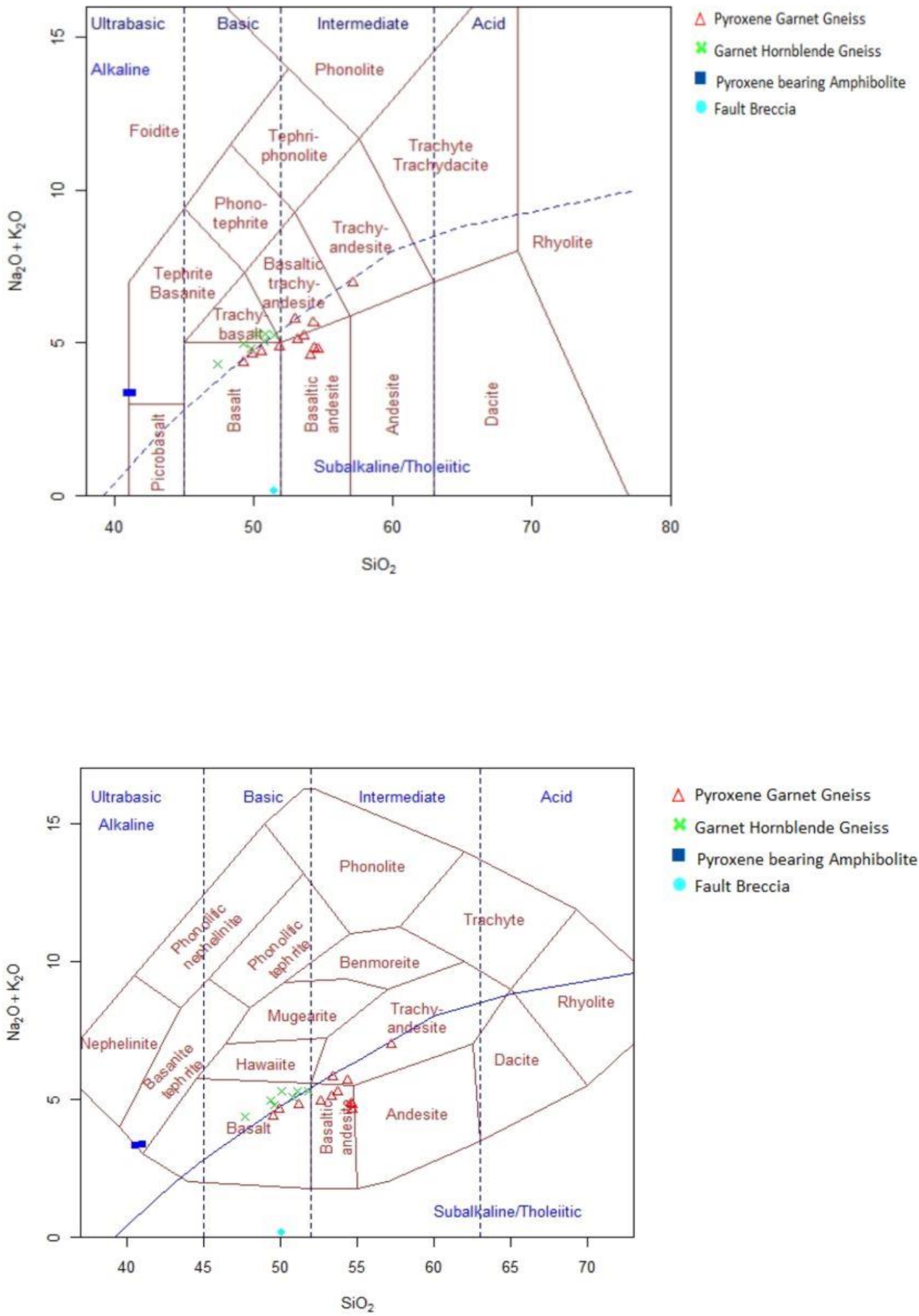

Figure 5.3: Geochemical classifications of rocks in the study area using TAS diagram (a) Le Bas et al., (1986) (b) Cox et al., (1979).

University of Ghana http://ugspace.ug.edu.gh

According to Cox et al. (1979)'s scheme, the mafic garnet gneisses mostly classify as subalkaline/tholeiitic series rocks. On the classification plot of SiO_2 versus K_2O of Peccerillo and Taylor., (1976) (Fig 5.4), the rocks plot mainly in the low K tholeiitic series. Almost all the pyroxene garnet gneisses plot in the low K tholeiitic field. The garnet hornblende gneisses plot also in the low K tholeiitic fields with few fallling in the calc alkaline series field.

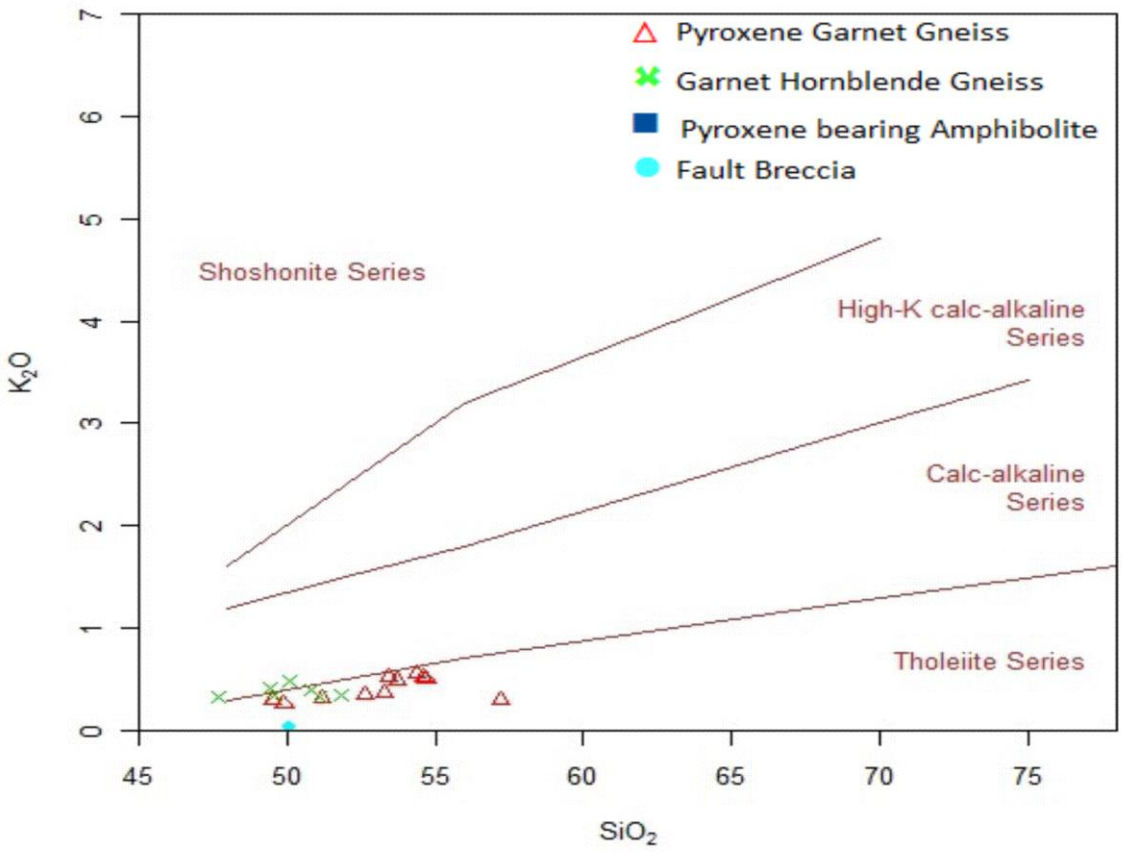

Figure 5.4: Classification plot of SiO_2 Versus K_2O (after Peccerillo and Taylor, 1974).

University of Ghana http://ugspace.ug.edu.gh

5.4.2 Tectonic Setting

The tectonic settings of the mafic garnet gneisses in the study area have been discussed using mostly immobile elements and their ratios and some major elements. Numerous discrimination diagrams have been plotted for the mafic garnet gneisses and its associated rocks. This work thus mainly relied on high field strength immobile elements such as Ti, Zr, Y, Nb, and immobile transition elements such Cr and some major elements in discussing the tectonic setting. These immobile elements may be less affected by metamorphic processes compared to the mobile trace elements. Furthermore, despite evidence for mobility of many trace and major elements during metamorphism (Rudnick and Presper, 1990), the preserved trace element concentrations mimic those of the protolith (Jahn, 1990).

Figure 5.5 shows a Cr versus Y plot of these mafic garnet gneisses to distinguish basalts with N-MORB compositions from those of island arc tholeiite affinities (Pearce et al., 1984). The Cr and Y discriminates effectively between MORB and volcanic arc basalts, with small amount of overlap between the two fields. Y is more depleted in volcanic basalts relative to other basalt. The mafic garnet gneisses fall broadly in the field of Island Arc tholeites (IAT). They showed depletion in Y with respect to MORB but with wide range of Cr contents.

University of Ghana http://ugspace.ug.edu.gh

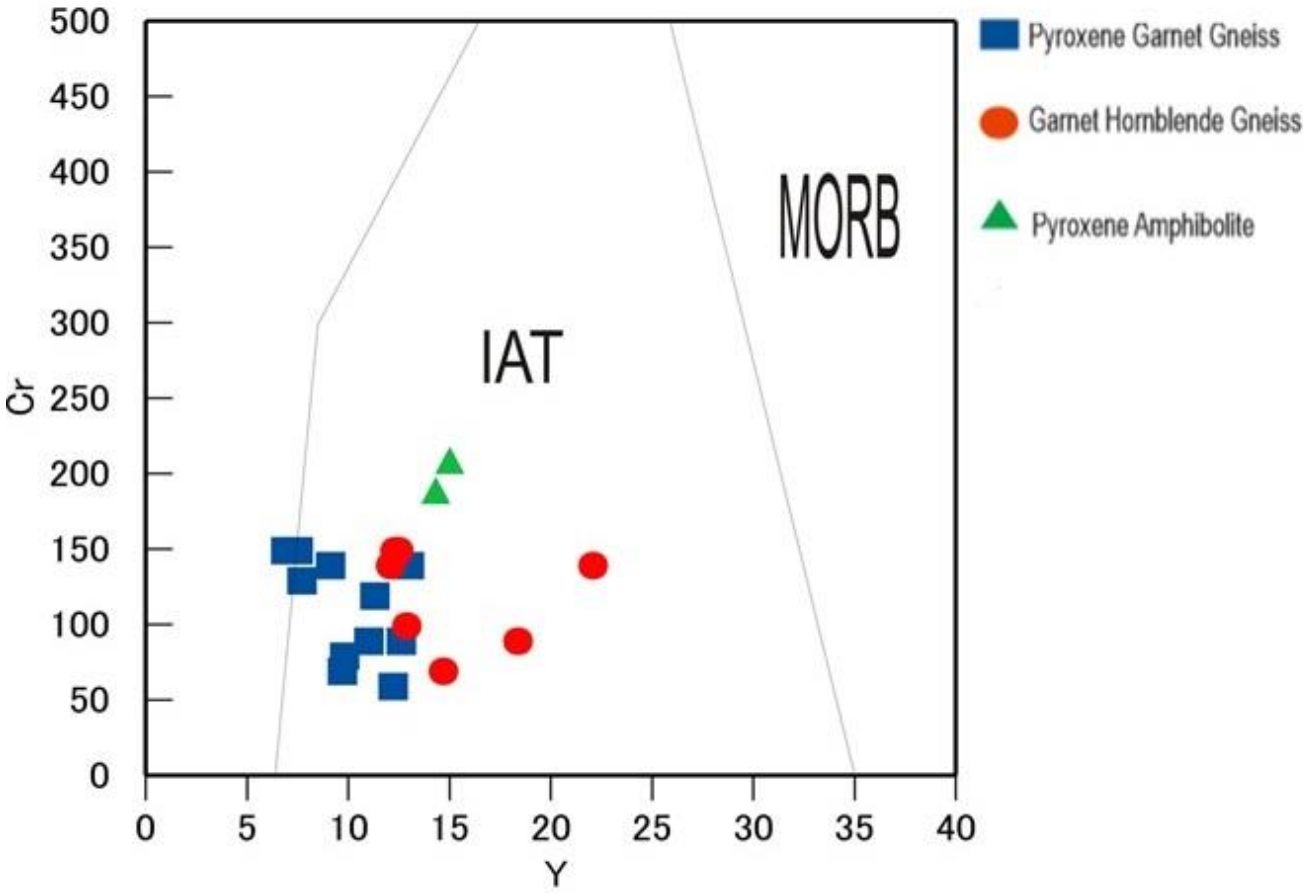

Figure 5.5: Tectonic discrimination diagram Cr vs Y plot (Fields for MORB and IAT after Pearce et al., 1984)

Pearce and Can (1973) proposed the Ti-Zr diagram which can be used to infer the tectonic setting of basalts. The diagram has four fields. Field A contains island arc tholeiites, C contains calc alkaline basalts and D contains MORB. Field B contains all three types (Fig 5.6). Most of the pyroxene garnet gneisses plotted in field A, the garnet hornblende gneisses plotted within Field A, B with two samples plotted within Field D.

University of Ghana http://ugspace.ug.edu.gh

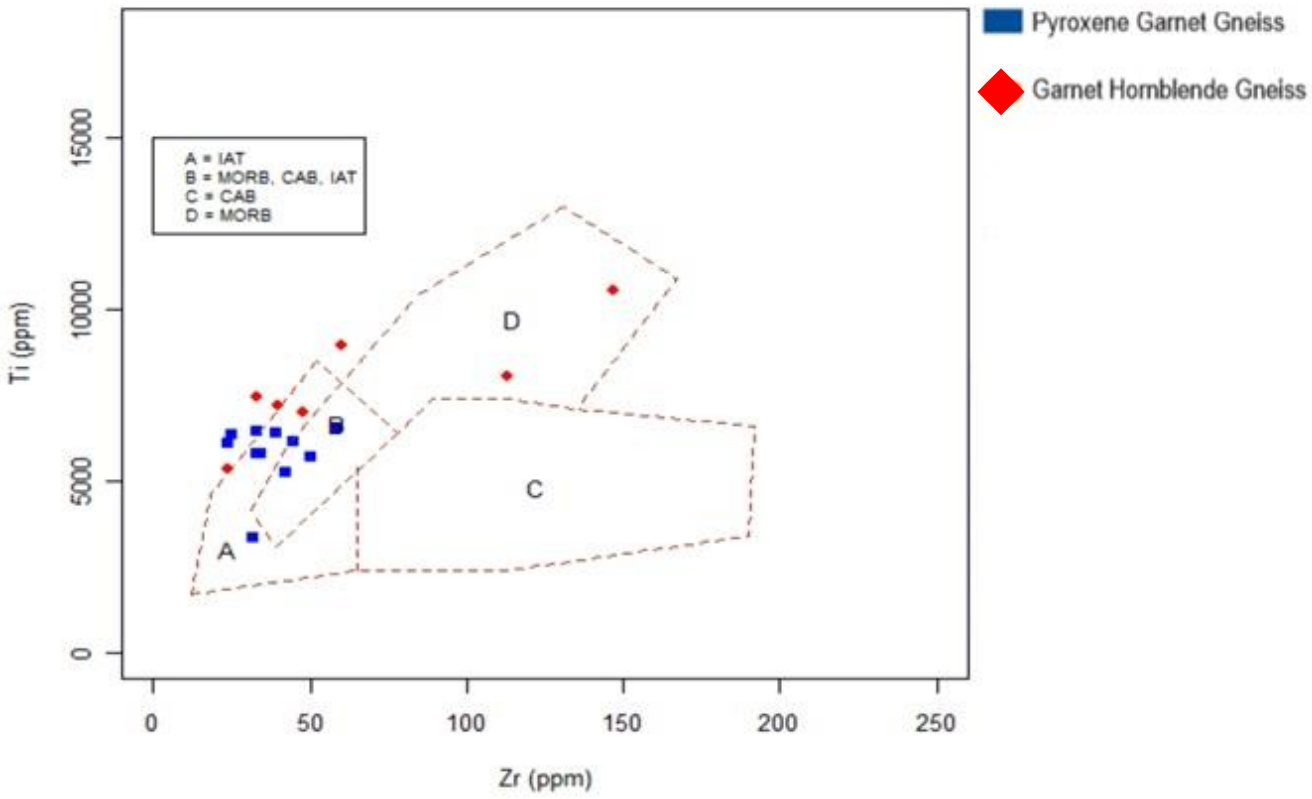

Figure 5.6: Tectonic discrimination diagram of Ti vs Zr plot (Pearce and Can, 1973)

Pearce et al., (1977), proposed MgO-FeO-Al_2O_3 discriminatory tectonic diagram to distinguish between different basalts from different tectonic environments. It applies to subalkaline basalts and basaltic andesites. This diagram discriminates between the following tectonic environments; ocean ridge basalt and floor basalts (MORB), ocean island basalts, continental basalts, volcanic arc basalts and active continental margin basalts and island arc basalts, and spreading centre basalts (Fig 5.7). Almost all the samples plotted in the island arc and active continental margin that is the orogenic field.

University of Ghana http://ugspace.ug.edu.gh

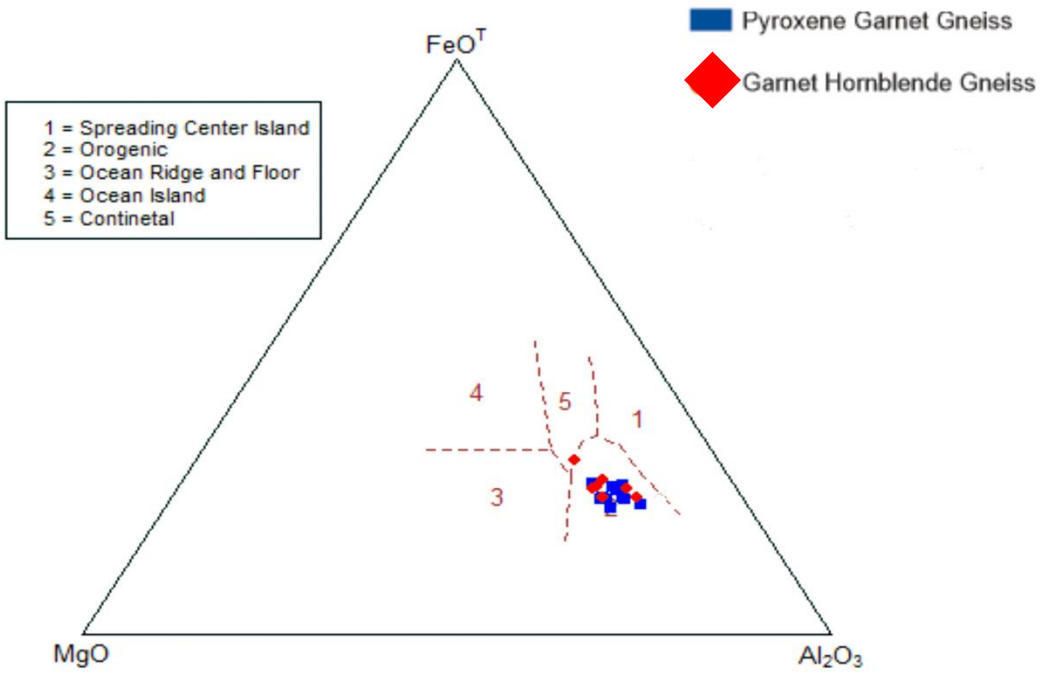

Figure 5.7: Tectonic discrimination diagram of MgO-FeO-Al2O3 (Pearce et al., 1977).

Although major elements discriminant diagrams are proposed for relatively unaltered basaltic rocks, it is used here to compare the concentrations of these elements in the mafic garnet gneisses with those estimated for basaltic rocks formed in various tectonic environments

Mullen (1983) proposed a discriminatory diagram for Basalt and basaltic andesites with silica content from 45 to 54 wt% using MnO_2, TiO_2 and P_2O_5 concentrations. This diagram

University of Ghana http://ugspace.ug.edu.gh

discriminates the following; MORB, ocean island tholeiites; ocean island alkali basalts; isaland arc tholeiites; calc alkaline basalts (Fig 5.8).

The samples plotted mainly in the island arc basalts fields and the ocean island alkali basalts (OIA) with few in the MORB fields.

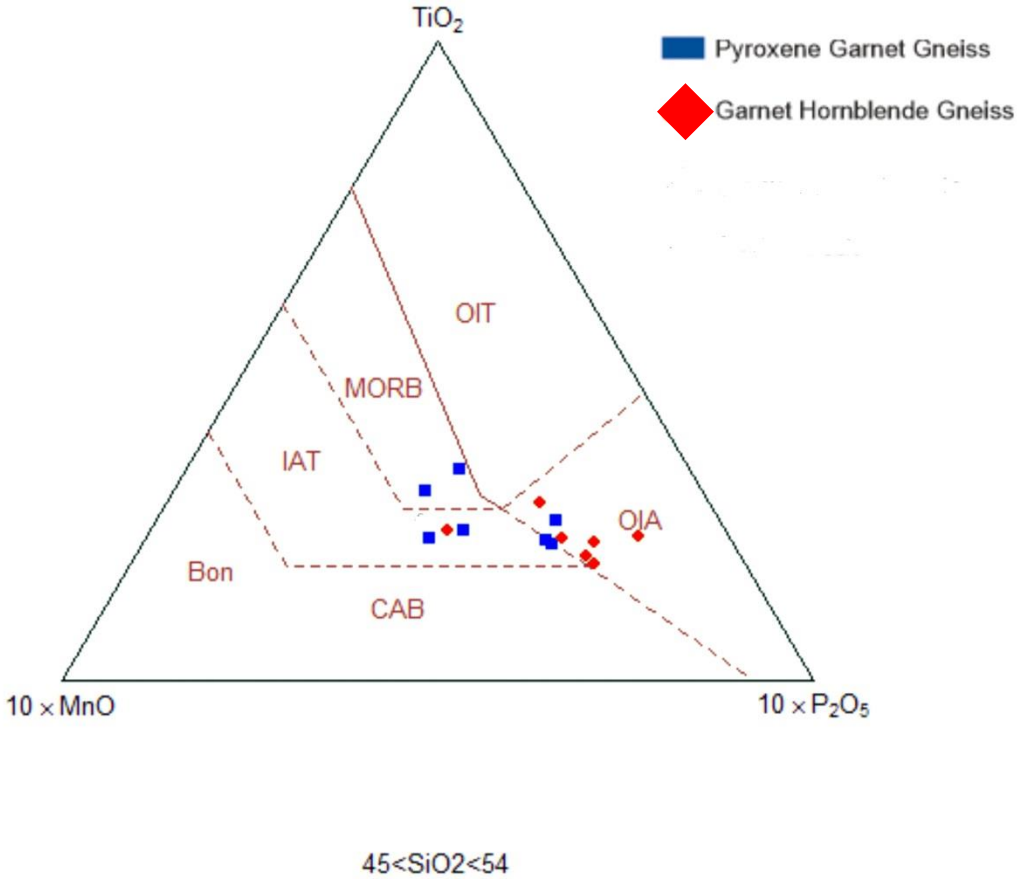

Figure 5.8: Tectonic discrimination diagram of MnO_2, TiO_2 and P_2O_5 (Mullen, 1983)

University of Ghana http://ugspace.ug.edu.gh

From the REEs plots (Fig 4.31 and Fig 4.32), generally the rocks display pattern similar to the Lower Crust (LC) with enrichment of light rare earth elements (LREEs) and relative depletion in the heavy rare earth elements (HREEs). Rudnik and Fountain (1995) proposed enrichment of LREEs and small positive europium anomaly for Lower Crust (LC). All the pyroxene garnet gneisses have positive anomaly of europium. These pyroxene garnet gneisses also display enrichment in the LREEs and have depleted Heavy HREEs. They show very similar pattern to the lower crust (LC).

The garnet hornblende gneisses display similar trend displayed by the pyroxene garnet gneisses and the Lower Crust. They have slight enrichment of LREEs and depleted HREEs with positive europium anomaly. Few samples displayed almost flat to negative europium anomalies.

The pyroxene bearing amphibolite also displayed similar pattern to the Lower Crust (LC). It displayed apparent enrichment in the LREEs. Ce, Nd and Sm yielding a relatively flat $(La/Sm)_N$ with slight negative to flat Eu anomaly.

The fault rock or breccia displayed similar pattern as the pyroxene garnet gneisses and the Lower Crust (LC). It has slight enrichment of LREEs relative to the HREEs with very pronounced positive Eu anomaly. Even though pattern resembles Lower Crust (LC); the rare earth elements (REEs) of the Fault Breccia are more depleted relative to the Lower Crust (LC) and the mafic garnet gneisses.

Humphries (1984) showed that there is no simple relationship between degrees of mobility of REEs and the rock or metamorphic grade and emphasizes the mineralogical and fluid

University of Ghana http://ugspace.ug.edu.gh

control. REEs may be mobilized by halogen rich or carbonate rich mineralizing fluids in the rock in which they would otherwise be stable with respect to the movement of an aqueous fluid. This is to say even though REEs are immobile, they can become mobile in certain fluids such as carbonate rich fluids.

The pyroxenite displays almost flat pattern of REEs with negative Eu anomaly. It has slightly enrichment in the LREEs with slightly higher Ce, Nd and Sm.

The incompatible trace elements of the mafic garnet gneisses also show similar pattern in Lower Crust (LC). Rudnik and Fountain (1995), proposed that the Lower Crust (LC) is depleted in Rb, Th, K and Pb. The pyroxene garnet gneisses and garnet hornblende gneisses display similar pattern to the Lower Crust (LC). The positive peak of Sr observed may be controlled by plagioclase in the rocks. Sr substitutes for Ca in the plagioclase. The pyroxene bearing amphibolites show pattern almost similar to the mafic garnet gneisses and the Lower Crust (LC).

The slight Ti peaks in the garnet hornblende gneisses, the pyroxene garnet gneisses and the pyroxene bearing amphibolite might be as a result of accessory opaque phases such as rutile and ilmenite in them. The fault rock also displays similar pattern to the Lower Crust (LC) and the mafic garnet gneisses, but is more depleted in the incompatibles such as Ba, Rb, Th and K due to fluid activities within the fault breaks since these elements are more mobile. Even though Sr is also mobile, it displays high positive peaks and enriched. This is due to the substitution of a Sr for Ca in plagioclase.

University of Ghana http://ugspace.ug.edu.gh

General enrichment in the LILE in the mafic garnet gneisses compared to N MORB and HFSE can be as a result of participation of H_2O rich fluids in the genesis of subduction zone magmas. These fluids are enriched LILE from the crust.

5.4.3 Petrogenesis

5.4.3.1 Magma type

The origin and the magmatic type of the Shai Hill gneisses from the Dahomeyide belt, Southeastern Ghana have been evaluated using the major and trace elements compositions and discussed in this section.

Several criteria have been used to evaluate the composition of primary magmas. Some of these criteria include low SiO_2, high magnessium number (Mg#) and low alkalis among others. According to Winter (2001), primary magmas have Mg# > 65, Cr > 1000 ppm and Ni > 400 – 500 ppm. The mafic garnet gneisses have magnessium number (Mg#) between 50.63 and 60.30. These suggest the rocks are not primary magmas and that they are evolved magmas in which their parent magmas may have experienced some degree of fractionation. Their Cr content ranges from 10 ppm to 150 ppm and Ni content of 6 ppm to 90 ppm. This shows that the magma that formed the mafic garnet gneisses are not primary magmas and probably might have undergone some degree of fractionation. These rocks also have relatively high SiO_2 content (Table 10 and Table 11). The fault breccia has relatively low magnessium number (Mg#), low Ni and Cr content and have high SiO_2 (Table 12), also giving indications of fractionation.

University of Ghana http://ugspace.ug.edu.gh

The magnessium number (Mg#), the Cr, Ni and the SiO_2 contents of the pyroxene bearing amphibolite (Table 12), also suggests that the rocks are not from primary magmas. The magmas have undergone fractionation during ascent of the magma and subsequent subduction. The pyroxene bearing amphibolites have relatively higher magnessium number (Mg#) and higher Cr and Ni content with low SiO_2 compared to the mafic garnet gneisses. This indicate that the mafic garnet gneisses are more evolved than the pyroxene bearing amphibolite. The pyroxenite has the highest magnessium number (Mg#) of 62.51 and has high Ni and Cr content relative to the mafic garnet gneisses. These indicate some level of fractionation but less evolved relative to the mafic garnet gneisses.

The evolution of these rocks were further analyzed using the Irvine and Baragar (1971), AFM diagram (Fig 5.9). In the diagram, the mafic garnet gneisses (i.e, pyroxene garnet gneisses and the garnet hornblende gneisses) plot closer to the FeO and the total alkali end, away from the MgO end. This suggests that these mafic garnet gneisses were metamorphosed from evolved magmas. One sample of the pyroxene garnet gneisses plots very close to the total alkali giving indication of high degree of fractionation. The fault breccia also plots closer to the FeO and further away from the MgO ends showing higher degree of fractionation. Pyroxene bearing amphibolite and the pyroxenite plot relatively closer to the MgO and suggest lesser degree of fractionation relative to the mafic garnet gneisses.

University of Ghana http://ugspace.ug.edu.gh

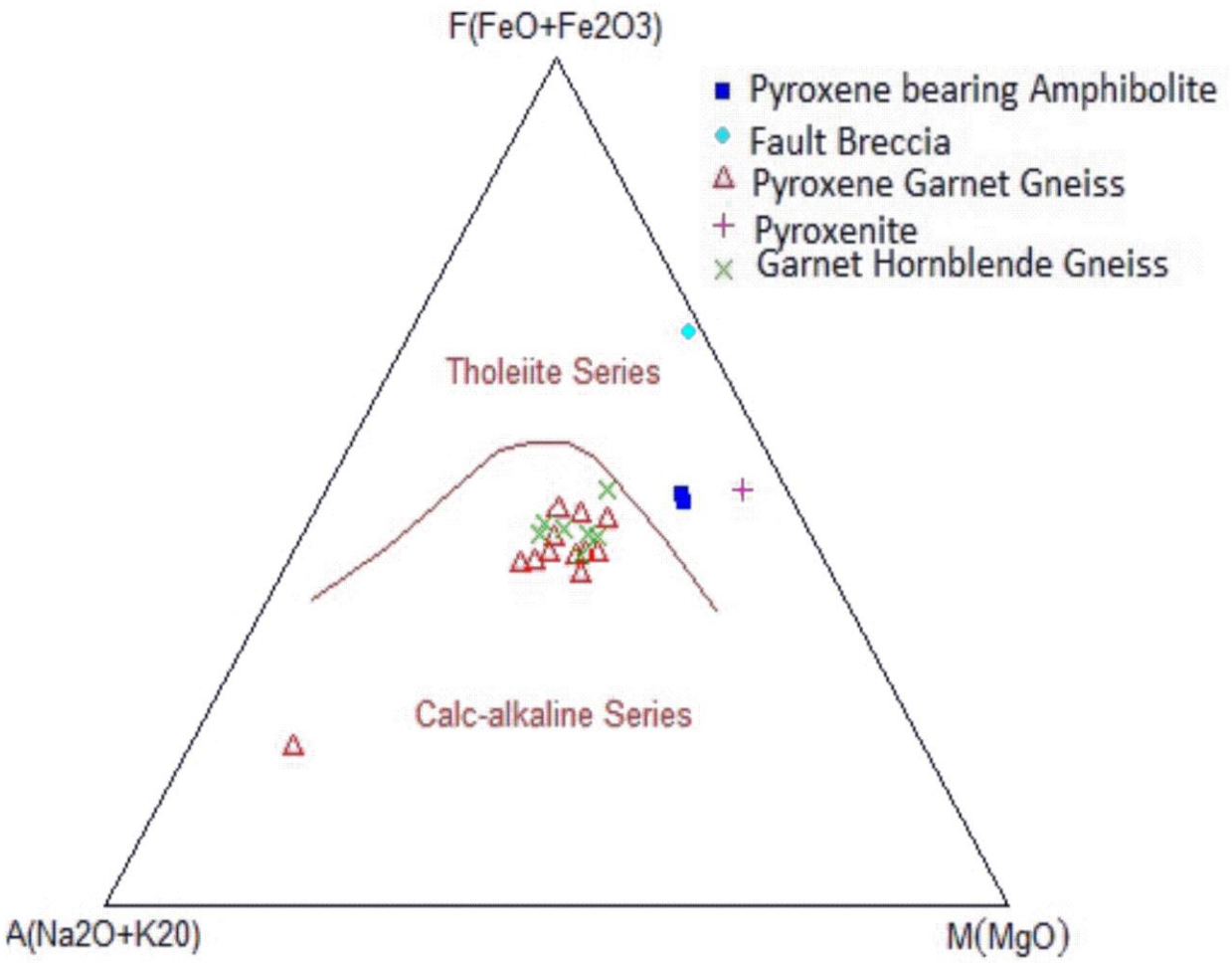

Figure 5.9: AFM diagram showing samples from the study area (After Irvine and Barager, 1971).

University of Ghana http://ugspace.ug.edu.gh

5.4.3.2 Magmatic Protolith

From the major elements composition, the mafic garnet gneisses are mainly basaltic and basaltic andesite with N67 exhibiting andesite composition. The association of basaltic, basaltic andesite and andesite rocks indicates an arc setting. The mafic garnet gneisses averagely display high Al_2O_3 content with low K_2O (Table 10 and 11). High Al_2O_3 is particularly common in association with calc alkaline magmas which is an arc tholeiite signature (Winter 2001). According to Winter (2001), high alumina basalts are parental to the calc alkaline arc series. The rocks are tholeiite and have arc characteristics. From Fig 5.2, the rocks plot mainly in the tholeiite series and few in the calc alkaline series with mainly low K to medium K series showing arc signatures.

The association of calc alkaline and tholeiites magmas are restricted to an arc setting (Winter 2001) which indicate that the protolith of these mafic garnet gneisses are from arc setting. Attoh and Morgan (2004) suggest that these mafic garnet gneisses have preserved the geochemical imprints of their magmatic protoliths display rare earth element (REE) and trace element patterns quite similar to mafic lower crust composition. They concluded that the High Pressure (HP) granulites were derived from two types of tholeiitic magmas: dominantly island arc tholeiites (IAT) together with subordinate N-MORB tholeiites with the island arc tholeiites (IAT) showing peculiar LREE enrichment with flat $(La/Yb)_N$ patterns where the N-MORB are slightly depleted in LREE and have low $(La/Yb)_N$ relative to the lower crust. Compatible element concentration for the more primitive island arc basalts have Ni values of 75 to 150 ppm, Cr and V content of 200 to 400 ppm (Winter

University of Ghana http://ugspace.ug.edu.gh

2001). From tables 10 and 11, the mafic garnet gneisses are characterized by very low Ni content and Cr and V compared to these values. This indicates that the basaltic protolith of these gneisses are not from primary magma but rather resulted from partial melting and fractionation of the primary magma.

From the REE plot (Fig 4.31), the mafic garnet gneisses display slightly enriched LREE relatively to the HREE. REE trace element data from the mafic garnet gneisses exhibit island arc with flat to LREE enriched patterns with $(La/Yb)_N$ ratios of 1.57 to 5.90. This can be due to low degree of partial melting of a primitive mantle (Winter 2001) or the mantle source for these island arc magmas is a heterogeneous mixture of depleted MORB and enriched Ocean Island Basalt (OIB) mantle sources giving it different incompatible element concentrations, reflecting variable enrichment and depletion (Thompson et.al., 1984). The HREE pattern is relatively flat and implies that garnet, which partitions among the HREE, may not have been a major phase during the generation of these magmas.

Again from the incompatible trace elements plots, the mafic garnet gneisses display slight enrichment in large ion lithophile elements (LILE) relative to the high field strength element (HFSE) with slight negative Nb and Ta anomaly. Also the HFSE are slightly depleted compared to N-MORB. The enrichment in the LILE is explained by the participation of water rich fluids in the genesis of subducted slab (Winter, 2001). The fluid from the subducted slab enriched in the mobile LILE lower the melting temperature of the solid rocks and concentrate LILE in the resulting hydrated magma. This may be the case for the generation of the mafic garnet gneisses. The lack of negative Yb anomaly suggests that the

University of Ghana http://ugspace.ug.edu.gh

magma source is not deep (Winter, 2001). Furthermore, the relatively flat HFSE pattern observed approximately one (1), means the concentration of these elements is similar to that of N-MORB and suggest the source of island arc magmas is similar to MORB which is from the depleted mantle but not the subducted slab (Winter, 2001).

McCulloch and Gamble (1991) concluded that the immobile HFSE concentrations are similar to those of MORB, and probably reflect overall mantle source characteristics, whereas the LILE reflect the more water soluble components from the slab. The enrichment in LREE is a feature of calc-alkaline suites (Donnelly and Rogers, 1978). In contrast, typical Island Arc Tholeiites (IATs) usually show nearly flat REE patterns. The samples display averagely lower Ti (Table 10 and 11) values showing Island Arc Tholeiites (IAT) characteristics with few having relatively high N-MORB Ti character.

In summary, the LILE enriched relative to the HFSE and the flat to slightly enriched LREEs compared to HREE is typical of Island arc magma origin. These mafic garnet gneisses exhibit geochemical patterns similarto LC.

University of Ghana http://ugspace.ug.edu.gh

Proposed Model: Formation and Subduction of the Shai hills Suture rocks

The history of the rocks in the study area can be traced back to the breakup of Rodinia and the rifting associated with the event about 750 million years ago. Ocean closure and subduction of ocean crust lithologies to lower crustal and mantle depths during the assemblage of NW Gondwana led to high and ultrahigh pressure metamorphism which is likely to have steered to the formation of the mafic garnet gneisses since the gneisses are said to preserve signatures of island arc tholeiites and subordinate imprints of N-MORBs (Attoh and Morgan, 2004). The mafic garnet gneisses (granulite) contain tholeiitic lavas formed in an oceanic island-arc environment. The mafic garnet gneisses experienced a different pressure-temperature-time (*P-T-t*) path during subduction as a result collision between the West African Craton (WAC) and group of eastern plates. Peak metamorphic conditions for the shai hill suture zone were reached at granulite facies and then later exhumation. This model for the subduction and exhumation of the shai hill suture zone is based on the metamorphic and deformation constraints. Fig 5.10 is a proposed geodynamic model for the evolution of Suture zone rocks in Ghana modified after Attoh and Nude (2008).

Stage A represents a stable West African Craton (WAC). Stage B represents initial rifting and continental breakout. This may be a result of plume of magma rising up from within the mantle. The Plume ponds at the base of the continent (WAC) and may have resulted into thermal swelling of the WAC and might have produce a broad dome which was then followed by normal faulting and rifting. The lithospheric breakup of the WAC resulted in

University of Ghana http://ugspace.ug.edu.gh

the formation of ocean basin on the eastern margin of the WAC represented in stage C. The granulite stage characterized by a pressure increase with relatively temperature decrease is related to the burial of the oceanic crust and part of the WAC within a subduction zone or during collisional processes. Stages D, E and F represent collision of the WAC and group of eastern plates to close up the ocean basin which might have created a subduction zone. The ocean crust break at some point and descended together with part of the WAC into lower crust to mantle depth. This resulted into the prograde metamorphism recorded in the mafic gniesses. This actually brought about the D_1 deformation and the granulite metamorphism at peak collision where subduction ceased.

The later retrograde P–T evolution may occur during exhumation. This resulted into the D_2 and the D_3 deformations and the hornblende-granulite to the greenschist metamorphism. This is represented in Stage G.

University of Ghana http://ugspace.ug.edu.gh

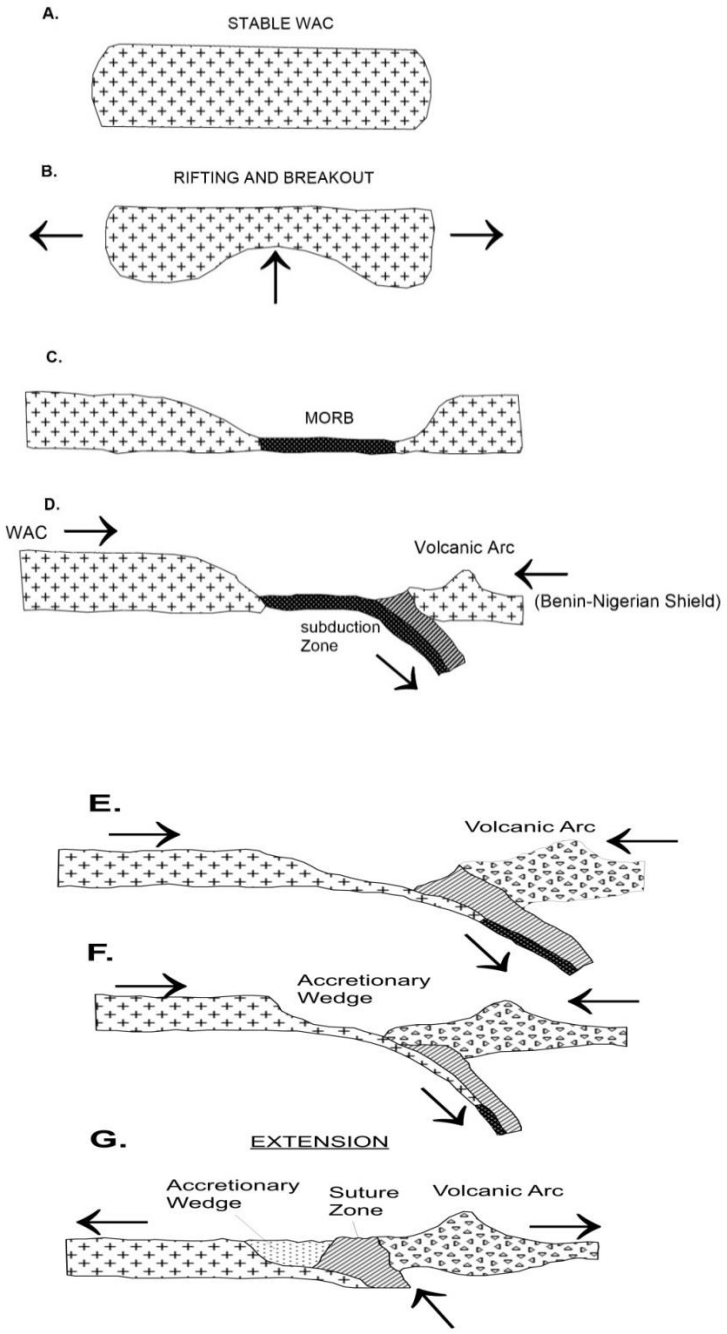

Figure 5.10: Proposed model for the Pan African suture zone in Ghana based on Wilson cycle reconstructions. (Modified after Attoh and Nude, 2008).

University of Ghana http://ugspace.ug.edu.gh

CHAPTER SIX

6.0 CONCLUSIONS AND RECOMMENDATIONS

6.1 Conclusions

The petrological and structural studies of the mafic garnet gneisses at the Shai Hills suture zone indicate that the suture rocks have undergone solid state poly deformational and poly metamorphic events and episodes as a result of subduction and later exhumation. Indications are that, these mafic garnet gneisses, were subducted under increased pressure and temperature conditions, and went through prograde metamorphism. Even though evidences of prograde metamorphic imprints are rarely seen, the observation of hornblende and ilmenite in stable mineral assemblages of porphyroblastic garnet and clinopyroxene at peak granulitic stage indicates prograde metamorphism. This suggests, the rocks were subjected to prograde metamorphism during subduction before their exhumation. Peak metamorphism is defined by granulitic metamorphic assemblages of garnet, clinopyroxene, plagioclase and some quartz. This was immediately followed by hornblende-granulite facies assemblages as a result of very early stages of exhumation. This stage was characterized by the development or crystallization of dark reddish hornblende in the rock and a corona texture of clinopyroxenes around garnet.

The amphibolite and the greenschist facies observed in the rocks define major retrogressive metamorphism as a result of exhumation accompanied by a decrease in temperature and pressure conditions, as well as possible influx of water. The amphibolite facies followed the

University of Ghana http://ugspace.ug.edu.gh

hornblende-granulite with the introduction of green hornblendes around the rims of some clinopyroxenes and garnet. Greenschist facies which follows the amphibolite facies in the retrogressive path is characterized by development of chlorite mineral around the rims of garnet and some clinopyroxenes, also the introduction of epidotes from the alteration of plagioclase. This indicates that the rocks have undergone polymetamophic episodes.

From textural and structural evidence, it can be concluded that the rocks have undergone intense deformation. The rocks have undergone at least three deformational events. This can be seen from various structures observed in the area. The rocks were subjected to ductile deformation as a result of subduction. The development of foliations and gneissic bands indicate ductile deformation.

The first deformational event is characterized by the development of gneissic banding, foliations, and boudinage and mineral lineations in the rocks. The D_1 deformations is characterized by dextral non-axial shearing or simple shearing evidenced by the rotations of some garnet porphyroblasts, hornblende mineral lineation in the felsic compositional bands which developed into sigma and delta structures and stretched and lenticular pyroxenite boudins within the mafic garnet gneisses.

The D_2 deformation is also characterized by ptygmatic folds found in the area. The ptygmatic folds postdate the gneissic bands and foliations in the mafic garnet gneisses and hence are D_2 deformational event. The ptygmatic folds were formed from partial melting of the felsic compositional bands as a result of decompression during exhumation where

University of Ghana http://ugspace.ug.edu.gh

conditions must have been conducive for the felsic bands to melt. Conditions such as decrease pressure at relative constant temperature and with the introduction of fluids.

Further exhumation of these rocks introduces the rocks close to the surface, where deformation changed from the ductile deformation to a brittle deformation. Here temperature becomes very low and hence deformation at this stage was mainly brittle. This is evident in the rocks with various faults, fractures and joints observed in the rocks at macroscale. The D_3 deformational event is responsible for the crushing and producing the fault breccia. The D_3 deformations postdate both the D_1 and D_2 deformations. This stage of deformations is characterized by sinistral sense of shear as observed in the fractured thrusted pyroxenite in the mafic garnet gneisses.

The pyroxene bearing amphibolite has a gradational contact with the mafic garnet gneisses. This suggests that the pyroxene bearing amphibolite may have metamorphosed into the mafic garnet gneisses during prograde metamorphism thus from amphibolite facies to granulite facies. The pyroxenite rocks are older materials thrusted within the mafic garnet gneisses. The fault breccia formed as a result of crushing and cataclasis of the mafic garnet gneisses during brittle deformation.

Geochemical data show that the mafic garnet gneisses have major elements and trace elements pattern concentration similar those of the Lower Crust. The high pressure mafic garnet gneisses and associated rocks despite evidences of major and trace elements depletions associated with high temperature metamorphism, imprints of the trace elements pattern suggest magmatic protolith and with inference that the suture zone mafic granulites

University of Ghana http://ugspace.ug.edu.gh

consist of rocks largely of Island arc tholeiites (IAT) but also include suites of rocks with oceanic crust (MORB) geochemical signatures. This association of rock suites suggests the existence of a subduction zone complex where oceanic crust may have formed in either a back arc basin or intra-arc basin environment.

From the Rare Earth Element (REE) and incompatible trace elements plots, the mafic garnet gneisses have similar pattern to the lower crust (LC). The rocks generally displayed slight enrichments in the Light Rare Earth Elements (LREEs) relative to the Heavy Rare Earth Elements (HREEs) with small positive Europium anomaly. They also displayed enrichment in the LILE comapared to HFSE. The Magnessium number (Mg#) obtained for the mafic garnet gneisses is also approximately equal to that of the Lower Crust (LC). The mafic garnet gneisses also displayed almost the same pattern as IAT from the incompatible trace elements plots normalized to N MORB. Geotectonic plots also showed that, the rocks have affinity for Island Arc Tholeiite (IAT) mainly with few MORB like materials. The rocks plotted mainly in the field of Island Arc Tholeiite (IAT), with few plots in the MORB and OIA. These results agree with the findings of Attoh and Morgan (2004).

The associations of the Island Arc Tholeiite (IAT) and the MORB imprints suggest that there may have been the formation of oceanic crustal materials within the West African Craton (WAC), in either a back arc basin or intra-arc basin environment. These materials together with part of the WAC later may have subducted to lower crustal or to mantle depth before exhumation by probable uplift or erosions.

University of Ghana http://ugspace.ug.edu.gh

6.2 Recommendation

It is recommended that detailed structural and petrologcal mapping need to be extended throughout the suture zone in Ghana in future research to permit better understanding of the suture zone as far as structures and petrology are concerned.

Also important geochemical techniques such as microprobe for mineral chemistry, geochronology and isopotic studies should be carried out together with geothermobarometric calculations on the mafic garnet gneisses and its associated rocks that occur in the suture zone to provide complementary and useful data for thermobarometry and age of the HP metamorphism deductions.

University of Ghana http://ugspace.ug.edu.gh

REFERENCES

Affaton, P., 1990. Le bassin des Volta (Afrique de l'Ouest): une marge passive du protérozoïque supérieur, tectonisé au panafricain (600+/-50Ma). Thèse d'Etat, vol. 2, 499p. Collection Etudes et Thèses, Ed. ORSTOM, Paris.

Affaton, P., Aguirre, L., Menot, R.P., 1997. Thermal and geodynamic setting of the Buem volcanic rocks near Tie´le´, Northwest Benin, West Africa. Precambrian Research 82, 191–209.

Affaton, P., Kroner, A., Seddoh, K.F., 2000. Pan-African granulite formation in the Kabye massif of northern Togo (West Africa): Pb–Pb zircon ages. International Journal of Earth Science 88, 778–790

Affaton, P., Rahman, M.A., Trompette, R., and Sougy, J., 1991. The Dahomeyide orogeny: Tectonothermal evolution and relationship to Volta basin, In Dallmeyer, R.D., and Lecorche, J-P., (eds.), The West Africa Orogens and Circum- Atlantic Correlatives: New York, Springer-Verlag, p. 95-111.

Affaton, P., Sougy, J., Trompette, R., 1980. The tectono-stratigraphic relationships between the Upper Precambrian and Lower Paleozoic Volta Basin and the Pan-African Dohomeyide orogenic belt (West Africa). American Journal of Science 280, 224–248.

University of Ghana http://ugspace.ug.edu.gh

Agbossoumondé, Y "The Ultrabasic Complexes of the Pan-African Belt in Togo (Agou-Atakpame Axis, SouthTogo) Petrologic, Mineralogical and Geochemical Study," Ph.D. Dissertation, Université Jean Monnet, St. Etienne, 1998.

Agbossoumondé, Y., 1998. Les massifs ultrabasiques-basiques de la chaine panafricaine au Togo: axe Agou-Atakpamé. Etudes pétrographique, minéralogique et géochimique. Thèse Saint-Etienne, 306p.

Agbossoumondé, Y., Guillot, S., Ménot, R.P., 2004. Pan-African subduction–collision event evidenced by HP granulites from the Agou Massif, southern Togo. Precambrian Research. 135, 1–21.

Agbossoumondé, Y., Guillot. S., Ménot, R.P "Pan-African Subduction-Collision Envent Evidence by High-P Coronas in Metanorites from the Agou Massif (Southern Togo)," Precambrian Research, Vol, 135. No.1-2. 2004.

Agbossoumonde, Y., Menot, R. P., Nude, P.M., 2013. Geochemistry and Sm-Nd isotopic composition of the Agou igneous complex (AIC) from the Pan-African orogeny in Southern Togo, West Africa: Geotectonic Implication. Journal of African Earth Science 82, pp. 88-99

Agbossoumondé, Y., Ménot, R.-P., Guillot, S., 2001. Metamorphic evolution of Neoproterozoic eclogites from south Togo (West Africa): geodynamic implications for the reconstruction of West Gondwana. Journal of African Earth Science 33(2), 227–244.

University of Ghana http://ugspace.ug.edu.gh

Agbossoumondé, Y., Ménot, R.P., Paquette, J.L., Guillot, S., Yessoufou, S., Perrache, C., 007. Petrological and geochronological constraints on the origin of Palimé-Amlamé granitoids (South Togo, West Africa): a segment of the West African Craton Palaeproterozoic margin reactived during Pan-African collision. Gondwana Research. 12, 475–48

Agyei, E.K., van Landewijk J.E.J.M., Amstrong R.L., Harakal L.F. Scott K.L., 1986. "Rb-Sr and K-Ar Geochronometry of Southeastern Ghana," Journal of African Earth Sciences, Vol. 6, 1987, pp. 153-161.

Attoh, K. (1990). Dahomeyides of southeastern Ghana: Evidence for oceanic closure and crustal imbracation in a Pan African orogeny. 15th coll. African Geology, pp150-164.

Attoh, K., 1990. Dahomeyides of Southeastern Ghana: Evidence for oceanic closure and crustal imbrication in a Pan-African orogen. Publication occasionnelle du C.I.F.E.G., BRGM, Orleans Tr. No. 21.

Attoh, K., 1998a. High-pressure granulite facies metamorphism in the Pan-African Dahomeyide orogen. West Africa Journal of Geology 106, 236–246.

Attoh, K., Corfu, F., Nude, P.M., 2007. U-Pb Zircon age of deformed carbonitite and alkaline rocks in the Pan-African Dahomeyide suture zone, West Africa. Precambrian Research 155 (2007) 251-260.

University of Ghana http://ugspace.ug.edu.gh

Attoh, K., Dallmeyer, R. D. and Affaton, P. 1997. Chronology of nappe assembly in the Pan-African Dahomeyide orogen: evidence from $^{40}Ar/^{39}Ar$ mineral ages. Precambrian Research, 82, 153–171.

Attoh, K., Hawkins, D. and Bowring, S. 1991. U–Pb zircon ages of gneisses from the Pan-African Dahomeyide orogen, West Africa. EOS Transactions, American Geophyical Union, 72, S299.

Attoh, K., Morgan, J., 2004. Geochemistry of high-pressure granulites from the Pan-African Dahomeyide orogen, West Africa: constraints on the origin and composition of the lower crust. Journal of African Earth Sciences, 39, 201–208.

Attoh, K., Nude, P.M., 2008 Tectonic significance of carbonatite and ultrahigh-pressure rocks in the Pan-African Dahomeyide suture zone, southeastern Ghana, from: ENNIH, N. and LIE´GEOIS, J.-P. (eds). The Boundaries of the West African Craton. Geological Society, London, Special Publications, 297, 217–231.the Geological Society of London 2008.

Bates, D.A. (1955). The geology of $1/4^0$ field sheets 3 and 5 Axim NE, 1, -Ghana Geological Survey Accra. Arch. Rep., 16 (1991): 78pp.

Benneh, M.P., Dickson, K.B., 1990, A New geography of Ghana. p. 20-32, 36-38

Bessoles, B., Trompette, R., 1980. Géologie de l'Afrique. La chaîne panafricaine ''zone mobile d'Afrique centrale (partie sud) et zone soudanaise''. Orléans, Fr., B.R.G.M. mém. n 6.

University of Ghana http://ugspace.ug.edu.gh

Boynton, W.V., 1984. Geochemistry of the rare earth elements: meteorite studies. In: Henderson, P. (ed.). Rare earth element geochemistry. Elsevier, pp. 63-114

Burke, K., 1959. Replacement veins in Dahomeyan of Ghana. Geological Magazine / Volume 96 / Issue 05 / October 1959, pp 353-360. Copyright © Cambridge University Press 1959. DOI: http://dx.doi.org/10.1017/S0016756800062324, Published online: 01 May 2009.

Caby, R. 1987. The Pan-African belt of West Africa from the Sahara Desert to the Gulf of Guinea. In: SCHAER, J. P. and RODGERS, J. (eds) Anatomy of Mountain Ranges. Princeton University Press, Princeton, NJ, 129–170.

Castaing, C., Triboulet, C., Feybesse, J.L. and Chevromont, P. 1993. Tectonometamorphic evolution of Ghana, Togo, and Benin in the light of the PanAfrican/Brasiliano orogeny. Tectonophysics, 218, 323–342.

Cox, K.G., Bell, J.D., and Pankhurst, R.J. 1979. The interpretation of igmeous Rocks: George Allen and Unwin, London, 445p.

Davis, D.W., Hirdes, W., Schaltegger, U., Nunoo, E.A., 1994. U-Pb age constraints on deposition and provenance of Birimian and gold-bearing Tarkwaian sediments in Ghana, West Africa. Precambrian Research, 67, 89–107.

Davis, G.H., Reynolds, S.J. (2011) Structural Geology of rocks and regions.

Dickson, K.B., Benneh.G. (1988), A new geography of Ghana. Longman Group UK limited. 170pp.

University of Ghana http://ugspace.ug.edu.gh

Donnelly, T.W. and Rogers, J.J.W., 1978. Igneous series in island arcs: The northern Caribbean compared with world-wide island-arc assemblages. Bulletin Volcanol., 43: 347-382.

Donnelly, T.W., and Rogers, J.J.W., 1978, The distribution of igneous rock suites around the Caribbean: Geologie en Mijubouw, v. 57, p. 151–162.

Duclaux, G., Menot, R. P., Guillot S., Agbossoumonde, Y., and Hilairet, N., 2006. The mafic layered complex of the Kabye massif (north Togo and north Benin): Evidence of a Pan-African granulite continental arc root. Precambrian Research (2006), Elsevier B.V. doi: 10.1016/j. precamres. 2006. 08. 012

England, P.C., Thompson, A.B., 1984. Pressure- Temperature-time path of Regional metamorphism1. Heat transfer during evolution of regions of thickenedcontinental crust. Journal Petrology 25 (4), 894-928.

Grant, N.K., 1969. The late Precambrian to early Paleozoic Pan-African orogeny in Ghana, Togo, Dahomey and Nigeria. Geological Society of America Bulletin 80, 45–55.

Hasting, D.A (1982). On the tectonics and metallogenesis of West Africa: a model incorporating new geophysical data. Geoexploration, 20: p295-327.

Hirdes, W., Davis, D.W., 2002. U-Pb zircon and rutile metamorphic ages of the Dahomeyan garnet-hornblende gneiss in southeastern Ghana, West Africa. Journal of African. Earth Sciences. 35, 445–449.

University of Ghana http://ugspace.ug.edu.gh

Hoffman, P.F., 1991. Did the breakout of Laurentia turn Gondwana inside-out? Science 252, 1409–1412.

Hoffmann, A.W., 1988. Chemical differentiation of the Earth: the relationship between mantle, continental crust, and oceanic crust. Earth and Planetery Sciences, Letters 90, 297–314.

Holm, R.F., 1974. Petrology of alkalic gneiss in the Dahomeyan of Ghana. Geological Society of America. Bulletin 85, 1441–1448.

Humphris, S. E. and G. Thompson. (1978). Hydrothermal alteration of oceanic basalts by seawater. Geochimica et Cosmochimica Acta, 42,107-125.

Humphris, S.E., and Thompson, G., 1978, Trace element mobility during hydrothermal alteration of oceanic basalts: Geochemica et Cosmochemica Acta.V.42, p 127-136

Humpris, S.E., 1984. The mobility of the rare earth elements in the crust. In. Henderson P. (ed.) Rare earth elements geochemistry. Elsevier, Amsterdam, pp.315-341.

Irvine, T.N., Baragar, W.R.A., 1971. A guide to chemical classification of the common volcanic rocks. Canadian Journal of Earth Sciences. 8, 523–548.

Jahn, B.M., 1990. Origin of granulites: geochemical constraints from Archean granulite facies rocks of the Sino-Korean eraton, China. In: Vielzeuf, D., Vidal, Ph. (Eds.), Granulites and Crustal Evolution. Kluwer Academic Publishers, Boston, pp. 471–492.

University of Ghana http://ugspace.ug.edu.gh

Jones, W.B., 1990. The Buem volcanic and associated sedimentary rocks, Ghana: a field and geochemical investigation. Journal of African Earth Sciences. 11, 373–383.

Jung. S. 1999. The role of Crustal Contamination during the evolution of Continental rift-related Basalts. A case study from the Vogelsberg area (Central Germany), Geolines (Praha) 9, 48-58

Junner, N. R. and Harwood, H. F. 1928. Microscopical features and chemical analyses of certain representative igneous rocks from the Gold Coast, British West Africa. Gold Coast Geological Survey Bulletin, 4, 10–11.

Junner, N.R., 1940. Geology of the Gold Coast and Western Togoland. Gold Coast Geological Survey Bulletin 11.

Kesse, G.O., (1985). The Mineral and Rock Resources of Ghana, A.A. Belkema Publishers, Netherlands.

Kitson, A.E. 1919. Gold Coast Geological Survey Annual Report. 1919 13.

Kitson, A.E., 1928. Provisional geological map of the Gold Coast and Western Togoland, with brief descriptive notes thereon. In: Gold Coast Geological Survey Bulletin 2. Accra, Ghana.

Knorring, V.O. and Kennedy, W. Q. 1958. The mineral paragenesis and metamorphic status of garnet–hornblende–pyroxene–scapolite gneiss from Ghana. Mineralogical Magazine, 31, 846–859

Kretz, R., 1983. Symbols for rocks-forming minerals. American Mineralogist. 68, 277–279.

University of Ghana http://ugspace.ug.edu.gh

Kutu, J.M., Hayford, E.K., Oddei, J.K., Gadasu, A (2014) Characterisation of engineering rock materials from the Shai-Akuse district, Southeastern Ghana. Journal of Ghana Science Association, Vol 15, No. 2

Langmuir, C.H., Bender. J.F., Bance A.F., Hanson. G.N, and Taylor, S.R., 1977. Petrogenesis of basalts from the famous area: mid-Atlantic ridge. Earth and Planetery Sciences. Letters 36, 133-156.

Le Bas, M. J., R. W. LeMaitre, A. L. Streckeisen, and Zanettin B. (1986). A chemical classification of volcanic rocks based on the total alkali-silica diagram. /. Petrology 27,745-750.

Mani, R. (1977). The geology of $1/4^0$ Field sheet 145, Honuta SW.

McCulloch, M. T. (1993). The role of subducted slabs in an evolving Earth. Earth and Planetery Sciences. Letters, 115, 89-100.

McCulloch, M. T. and J. A. Gamble (1991). Geochemical and geodynamical constraints on subduction zone magmatism. Earth and Planetery Sciences. Lett., 102, 358-374

Menot, R. P. and Seddoh, K. F. 1985. The eclogites of Lato Hills, south Togo, West Africa: Relics from the early tectonometamorphic evolution of the Pan-African orogeny. Chemical Geology, 50, 313–330.

University of Ghana http://ugspace.ug.edu.gh

Menot, R. P., 1980. The massive basic and Ultrabasic mobile belt Pan-African in Ghana, Togo and Benin. State of the question. Bulletin de la Société Géologique France 22, 297-303.

Middlemost, E.A.K., 1994. Naming materials in the magma/igneous rock system. Earth Science Reviews 37, 215–224.

Morgan, J., Attoh, K., Gorring, M., Brown, N., 1996. LREE depleted partial melts in eclogitic granulites of the Panafrican Dahomeyide suture zone, West Africa. Geological Society of America Abstracts with Programs 28, 84.

Mullen, E.D., 1983. MnO–TiO2–P2O5 a major element discriminant diagram for basaltic rocks of the oceanic environments and its applications for petrogenesis. Earth and Planetary Science Letters 62, 53–62.

Nude, P.M., Shervais, J.W., Attoh, K., Vetter, S.K., Corey Barton, C., 2009. Petrology and geochemistry of nepheline syenite and related carbonate-rich rocksin the Pan-African Dahomeyide orogen, southeastern Ghana, West Africa. Journal of African Earth Sciences. 55 (3–4), 147–157.

Pearce, J.A and Cann, J.R. 1973. Tectonic setting of basic volcanic rocks determined using trace element analyses. Earth and Planetary Science Letter, 19, 290-300

Pearce, J.A., Lippard, S.J., Roberts, S., 1984. Characteristics and tectonic significance of supra-subduction zone ophiolites. In: Kokelaar, B.P., Howells, M.F. (Eds.), Marginal

University of Ghana http://ugspace.ug.edu.gh

basin geology; volcanic and associated sedimentary and tectonic processes inmodern and ancient marginal basins. Geological Society Special Paper, pp. 74–94.

Pearce, T.H., Gorman, B.E., and Birkett, T.C., 1977. The relationship between major elements chemistry and tectonic environment of basic and intermediate volcanic Rocks. Earth and Planetery Sciences. letter, 36 121-132.

Peccerillo, A and Taylor, S.R. (1976). Geochemistry of Eocene calc-alkaline volcanic rocks from the Kastamonu area, Northern Turkey. Contributions to Mineralogy and Petrology, 58, 63-81.

Rollinson, H. R. (1993). Using geochemical data: evaluation, presentation, interpretation. Longman Group UK Limited.

Rudnick L., Roberta, Fountain M., David, 1995. Nature and composition of the continental crust: a lower crustal perspective.

Rudnick, R., Presper, T., 1990. Geochemistry of intermediate to highpressure granulites. In: Vielzeuf, D., Vidal, Ph. (Eds.), Granulites and Crustal Evolution. Kluwer Academic Publishers, Boston, pp. 523–550.

Rudnick, R.L., McDonough, W.F., OConnell, R.J., 1998. Thermal structure, thickness and composition of continental lithosphere. Chemical Geology 145, 395–411.

University of Ghana http://ugspace.ug.edu.gh

Saunders, A.D., and Tarney J., 1984, Geochemical characterisatics of basaltic Volcanism within back-arc basins. In: Kokelar B.P and Howells M.F., (eds.). Marginal basin geology, space. Publish Geological Society London 16, pp 59-76

Stephens, M. B., M. J. Glasson, and R. R. Keays, (1979). Structural and chemical aspects of metamorphic layering development in metasediments from Clunes, Australia. Amererican Journal of Science, 279,129-160.

Sun, S.S., McDonough, W.F., 1989. Chemical and isotopic systematics of oceanic basalts: implications for mantle composition and processes. In: Saunders, A.D., Norry, M.J. (Eds.), Magmatism in the Ocean Basins, 42. Geological Society Publication, pp. 313–345.

Sylvain, J.P., Assih-Edeou, P., Castaing, C., Chevremont, Ph., Collart, J., Ouassane, I., 1986. Notice explicative de la carte g´eologique 1/200000, feuille Atakpam´e. In D.G.M.G./B.N.R.M., Lome, Togo.

Tairou, M.S., Affaton P. (2012). Structural organization and Tectono- Metamorphic Evolution of the Pan African Suture Zone: Case of the Kabye and Kpasa Massifs in the Dahomeyides orogeny in Northern Togo. International Journal of Geosciences, 2013, 4, 166-182

Thompson, J. B. Jr. (1982a). Composition space: An algebraic and geometric approach. In J. M. Ferry (ed.), Characterization of Metamorphism Through Mineral Equilibria. Rev. in Mineralogy, 10, Mineralogical Society of America, pp. 1-31.

University of Ghana http://ugspace.ug.edu.gh

Thompson, J. B. Jr. (1982b). Reaction space: An algebraic and geometric approach. In J. M. Ferry (ed.), Characterization of Metamorphism Through Mineral Equilibria. Rev. in Mineralogy, 10, Mineralogical Society of America, pp. 33-52.

Thompson, R. N. (1972). Melting behavior of two Snake River lavas at pressures up to 35 kb. Carnegie Inst. Washington yeark, 71, 406-410.

Thompson, R. N. (1982). Magmatism of the British Tertiary Volcanic Province. Scotland Journal of Geology, 18, 49-107.

Thompson, R. N., M. A. Morrison, G. L. Hendry, and S. J. Parry (1984). An assessmant of relative roles of crust and mantle in magma genesis: An elemental approach. Philosophical Transactionof the Royal Society London, A310, 549-590.

Veevers, J.J. (2003) Pan-African is Pan-Gondwanaland: Oblique convergence drives rotation during 650–500 Ma assembly.

Weaver, B.L., Tarney J., 1984, Empirical approach to estimating the composition of the continental crust.

Wilson, M., 1989. Igneous Petrogenesis, A Global Tectonic Approach. Unwin Hyman, London, p. 400.

Winter, J.D. (2001). An Introduction to Igneous and Metamorphic Petrology. USA; Prentice Hall. Whitney, D.L, Evans, B.W. (2010) Abbreviations for names of rock-forming minerals, From: American Mineralogist, Volume 95, 2010.

University of Ghana http://ugspace.ug.edu.gh

Yurtmen, S., Guillou, H., Westaway, R., Rowbotham, G. and Tatar, O. 2002. Rate of strike slip motion on the Amanos Fault (Karasu Valley Souhtern Turkey). Constrained by K-Ar dating and geochemical analysis of Quaternary Tectono Physics, 344, 207-246

Zhang, R. Y. & Liou, J. G. 1999. Clinopyroxene from the Sulu ultrahigh-pressure terrane, eastern China: Origin and evolution of garnet exsolution in clinopyroxene. American Mineralogist, 88, 1591–1600.

Zhang, R. Y., Zhai, S. M., Fei, Y. W. and Liou, J. G. 2003. Titanium solubility in coexisting garnet and clinopyroxene at very high pressure: the significance of exsolved rutile in garnet. Earth and Planetary Science Letters, 216, 591–601.

University of Ghana http://ugspace.ug.edu.gh

APPENDIX

Table 1: Some selected data

	Pyroxene Garnet Gneiss											
	S11	S15	S16A	S20	S24	N58A	N58h	N58f	N62A	N63	N67	N68
Zr/Hf	38.46154	32.5	30	30.90909	36.875	31.25	33	36.66667	35.55556	32.30769	42.5	40.90909
Th/U	1.9	1	1	3.6	1.136364	1	2	1	1.5	2.222222	1	1.4
K/U	46487.28	61429.62	43166.76	81352.74	19243.92	48147.54	58109.1	53128.32	52920.79	48885.43	49807.8	87993.78
Rb/Cs	80	56.66667	60	75	80	25	100	50	190	230	50	70
Sr/Nd	58.11475	49.79167	83.93258	67.89474	47.11111	74.78261	71.47059	85.82418	101.6418	67.26316	427.1429	52.44898
La/Nb	3.36	3.076923	1.666667	1.314815	2.486486	1.5	3.466667	1.722222	5.333333	3.25	0.28	3.947368
Sm/Nd	0.202459	0.225694	0.280899	0.227193	0.222963	0.283696	0.228431	0.278022	0.244776	0.250526	0.22	0.220408
U/Pb	0.01	0.025	0.025	0.025	0.11	0.025	0.025	0.025	0.04	0.045	0.025	0.025
Eu/Eu*	1.361682	1.16659	1.14548	1.166483	1.158913	1.20914	1.278203	1.272986	1.547789	1.234954	1.536499	1.209778
LaN/YbN	5.899194	5.186104	2.268921	5.092313	5.851491	1.576037	4.552995	3.119403	4.433053	4.979839	28.31613	5.056452
LaN/SmN	2.139219	1.548387	0.880645	1.724374	1.922624	0.867631	1.403849	0.770751	1.84107	1.717945	1.715543	1.456093
CeN/YbN	5.065491	4.87481	2.313047	4.595402	5.026854	1.64604	4.299859	3.435976	3.578767	4.173886	24.31436	4.837005
CeN/SmN	1.836894	1.455446	0.897772	1.556109	1.651673	0.906168	1.325798	0.848971	1.48628	1.439908	1.473094	1.3929
EuN/YbN	3.25822	3.390372	2.734171	2.994789	3.165447	1.846453	3.471331	4.159204	3.194111	2.972789	19.90476	3.582857
Zr/Nd	4.098361	2.708333	2.696629	2.982456	4.37037	2.717391	3.235294	3.626374	4.776119	4.421053	4.857143	3.061224
K/Rb	1452.728	1806.754	3597.23	677.9395	1323.02	2407.377	2905.455	2656.416	2228.244	1912.908	2490.39	3142.635
Rb/Cs	0.004513	0.002371	0.000803	0.007752	0.005031	0.001453	0.001372	0.00128	0.00279	0.003599	0.000669	0.001816

University of Ghana http://ugspace.ug.edu.gh

Table 2: Some Selected Data

	Garnet Hornblende Gneiss							**Pyroxene Bearing Amphibolite**		**Fault Breccia**	**Pyroxenite**
	M2	M5A	M5B	M3	M4A	M4B	M6C	M5C	M5D	N58d	N58g
Zr/Hf	40.35	30	33.33	42	40	36.92	30	31.66	28.42	31.66	32.94118
Th/U	1.12	1	2	2.090909	1.285714	2	1.8	1.8	0.833333	1	3
K/U	34242.86	1791.34	1791.34	814.2455	2559.057	1279.529	895.67	97955.34	80245.9	6641.04	24903.9
Rb/Cs	60	130	100	40	190	70	60	150	100	8.333333	38
Sr/Nd	61.60305	78.36957	72.16981	23.1746	42.89773	62.57143	57.22628	9.62766	9.893617	303.5714	16.07143
La/Nb	0.919355	2	1.736842	2.06	4.692308	1.428571	2.65	0.833333	0.53	0.513514	2.111111
Sm/Nd	0.273282	0.272826	0.293396	0.228571	0.2625	0.255	0.278832	0.254255	0.276596	0.25	0.2625
U/Pb	0.04	0.025	0.025	0.055	0.035	0.035	0.05	0.025	0.03	0.005556	0.035
Eu/Eu*	0.913034	1.078565	1.014354	0.836539	0.923315	0.982159	0.97139	0.910539	0.978195	1.43724	0.702345
LaN/YbN	2.066077	1.599781	1.794225	3.306759	3.639452	3.111663	3.080367	4.262143	3.435794	2.099947	1.515938
LaN/SmN	1.001532	0.701709	0.667462	1.124832	0.83054	1.057197	0.872741	0.723782	0.641129	1.138249	0.813035
CeN/YbN	2.099902	1.709809	1.981695	3.559701	4.120301	3.183549	3.188695	5.351656	4.402252	2.035384	1.729524
CeN/SmN	1.017928	0.74997	0.737202	1.210873	0.940273	1.081621	0.903433	0.908799	0.821473	1.103253	0.927586
EuN/YbN	1.727525	2.216995	2.384902	2.139423	3.246162	2.581057	2.843537	4.608492	4.374673	2.703691	1.245099
Zr/Nd	8.625954	2.608696	3.773585	5.833333	3.409091	3.428571	2.408759	3.031915	2.87234	4.52381	5
K/Rb	4565.715	68.89769	89.567	111.9588	94.28105	127.9529	74.63917	3265.178	4814.754	664.104	917.5121
Rb/Cs	0.000743	0.001803	0.001307	0.00137	0.002517	0.000799	0.001531	0.008287	0.005376	0.000392	0.010556

University of Ghana http://ugspace.ug.edu.gh

Table 3: Some trace element ratios of the mafic garnet gneiss.

Sample	La/Nb	K/Nb	Zr/Hf	Nb/Ta	Zr/Nb	Ba/Nb	Ce/Pb
S11	3.36	1859.49	38.4615	25	20	102.40	1.88
S15	3.07	1181.33	32.5	13	15	65.38	9.80
S16A	1.66	1027.78	30	21	11.42	43.95	4.65
S20	1.31	753.26	30.90	27	6.29	35.92	8.35
S24	2.48	1144.23	36.87	18.5	15.94	61.35	10.30
N58A	1.50	1003.07	31.25	24	10.41	31.75	4.90
N58h	3.46	1936.97	33	15	22	74	6.40
N58f	1.72	1475.78	36.66	18	18.33	48.77	4.45
N62A	5.33	4704.07	35.55	9	35.55	218.88	5.05
N63	3.25	2199.84	32.30	20	21	94	7.1
N67	0.28	332.05	42.5	18.75	2.26	14.13	2.35
N68	3.94	2315.62	40.90	19	23.68	111.05	9.35
M2	0.91	441.84	40.35	15.50	18.22	18.30	7.55
M5A	2	63.97	30	14	17.14	64.64	3.90
M5B	1.73	47.14	33.33	19	21.05	53.42	4.75
M3	2.06	17.91	42	25	29.40	13.22	14.45
M4A	4.69	137.79	40	13	46.15	110.76	9
M4B	1.42	21.32	36.92	14	11.42	27.50	8
M6C	2.65	44.78	30	20	16.50	53	7.15